The Role of Melanoma Cancer Stem Cells in Metastasis

Dissertation

zur

Erlangung der naturwissenschaftlichen Doktorwürde

(Dr. sc. nat.)

vorgelegt der

Mathematisch-naturwissenschaftlichen Fakultät

der

Universität Zürich

von

Gregor Kiowski

von

Zollikon, ZH

Promotionskomitee

Prof. Dr. Lukas Sommer (Vorsitz und Leitung der Dissertation)

Prof. Dr. Alex Hajnal

Prof. Dr. Burkhard Becher

Zürich, 2012

To my wife Celine,
who truly knows what this is about
because she helped me through all of it.

Contents

Zusammenfassung

Aufgrund seines sehr aggressiven Charakters ist schwarzer Hautkrebs, auch Melanom genannt, der gefährlichste aller Hauttumore. Dies ist darauf zurückzuführen, dass Heilung momentan nur durch die chirurgische Entfernung von lokalisierten, nicht metastasierenden Tumoren erreicht werden kann. Daher ist eine frühzeitige Erkennung von metastasierenden Zellen und ein besseres Verständniss der Mechanismen, die der Metastasierung zugrunde liegen, wichtig für die Entwicklung besserer Therapieansätze.

Melanome entstehen aus entarteten Hautpigmentzellen, die entwicklungsbiologisch von der so genannten Neuralleiste abstammen. Aufgrund der Identifizierung von Melanomstammzellen, die Merkmale von ebensolchen Neuralleistenzellen besitzen, war das Ziel dieses Projektes deren Einfluss auf die Metastasierung zu untersuchen.

Bedenkt man aber die Komplexität der Melanomentwicklung beim Menschen, die mehrere aufeinanderfolgende Schritte beinhaltet, konnte dieses Ziel nicht direkt in Angriff genommen werden. Anstatt dessen musste erst ein neues Modelsystem entwickelt werden, welches den genauen pathologischen Verlauf der Krankheit widerspiegelte. Um dies zu erreichen haben wir uns ein menschliches

Hautmodel zu Nutzen gemacht, welches es uns ermöglicht hat alle Schritte des Krankheitsverlaufes in Ratten zu rekonstruieren. Diese Schritte umfassten die korrekte Ansiedlung der Tumorzellen an ihrem Ursprungsort, das Fortschreiten des Krankheitsverlaufes von radialem zu vertikalem Wachstum, sowie die Entstehung von gut durchbluteten, aggressiven Tumoren.

Aufbauend auf diesem Model haben wir abschliessend noch einige Experimente bezüglich der Rolle von Melanomstammzellen währende der Metastasierung durchgeführt. Obwohl kein Zusammenhang zwischen den schon beschriebenen $CD271^{Pos}$ Melanomstammzellen und einem erhöhtem Wachstumspotentials festgestellt werden konnte, haben wir einige Hinweise darauf gefunden, dass $CD271^{Pos}$ Zellen in die Invasion verwickelt sein könnten. Dies wurde unterstützt durch die Beobachtung, dass in migrierenden Tumorzellen CD271 dynamisch reguliert wird. Das ist insofern interessant wenn man bedenkt, dass ein Prozess aus der Embryonalentwicklung, genannt 'Epithelial-to-Mesenchymal Transition', kürzlich als Treibende Kraft für die Entsehung von Krebsstammzellen identifiziert wurde. Im Bezug darauf konnten wir in ersten Experimenten zeigen, dass der Verlust von E-cadherin, einem bestimmenden Faktor des EMT Prozesses, ein aggressives Verhalten hervorrufen kann. Interessanterweise wurden in diesen aggressiven Tumoren vermehrt einzelne, invasiven Zellen gefunden, die stark positiv für CD271 waren.

Zusammengenommen liefert diese Studie erste Hinweise darauf, dass auch im Melanom Stammzelleigenschaften dynamisch reguliert sein könnten. Darüber hinaus konnten wir durch die Transplantation von genetisch veränderten Zellen erstmals das Potential des neu entwickelten Modells für zukünftige Studien unter Beweis stellen.

Summary

Due to its extremely high metastatic capacity, cutaneous malignant melanoma represents the most fatal skin tumor in industrialized countries. This is because, up to date, the only possible therapy to cure melanoma remains surgical excision of localized, non-metastatic primary tumors. Thus, to improve current therapy an early identification of metastasizing melanoma cells and a better understanding of the mechanisms governing their dissemination is fundamental.

Melanoma results from transformation of cells of the melanocytic lineage, which originally is derived from the neural crest. Considering that human melanoma can arise from melanoma stem cells (MSCs) displaying neural crest stem cell features, this project aimed at assessing the metastatic capacity of MSCs and the contribution of neural crest migratory pathways therein.

However, considering the complex nature of melanoma progression involving several consecutive steps, a novel model system closely resembling human disease initiation and progression had to be established first. To this end we employed a tissue engineering approach, which allowed us to recapitulate all initial steps of disease progression in a humanized environment *in-vivo*. These

included the incorporation of the tumor cells into their physiological microenvironment, transition of radial to vertical growth, and establishment of highly vascularized, aggressive tumors with dermal involvement.

Based on this novel approach, we conducted several preliminary experiments addressing the role of melanoma stem cells in metastasis. However, no direct evidence for an enhanced tumor induction potential for the previously described $CD271^{Pos}$ melanoma stem cells was found. Nevertheless, several findings pointed to a potential implication of $CD271^{Pos}$ cells in invasion. In line with this theory, CD271 expression was discovered to be dynamically regulated in migrating human melanoma cells. This was of particular interest, considering that an embryonic signaling cascade termed 'Epithelial-to-Mesenchymal Transition' (EMT) was recently shown to induce cancer stem cell behavior. In accordance with these findings, we were able to obtain first evidence confirming that loss of E-cadherin, a determinant of EMT, induces an aggressive behavior in melanoma. Intriguingly, the resulting aggressive tumors revealed an abundance of single, invasive cells strongly positive for CD271.

Taken together, this study provides the first experimental evidence indicating that in melanoma stem cell traits may be dynamically regulated. Furthermore, in transplanting genetically manipulated cells, we were able to show the great potential inherent to the developed system for future studies.

Abbreviations

ADAM	A Disintegrin And metalloproteinase
AJCC	American Joint Committee on Cancer
Akt	Same as PKB
AML	Acute Myeloid Leukemia
ARF	Alternate Reading Frame protein from the CDKN2A locus
BMP	Bone Morphogenetic Protein
CDK	Cyclin-Dependent Kinase
CDKN2A	Cyclin-Dependent Kinase Inhibitor 2A
CSC(s)	Cancer Stem Cell(s)
CTF	C-Terminal Fragment
DCT	Dopachrome Tautomerase
DNA	Deoxyribonucleic Acid
E2F	Elongation Ffactor 2 F
EMT	Epithelial-to-Mesenchymal Transition
ERK	Extracellular signal-Regulated Kinases
FACS	Fluorescent Activated Cell Sorting
FDA	(American) Food and Drug Administration

GFP	Green Fluorescent Protein
GSK-3β	Glycogen Synthase Kinase-3β
H/E	Hematoxylin and Eosin stain
IRES	Internal Ribosome Entry Site
LDH	Lactate-Dehydrogenase
MAPK	Mitogen-Activated Protein Kinase
MC1R	Melanocortin Receptor 1
MDM-2	Murine Double Minute protein
MET	Mesenchymal-to-Epithelial Transition
MITF	Microphthalmia-Associated Transcription Factor
MSC(s)	Melanoma Stem Cell(s)
α-MSH	α-Melanocyte-Stimulating Hormone
NCSC(s)	Neural Crest Stem Cell(s)
NGF	Nerve Growth Factor
NK cells	Natural Killer cells
NMM	Nodular Malignant Melanoma
NOD/SCID	Non-Obese Diabetic mice with Severe Combined Immunodeficiency Disease
NSG	NOD/SCID/IL2rγ^{null} mice
P75-ICD	P75 Intracellular Domain
P75-NTR	low-affinity Neurotrophin Receptor P75
P75-TMD	P75 Transmembrane Domain
PIP_3	Phosphatidylinositol Phosphate

PKB	Protein Kinase B
PTEN	Phosphatase and Tensin Homolog Deleted from Chromosome Ten
Raf	Rat Fibrosarcoma Protein
Ras	Rat Sarcoma Protein
Rb	Retinoblastoma Protein
RFP	Red Fluorescent Protein
RGP	Radial Growth Phase
RNA	Ribonucleic acid
scr shRNA	scrambled shRNA
shRNA	Small Hairpin RNA
SSM	Superficially Spreading Melanoma
TNF	Tumor Necrosis Factor
TNM	Tumor-Node-Metastasis
TRP1	Tyrosinase-Related Protein 1
VGP	Vertical Growth Phase

Introduction

Carcinogenesis: Models and concepts

Cancer epidemiology

Based on global estimations of the World Health Organisation [1], deaths from cancer account for around 12% of all deaths world wide. This makes cancer one of the leading causes of mortality and poses, besides cardiovascular diseases, the most serious health problem for the population. Despite the increasing risk of developing cancer with age, cancer is not exclusively an age disease. The global risk of developing cancer at an age younger than 64 years is 10.3% for males and 9.5% for females [2]. This makes cancer the most common cause of death in the age group between 40-60 in industrialized countries [3]. With an estimated increase of global cancer deaths from currently approximately 7.6 millions to 11.5-17 millions over the next 20 years [1], better understanding of the various forms of cancer remains paramount to improve therapy.

The main treatment possibilities for cancer, up to date, remains a combination of surgery, radiotherapy and chemotherapy. Whereas advances in these therapeutic areas have led to a steady decrease in mortality rates over the last two decades [4], major break-throughs have only recently been achieved

by incorporating specifically designed drugs into standard treatment [5]. This novel class of drugs are rationally designed based on the growing knowledge of the molecular pathways driving cancer development and progression. Importantly, exclusively targeting tumor cells, these drugs are anticipated to improve efficacy while minimizing toxicity as compared to conventional chemotherapy. However, despite very successful examples like Imatinib (Gleevec ®, Novartis) for the treatment of chronic myelogenous leukemia, most target-specific drugs that enter clinical evaluation fail in producing survival benefits [6, 7]. This poor translation of basic oncology research to the clinics clearly shows that a deeper understanding of all aspects of disease progression as well as the development of more relevant model systems reflecting the human disease remains important [6, 7].

The hallmarks of cancer

On a cellular basis cancer arises when tissue cells escape growth control and start to proliferate indefinitely. For this to happen a cell needs to acquire various genetic and epigenetic alterations that allow it to overcome a multitude of intrinsic and extrinsic control mechanisms. Although germ-line mutations can predispose a person to heritable cancer, most tumors arise as a result of an accumulation of somatic mutations invoked by etiological agents like smoking, chronic virus infection (e.g. Hepatitis B/C or Papilloma virus), excessive sun exposure, carcinogenic chemicals etc. Because of this progressive nature of neoplastic transformation, increasing age constitutes the highest risk factor for most types of cancer [10]. Currently over 100 distinct cancer types are known, which can arise in every possible body tissue and carry an almost unlimited variation of somatic mutations. Paradoxically, it was this remarkable

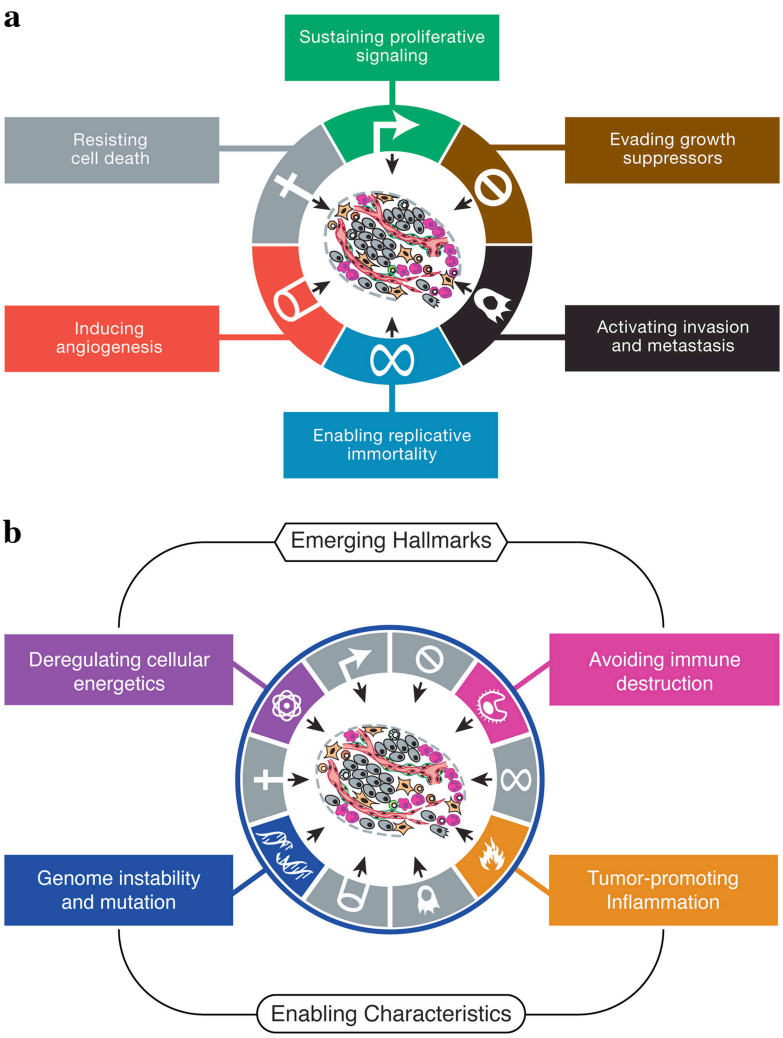

Figure 1. The hallmarks of cancer. (**a**) The six hallmarks of cancer as originally proposed in 2000 [8]. (**b**) Over the next decade the concept has been augmented with two emerging core hallmarks and two enabling characteristics [9].

complexity that led to the notion of a common organizing principle underlying neoplastic transformation: The Hallmarks of Cancer (Figure 1a). Based on the fact that virtually all mammalian cells carry a similar machinery regulating their proliferation and death, these hallmarks represent the six basic alterations in cell physiology that are essential for malignant growth [8]:

- Self-sufficiency in growth signals
- Insensitivity to growth-inhibitory (antigrowth) signals
- Evasion of programmed cell death (apoptosis)
- Limitless replicative potential
- Sustained angiogenesis
- Tissue invasion and metastasis

Starting from these initial hallmarks, the conceptual framework has been further refined over the next 10 years [9]. With respect to that, the most important contributions have been linked to two newly emerging core hallmarks and two enabling characteristics (Figure 1b). Core hallmarks, which are defined as essential for tumor development, have been proposed to additionally comprise the capability of cancer cells to reprogram their cellular energy metabolism to support continuous proliferation [11, 12] and the evasion of immunological destruction [11, 9]. In contrast, enabling characteristics are thought to establish a permissive state, which facilitates the acquisition of the core hallmarks. As such genetic instability, for example induced by mitotic, oxidative or metabolic stress [13, 14], has been conjectured to endow cells with the ability to produce the chromosomal rearrangements required for tumor progression [15, 9]. Furthermore, it has become increasingly clear that neoplastic progression is not solely contingent on cell intrinsic changes, but also on contributions of the tumor microenvironment. These have been suggested to include growth promoting signaling directly exerted by the tumor stroma cells as well as tumor-promoting inflammation [16].

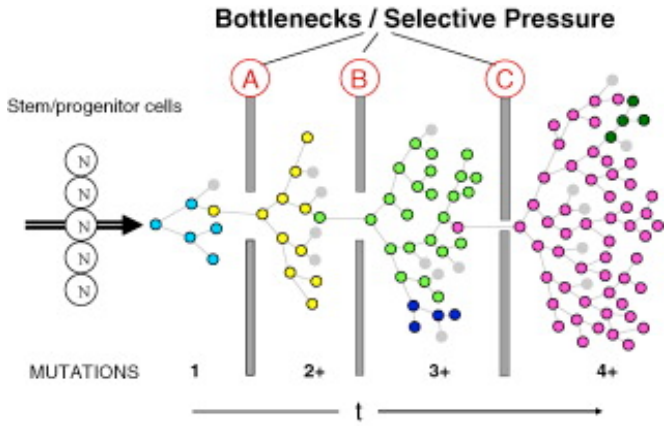

Figure 2. The clonal evolution of cancer. Induced by a mutation, a normal somatic cells (N) acquires a selective growth advantage and starts to overgrow its parental population of cells, which results in a selective sweep. Subsequent rounds of mutation and selective sweeps drive the stepwise evolution from a precancerous lesion towards the final neoplasm (depicted as A,B,C) [17].

The linear model of clonal evolution

Cancer is a genetic disease resulting from the accumulation of aberrations in the genome of somatic cells. Based on early cytogenetic studies showing that most tumors originate from a single transformed cell, cancer has been considered a disease of clonal evolution within the body [14]. First introduced by Nowell in 1976 [18], the clonal evolution model states that the pathogenesis of cancer proceeds by sequential steps of mutational events that are subjected to a Darwinian process of evolution. In a simple representation, this means that every somatic cell has the same chance to acquire a mutation that confers selective growth advantage, a so call driver mutation. This mutation enables it to expand more than the surrounding cells, which over time will result in its clonal domination - an evolutionary process known as selective sweep. Starting the next round of neoplastic evolution, eventually an additional driver mutation is introduced into this expanding population, which results in another

selective sweep. Thus, according to this traditional linear model, the accumulation of driver mutations in successive rounds of clonal expansion drives the stepwise progression from a precancerous lesion to the final neoplasm including metastasis (Figure 2).

However, despite being clonal in origin, most human tumors display a substantial genotypical and phenotypical intra-tumoral heterogeneity, which cannot be explained by the linear model [19, 20, 21, 22, 23, 24, 25, 26, 27, 28, 29]. This is because, assuming that every emerging dominant clone results in a selective sweep, a neoplasm evolving in a linear fashion consequently should be homogeneous in terms of its genotypic and phenotypic composition. Thus, resolving the mechanisms underlying these dichotomous observations has been a central dogma in tumor biology. So far two main concepts have emerged: the stochastic model of clonal evolution and the cancer stem cell model.

The stochastic model of clonal evolution

For the last three decades the main explanation for the observed intra-tumoral heterogeneity has been based on an extended clonal evolution model. Different from the simplistic linear model, in which monoclonal expansion of one dominant clone drives each step of disease progression (Figure 3a), in this model tumor evolution is considered a stochastic process. Based on their increasing genetic instability, all cells in an evolving neoplasm accumulate random mutations, which are subjected to Darwinian selection. This renders a neoplasm a genetically and epigenetically heterogenous entity of clonal populations with differing proliferative and survival capacities. Within this microcosmos of evolution, all evolving clones are in constant competition with each other, which consequently leads to the co-existence of multiple genetically divergent tumor

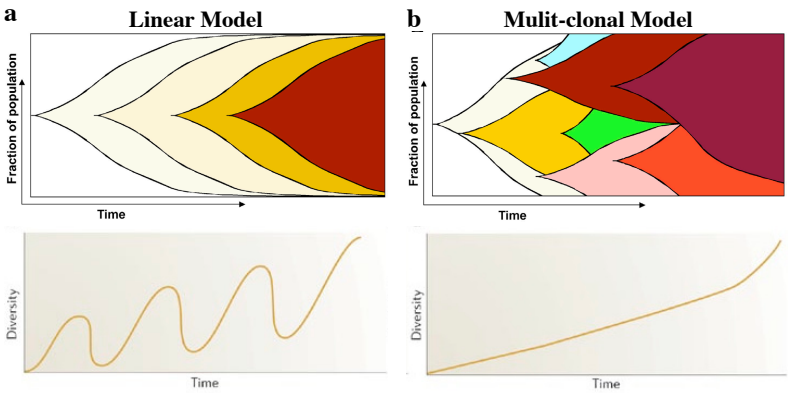

Figure 3. The extended clonal evolution model. (**a**) In the linear model, a succession of increasingly aggressive clones sweep through the population and become fixed (upper panel). Consequently, the genetic diversity should fluctuate, increasing when genetic instability generates new clones in an expanding population, and decreasing when a new clone strives towards fixation (lower panel). (**b**) In the multi-clonal approach several genetically diverse populations evolve simultaneously. Because the fitness of every clone depends on its immediate microenvironment, selective sweeps tend to be restricted to individual subpopulations (upper panel). In this model the genetic diversity increases constantly because genetic sweeps cannot affect the entire population (lower pannel). Figure adapted from [14, 30].

clones at any time [14] (Figure 3b). Interestingly, according to this model, selective sweeps homogenizing the entire population are very unlikely to occur for two reasons. First, some mutations are silent passenger mutations that do not confer any growth advantage and, therefore, do not present a selectable trait. And second, because the fitness of any given clone presumably depends on its immediate microenvironment, only selective sweeps within this particular environment are possible. Consequently, despite being in constant competition, it is conceivable that several clonal populations can evolve simultaneously explaining the frequently observed clonal heterogeneity in human neoplasms [30, 31]. Interlinked with this genetic heterogeneity, also the observed morphological diversity is explained by the same underlying principle.

Assuming that some of the acquired mutations manifest in a functional and, therefore, heritable morphological phenotype, selective pressure will also drive the evolution of multiple, morphologically diverse tumor cell populations.

Importantly, the genetic and phenotypic heterogeneity inherent to most human neoplasms has been shown to have direct consequences for treatment. The underlying principle is best demonstrated by depicting the tumor cell populations on a fitness landscape (Figure 4). In this graphical representation every possible genotype and its corresponding fitness value is represented by a single dot. Peaks correspond to the most aggressive genotypes as a function of proliferation and survival. Considering that a specific genotype (Figure 4, crosses) can only spawn offspring that are in its genotypic vicinity (Figure 4, dots), positive selection will only occur when a progeny acquires a mutation that allows it to go uphill (become more aggressive). As a consequence, if the genotypic vicinity of a given clone only includes a small fitness peak (Figure 4, green clone), the probability of its progeny to reach a higher peak becomes very low. Based on this simple model, it becomes obvious that clonal heterogeneity results in an increased probability for tumor progression (Figure 4a). This is because clonally heterogeneous tumors are able to explore larger areas in the adaptive landscape, which increases their chances that one clone eventually reaches a peak (Figure 4a, blue clone). Intriguingly, the same principle also applies for disease recurrence (Figure 4b). Assuming that the main effect of therapy is imposed by substantially changing the fitness landscape, the probability of a sub-clone reaching a new peak is again significantly higher in heterogeneous lesions [14, 30] (Figure 4b, red clone). In favor of this theory, several examples of sub-clones becoming dominant after treatment have been documented for lung cancer [32], chronic myeloid leukemia [33], melanoma

[34] and others [14]. As a consequence, the aim of current therapy remains to eradicate all residual cancer cells in order to minimize the chances of disease recurrence.

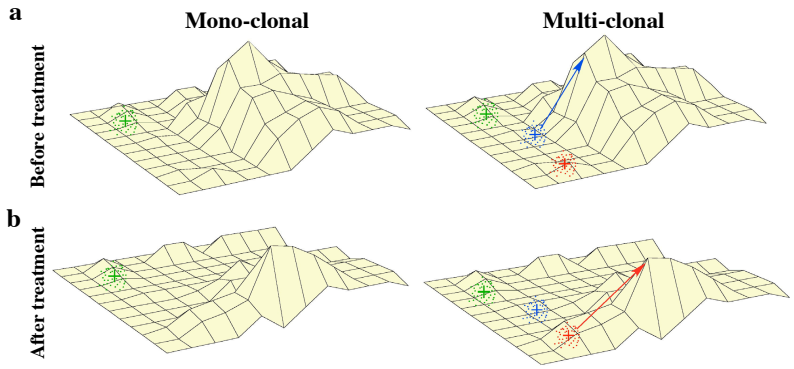

Figure 4. The consequence of clonal heterogeneity for treatment. In a fitness landscape every possible genotype is correlated to a fitness value in a graphical representation. Peaks represent the most aggressive phenotypes, colored crosses individual clones, and colored dots their respective mutant offspring. (**a**) Clonal heterogeneity increases the probability of a tumor to reach a fitness by sampling a larger area on the landscape. (**b**) Treatment renders the originally dominant clone (blue cross) harmless by altering the landscape. Following treatment, recurring disease results from a genetically diverse sub-clone (red cross) adapting to the new landscape [30].

The cancer stem cell model

The concept

Opposing the stochastic clonal evolution model, the cancer stem cell theory stipulates that the phenotypic heterogeneity in tumors arises from an inherent cellular hierarchy rather than random mutagenesis (Figure 5a). In this model, reflecting their corresponding normal tissue, tumors are sustained by a pathological counterpart of normal adult stem cells: cancer stem cells (CSC) [37]. Like normal tissue stem cells, CSC have the potential to self-renew and

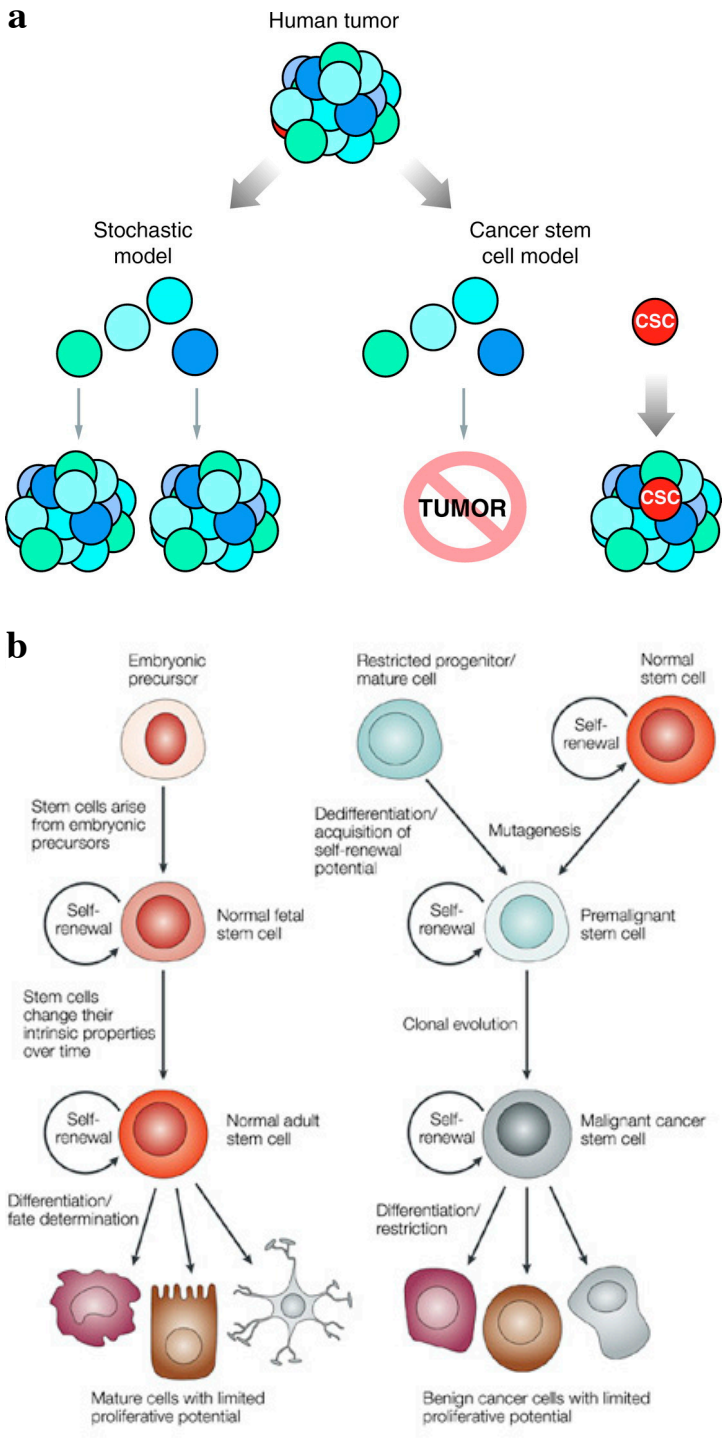
a
Human tumor
Stochastic model
Cancer stem cell model
CSC
TUMOR
CSC
b
Embryonic precursor
Restricted progenitor/ mature cell
Normal stem cell
Self-renewal
Stem cells arise from embryonic precursors
Dedifferentiation/ acquisition of self-renewal potential
Mutagenesis
Self-renewal
Normal fetal stem cell
Self-renewal
Premalignant stem cell
Stem cells change their intrinsic properties over time
Clonal evolution
Self-renewal
Normal adult stem cell
Self-renewal
Malignant cancer stem cell
Differentiation/ fate determination
Differentiation/ restriction
Mature cells with limited proliferative potential
Benign cancer cells with limited proliferative potential

Figure 5

Caption Figure 5. The cancer stem cell model. (**a**) Different from the stochastic model of tumor development, the cancer stem cell model assumes that only a small fraction of tumor cells, cancer stem cells, have the ability to sustain tumor growth. (**b**) Like their physiological counterparts, cancer stem cells have the potential to self-renew and to differentiate into phenotypically diverse progenitor cells with limited proliferative potential. Whether cancer stem cells can arise by transformation of adult stem cells or de-differentiation of more restricted progenitor cells is unknown for most types of cancer. Figure adapted from [35, 36].

to differentiate into phenotypically diverse progenitor cells with limited proliferative potential (Figure 5b). Consequently, tumor growth and maintenance can solely be perpetuated by the CSC population. Standing at the apex of the cellular hierarchy, CSCs give rise to differentiated progenitor cells, which constitute the main tumor mass. Although some of these progenitor cells might retain some limited proliferative capacity, they contribute little to disease progression and can be considered benign. Obviously, the ramifications of this theory for treatment are profound. Not the bulk cells of a tumor would have to be targeted, but the rare CSC population as they are the sole driver of tumorigenesis. This would also offer an intriguing explanation for the recurrence of many cancers after therapy considering that conventional therapy is mostly designed to eradicate bulk tumor cells (Figure 6). Albeit this would result in a temporal regression of the tumor mass, already a small population of residual CSCs resistant to therapy would be sufficient to induce *de-novo* tumor growth [38].

Experimental proof

Although the concept of a cancer stem cell has been proposed over a century ago by the pathologists Rudolph Virchow [40] and Julius Cohnheim [41]

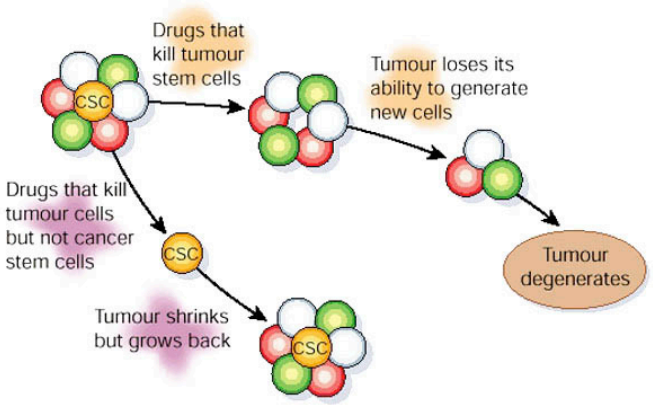

Figure 6. The consequence of cancer stem cells for treatment. Unless the cancer stem cell population is eradicated, the chances for recurrent disease remain high [39].

in their 'embryonal-rest hypothesis', experimental evidence has only been established recently. Pioneered by John E. Dick, CSCs were first identified in acute myeloid leukemia (AML) [42, 43]. Following the identification of a primitive $CD34^+/CD38^-$ hematopoietic stem cells able to recapitulate normal hematopoiesis in recipient mice, the detection of $CD34^+/CD38^-$ expressing cells in human AML patients provided the first indication of a putative CSC [42]. To address the potential of this putative CSC fraction, AML cells were fractionated on the basis of their $CD34^+/CD38^-$ vs. $CD34^+/CD38^+$ expression profile and serially passaged in immuno-compromized, non-obese diabetic mice with severe combined immunodeficiency disease (NOD/SCID). These experiments revealed that the capacity to transfer human AML to recipient mice, indeed, resided exclusively within the $CD34^+/CD38^-$ fraction [42]. Based on the consistent capacity of $CD34^+/CD38^-$ AML cells to recapitulate the human disease independent of the AML subtype they were originally isolated from, the authors concluded that AML follows a similar hierarchical organization as normal hematopoiesis [43] (Figure 7a). Importantly, this seminal study not

only provided the first proof of a CSC population, but also defined the gold standard for their experimental identification. These steps comprise the the prospective isolation of a putative CSC fraction from dissociated tumor material, the confirmation of their *in-vivo* tumor initiating capacity as opposed to bulk tumor cells, validation of their *in-vivo* self-renewal capacity by serial transplantation, and proof of their ability to phenotypically regenerate their original tumor (Figure 7b).

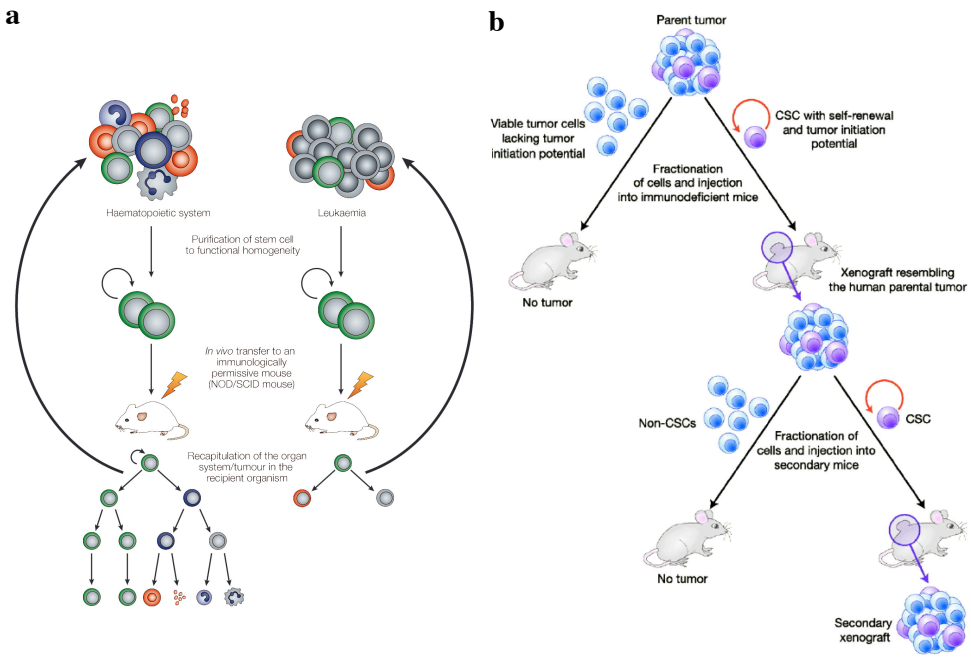

Figure 7. Experimental identification of cancer stem cells. (**a**) Based on the similarities to normal hematopoietic stem cells, cancer stem cells were first identified in human leukemia. (**b**) Experimental proof for cancer stem cells requires their isolation from dissociated tumor material, verification of their exclusive *in-vivo* tumor induction potential, proof of their capacity to self-renew *in-vivo*, and their ability to phenotypically recapitulate their parental patient tumor. Figure adapted from [44, 45].

Cancer stem cells in solid tumors

Following the discovery of CSCs in hematopoetic cancers, their existence was soon demonstrated also in solid tumors [46]. But unlike for hematopoetic tumors, the identification of CSCs in solid tumors has been hampered due to a lack of definitive assay systems and cell surface markers [44]. This fact is best reflected by the substantial controversy surrounding the frequency of CSCs in solid tumor populations. Sometimes ranging from 2% to over 25% in the same type of tumor [47], the experimental basis for an exact measurement of the CSC frequency is unknown [48]. This relates to the problem that many experimental variables like residual immunocompetence of the used animal host [49, 50], the site of engraftment (unpublished data), co-injection with extracellular matrix substrates [49] or the amount and quality of injected cells [51, 52] have been shown to substantially influence CSC measurements. Considering that the whole foundation of the CSC theory rests on its operational definition in such experimental model systems (Figure 7b), the development of relevant humanized model system has been deemed crucial to validate CSC populations in solid tumors [53].

The origin of cancer stem cells

Despite often confused, the term cancer stem cell does not *per se* imply that the neoplastic cell of origin actually is a stem cell. Nevertheless, normal stem cells have been proposed to be the most likely target for neoplastic transformation. This assumption relies on mathematical models, which predict neoplastic transformation to be a rare event requiring several rate-limiting mutations within the same cell [10]. As a consequence it has been presumed that only the stem cell pool in human tissues persists long enough to accumu-

late enough genetic and epigenetic alterations for transformation [39]. While compelling evidence for this theory exists for intestinal [54, 55] and prostate [56] cancer, for most neoplasms it remains elusive whether cancer stem cells arise from the transformation of normal stem cells or de-differentiation of more restricted progenitor cells (Figure 5b). Evidence for the latter model comes from skin [57, 58] and Chronic Myeloid Leukaemia [59], where more restricted progenitors were shown to be able to acquire stem cell properties. At present it appears conceivable that a combination of both mechanism might be operational during tumor initiation. The most compelling evidence for an integrated model relates to the fact that the same type of tumor in different patients often manifests in discrete subtypes with specific properties and expression profiles. Traditionally, this has been explained by the genetic mutation model, which assumes that the variety of discrete subtypes is determined by distinct oncogenic events transforming a common cell of origin (Figure 8a). In contrast, the hierarchical cell-of-origin model raises the possibility that the different subtypes arise as a consequence of common mutations transforming different cell populations along a lineage hierarchy [60] (Figure 8b).

Cancer stem cells vs. clonal evolution

An integrated concept

Regardless of the plethora of literature favoring one model of tumorigenesis over the other, both major paradigms, the clonal evolution as well as the CSC model, also harbor several caveats. On one hand, for the CSC model there still is no direct evidence that the difference between tumorigenic cells and non-tumorigenic cells emanates from epigenetically induced differentiation instead

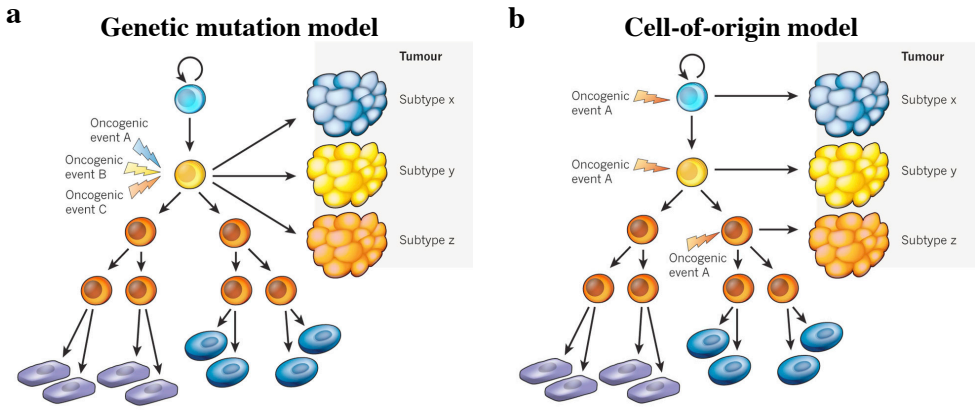

Figure 8. The cell of origin model. (**a**) In the genetic and epigenetic mutation model, a variety of distinct oncogenic events is responsible for the observed tumor subtypes. (**b**) In the cell-of-origin model tumorigenesis is driven by a common mutational event. The different subtypes result from the transformation of different cell population along the lineage hierarchy in a particular organ [60].

of genetic differences [52]. In fact, contradicting a simple hierarchy-based CSC model, in breast cancer the tumorigenic $CD44^+/CD24^-$ stem cell population was shown to be genetically divergent from the $CD44^-/CD24^+$ bulk tumor cells [61, 62]. On the other hand, also the clonal evolution model has its limitations. Based on the premise that there are simply more ways to damage a genome than to improve it, mathematic models show that an increasing mutation rate due to progressive genetic instability should lead to reduced fitness and, thus, clonal extinction; an effect known as negative clonal selection [63].

However, given the overwhelming experimental evidence for the clonal origin of cancer, the mutator theory can hardly be denied as the original driving force of neoplastic transformation. Thus, attempting to reconcile the clonal evolution and the cancer stem cell paradigm, an integrated model has recently been proposed (Figure 9). According to this model, clonal evolution does

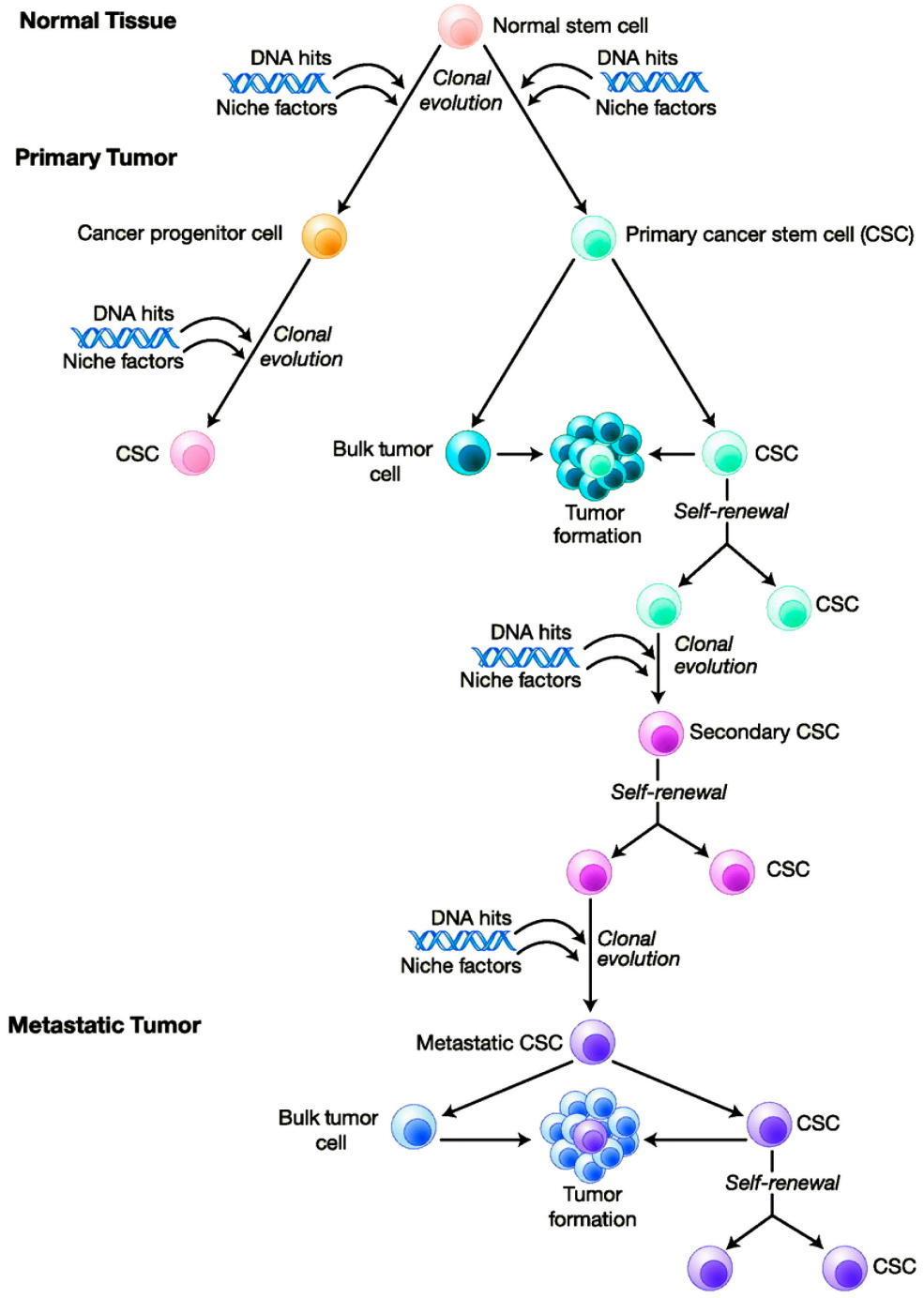
Normal Tissue
Normal stem cell
DNA hits
Niche factors
Clonal evolution
DNA hits
Niche factors
Primary Tumor
Cancer progenitor cell
Primary cancer stem cell (CSC)
DNA hits
Niche factors
Clonal evolution
CSC
Bulk tumor cell
Tumor formation
CSC
Self-renewal
CSC
DNA hits
Niche factors
Clonal evolution
Secondary CSC
Self-renewal
CSC
DNA hits
Niche factors
Clonal evolution
Metastatic Tumor
Metastatic CSC
Bulk tumor cell
Tumor formation
CSC
Self-renewal
CSC

Figure 9

Caption Figure 9. Clonal evolution and cancer stem cells: an integrated concept. Instead of working on the entire population of tumor cells, clonal evolution is restricted to the CSC pool. Genetic alterations in conjunction with microenvironmental niche factors constitute the selective pressure that drives the evolution of metastatic CSC [64].

occur, but is restricted to the CSC pool. Similar to the multi-clonal model of tumor evolution (Figure 3b), this would give rise to several genetically distinct CSC populations defined by their immediate microenvironment [64]. First evidence in support of this model comes from a recent report showing the stochastic evolution of the CSC population in metastatic colon cancer [65]. Intriguingly, this concept also offers the possibility to reconcile the CSC theory with the clonally heterogeneous nature of most human cancers. According to this model, the observed clonal heterogeneity reflects genetically diverse CSC subpopulations that are in evolutionary competition. Because every CSC population in turn gives rise to a large pool of genetically homogeneous progenitor cells, the resulting cancers as a whole are heterogeneous.

Tumor cell plasticity and epigenetic stability

However, restricting clonal evolution to a small CSC pool harbors yet another logic pitfall. Decreasing the number of cells evolution can work on would in return demand a corresponding increase in the mutation rate. And this often by two orders of magnitude above the rates that have been described for human tumor cells [48]. To resolve this paradox, it has been proposed that, different from a rigid hierarchical model, CSC can arise as a consequence of tumor cell plasticity. According to this model, the stem cell pool does not represent a stringent population within a neoplasm, but rather can be induced by

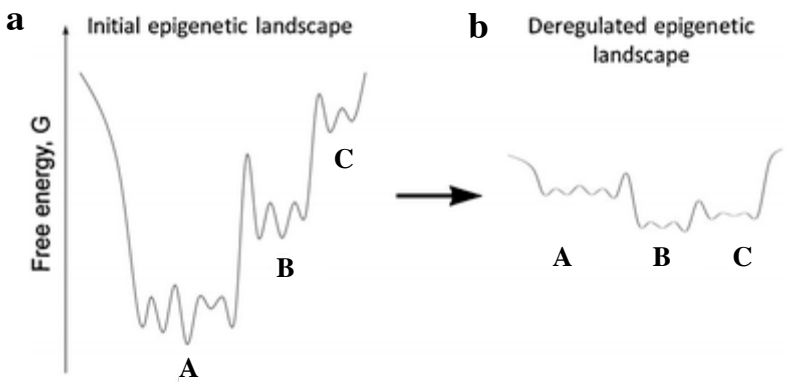

Figure 10. CSCs as a consequence of a deregulated epigenetic landscape. (**a**) In normal tissue cells and early stage tumors cells retain a stable epigenetic landscape. Similar to chemical reactions, the loss of free energy correlates with increasingly stable states. Depicted is the differentiation of a stem cell (C) to its final, mature cell type (A). (**b**) The increasing genetic and epigenetic instability found in late stage cancers causes the epigenetic landscape to flatten out. This allows cell to move freely between the different states including that of a stem cell (C) [63].

epigenetic changes contingent on microenvironmental cues [53, 48, 66]. That tumor cells indeed display a remarkable plasticity in response to their microenvironment has been demonstrated by a set of experiments subjecting tumor cells to an embryonic environment. In this set-up, malignant tumor cells were shown to be reprogrammed to follow their normal developmental programs and contribute to normal tissue formation [67, 68]. However, whether this observed plasticity reflected an inherent trait of pre-existent tumor stem cells that responded to their original microenvironment or a general feature of all transplanted tumor cells to acquire a transient stem cell state has not been addressed.

Clearly the possibility of normal tumor cells switching between stem cell and non-stem cell states adds yet another layer of complexity to an already ambiguous concept. However, at the same time, it also poses a promising theory

to resolve several disparate findings with respect to the frequency and nature of CSCs [69, 70, 17]. This follows from the fact that, in order to acquire stem cell features, neoplastic cells need to deregulate their epigenetic landscape. During the early stages of tumor development cancer cells, like normal tissue cells, retain a stable epigenetic landscape keeping them in defined, hierarchical states with a stem cell at the top (Figure 10a). Advancing to late stage tumors, increasing levels of genetic and epigenetic instability progressively deregulate the epigenetic landscape causing the discrete states of differentiation to distort. As a consequence cells acquire the potential to move freely between all possible states including that of a stem cell (Figure 10b).

Intriguingly, first evidence corroborating this concept was recently identified in malignant melanoma. In this study the histone 3 K4 demethylase JARID1B was shown to be essential for tumor maintenance, a typical feature of a CSCs. But in contrast to the hierarchical CSC model, the expression of JARID1B was not confined to a specific subpopulation of cells but was found to be dynamically regulated [71]. This raises the possibility that epigenetic regulation might indeed be responsible for the induction of transient stem cell features in some cancers. Interestingly, a potential mechanism triggering the induction of such transient, dynamic stem cells has recently been identified in breast cancer. By inducing a process reminiscent of an embryonic developmental program termed Epithelial-to-Mesenchymal Transition (EMT), it was demonstrated that transformed breast epithelial cells adopt CSC properties [72, 73]. This raises the possibility that for some tumors CSCs represent not a fixed entity, but rather a transient population of cells arising as a consequence of extrinsically induced epigenetic alterations.

Metastatic disease

The 'seed and soil' hypothesis

Regardless of all recent advances cancer remains a major cause of death. This is because metastases, rather than primary tumors, are the main cause of lethality due to cancer. But given the currently limited treatment options for systemic disease, only a better understanding of the cellular and molecular programs underlying metastatic progression will improve the chances of survival.

On a broad scale metastasis can be described as the process, during which tumor cells disseminate from the primary neoplasm to establish secondary tumors in distant organs. On a cellular basis, the metastatic process has been envisioned to be a sequence of discrete steps, all of which have to be overcome to induce metastatic growth at a distant site (Figure 11). These steps comprise the ability to escape from the primary tumor, enter the vasculature, survive in the circulation, arrest in a new organ, extravasate into the surrounding tissue, adapt to the new microenvironment, initiate proliferation, and attract new blood supply in order to progress to a macroscopic lesion [74]. Based on this striking complexity, it stands to reason that presumably only a minority of cells in a neoplasm are equipped with the required attributes to pass through all these steps. In line with this hypothesis, several seminal studies showed that the metastatic process is highly inefficient. Interestingly, the inefficiency was not caused by limited survival of the disseminated cells but by their failure to progress beyond the state of a micrometastasis [76, 77]. From this observation it was concluded that, in addition to cell inherent metastatic programs, also the environment of the target organ plays an active role in the

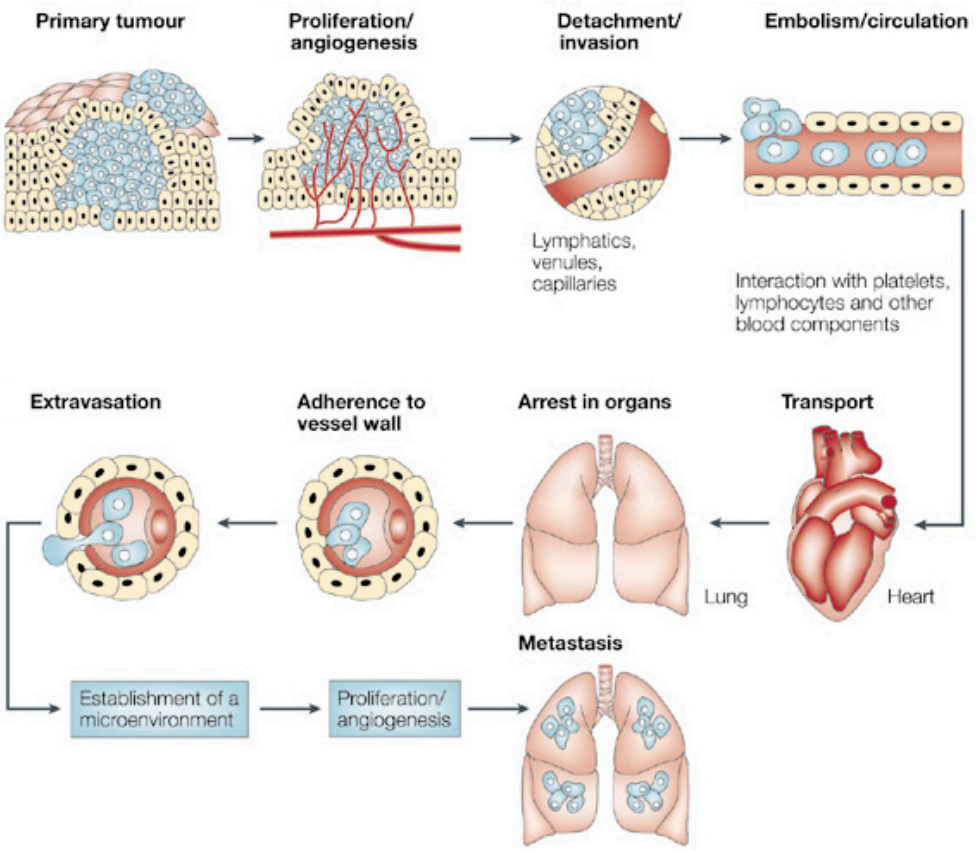

Figure 11. The metastatic process. The metastatic process requires a series of discrete steps. These include the detachment from the original tumor, intravasation, survival in the bloodstream, arrest in a new organ, extravasation into the surrounding tissue, adaptation to the new microenvironment, proliferation at the new site, and establishment of new blood supply [75].

tropism of metastatic disease. Interestingly, at the time these experiments were performed, the underlying concept had been postulated over a century ago. It was first described by the the English surgeon Stephen Paget in 1889, who noted a discrepancy between the frequency of metastases and the relative blood supply in certain organs. This observation of a non-random pattern of metastasis led him to postulate that 'when a plant goes to seed, its seeds are carried in all directions; but they can only live and grow if they fall on conge-

nial soil' [78]. This statement founded what today, 122 years later, is known as the as the 'seed-and-soil' hypothesis. It states that metastasis depends on a favorable interaction between the cancer cells, "the seeds", and the microenvironment of the target organ, "the soil". Although challenged 40 years later by James Ewing, who proposed that the observed organ specificity is exclusively attributed to mechanical forces and circulatory patterns between the primary tumor and the secondary site [79], Paget's theory has stood the test of time [75]. Validated by a set of *in-vivo* experiments performed in the 1970s, it was shown that, although mechanical arrest in the capillary bed of distant organs does occur, the progression to a macroscopic lesion is dependent on a favorable environment provided by the target organ [75, 80]. Thus, at present a combination of both theories appears most likely. Instead of actively 'seeking out' a specific organ, circulating cancer cells are passively transported along until they are arrested in a capillary bed due to physical size restrictions. At this point their subsequent growth will depend on favorable molecular interactions between the cancer cells and the environment of the new organ [74].

Metastatic heterogeneity and metastatic inefficiency

Following the observation that tumors display a strong intra-tumoral heterogeneity [30], several seminal studies started to explore the implication of this cellular heterogeneity on tumor progression [80]. From these studies two fundamental concepts arose, that of metastatic heterogeneity and that of metastatic inefficiency. The first model refers to the findings that individual cells within a tumor display a divergent propensity to metastasis [81]. The latter refers to the fact that the metastatic process overall is inefficient due to the stochastic nature of the genetic events underlying the acquisition of metastatic traits. Taken together, this points to the existence of specialized metastatic cells,

which are equipped with an enhanced capability to adapt to a new microenvironment and initiate *de-novo* tumor growth at a distant site [76, 82]. This is further corroborated by the fact that most metastases are monoclonal in origin [83, 84, 85, 86, 87, 88, 89]. However, the origin and nature of such specialized cells driving systemic disease remains elusive. But corresponding to the main concepts underlying tumorigenesis described above, only two potential mechanisms are conceivable, clonal evolution or cancer stem cells.

Clonal evolution and metastasis

Based on the clonal evolution model, systemic disease could be the final result of two differing processes, linear or parallel evolution of a metastatic clone. According to the linear model, metastatic cell dissemination would be the last step of tumor evolution. Bestowed with all malignant traits necessary to conquer a distant sites, metastatic cells are considered the pinnacle of evolution in a primary neoplasm [18]. In contrast, according to the parallel model, early disseminated tumor cells evolve independently parallel to the primary tumor [90]. Practically the difference between the two models should manifest in the clonal relationship between the primary tumor and the corresponding metastases. In the linear model, reflecting the late dissemination of already fully metastatic cells, the metastatic tumors should display a close clonal relationship to the primary tumor. In contrast, following the parallel model, metastases should represent genetically divergent clones [30].

Reflecting the long standing relationship between tumor size and metastasis, which forms the basis for the pathological tumor, nodes, metastasis (TNM) staging, linear progression has been accepted as the more likely mechanism.

Nevertheless, several conceptual caveats have challenged the idea of linear progression. Based on tumor growth rates, mathematical models predict that for linear progression to occur metastatic growth rates would have to exceed that of their primary tumors by far in certain conditions, for which there is no evidence [90]. Moreover, metastatic lesions already present in early stage tumors (T1M1 or T2M1) or growing without a detectable primary tumor are difficult to reconcile with linear progression. And last but not least, considering a Darwinian mode of selection towards the emergence of a metastatic clone, the assumption in itself presents a paradox. If metastatic clones leave the primary tumor, the primary tumor would suffer a decrease in fitness due to the loss of its fittest offspring, which eventually should result in its extinction [14]. Although evolutionary pressure towards dispersal appears conceivable based on the limitation of space and nutrients in a growing neoplasm, this conceptual problem has not yet been resolved. So far both models seem valid, as there is experimental evidence in favor of both theories emerging [87, 21, 91, 24, 92, 93, 94].

Cancer stem cells and metastasis

Defined as the only sub-set of cells capable of initiating *de-novo* tumor formation, it is clear that CSCs offer an auspicious candidate for the induction of metastasis. But besides this, CSCs would also offer an intriguing explanation for many peculiarities inherent to the metastatic process [37]. For example, like their 'normal' counterparts, CSCs are thought to reside in a distinct microenvironment called the 'stem cell niche', which regulates stem cell traits like proliferation, differentiation, and apoptosis resistance [95]. Strikingly, this idea is congruent with Paget's 'seed and soil' hypothesis, if one assumes that distinct CSC niches can only be found in particular organs. Along this line also

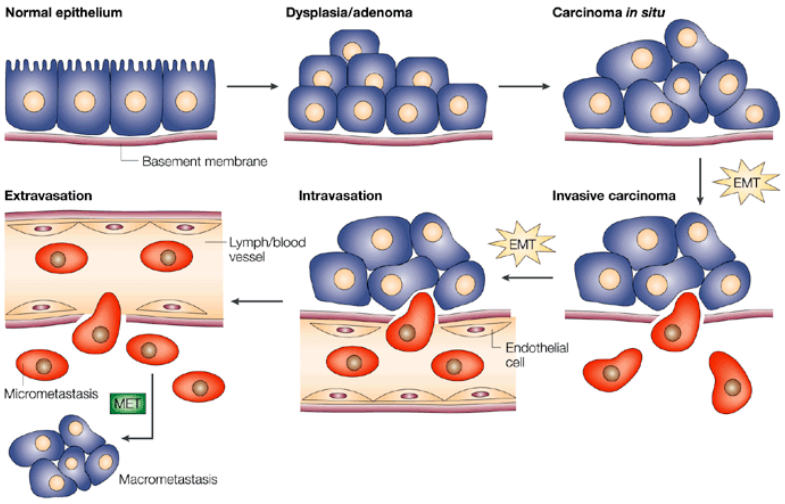

Figure 12. Epithelial-to-mesenchymal transition. Undergoing an epithelial-to-mesenchymal transition (EMT), benign carcinoma cells acquire the potential to push through the basement membrane and invade the underlying dermis. At a secondary site the reverse process, an mesenchymal-to-epithelial transition (MET), governs the progression from micrometstases to macrometastatic growth [96].

the observed dormancy of metastases, often evolving decades after resection of a primary tumor, could be explained. Residing in a niche, disseminated CSCs initially stay quiescent until a sudden change in the microenvironment activates their lethal potential.

Intriguingly, the strongest argument for the implication of CSCs in the metastatic process is, like the CSC concept itself, adapted from developmental biology. As such an embryonic migratory process called 'the epithelial-to-mesenchymal transition' has been proposed to constitute a major determinant for the progression of benign adenomas to malignant carcinomas [96]. During EMT tightly adherent, non-migratory, polarized epithelial cells transform into lose, unpolarized mesenchymal cells displaying an inherent migratory potential (Figure 12). Considering this, it appears conceivable that CSCs could

exploit remnants of this embryonic signaling pathways in order to disseminate, adapt, and survive at distant sites. However, at present convincing data proving the implication of CSC in the metastatic process remains fragmentary [97]. But nevertheless, first evidence for a link between EMT and CSCs has emerged from breast cancer. Surprisingly, in these studies EMT was no found to confer migratory potential to CSCs, but was identified as the determinant inducing CSC traits in transformed mammary epithelial cells [72, 73]. In this dual role, the EMT transdifferentiation program was suggested to serve as a regulatory interface, which concomitantly controls migratory and tumor inducing potential [72, 98] in response to contextual signals provided by the microenvironment [99].

Technical considerations studying metastasis

Metastasis is a systemic process 'hidden' away in the body and, therefore, notoriously difficult to observe. Thus, to faithfully model the complexity of the metastatic process, special care has to be applied choosing a relevant model system. Unfortunately, the most frequently used experimental metastasis models, intravenous and subcutaneous injections into mice [100], have been questioned with regard to their fidelity of the human process [90, 101, 102, 103]. As a consequence, it has been proposed that, in order to improve the relevance of the findings, the applied *in-vivo* models should mimic the autochthonous situation of tumor progression as closely as possible [104, 102, 103]. However, given the lack of such model systems for most human cancers, studying the metastatic process remains technically challenging.

Another difficulty impeding the investigation of metastatic traits is the genetic and epigenetic heterogeneity found in primary and secondary lesions. This applies in particular to micro-array studies, in which rare metastatic

traits are prone to submerge in the background noise inherent to a heterogenous sample [80]. This was made clear by a study sampling different areas within cervical tumors. Interestingly, whereas the majority of the genes in different regions of the same tumor were expressed relatively homogeneously, there remained a significant heterogeneity among a subset of genes involved in transcriptional regulation and cellular metabolism [105]. Thus, conducting micro-array analysis the intra-tumoral heterogeneity as well as the presence of non-tumor stroma cells has to be taken into account by sampling multiple areas from, if applicable, several patients [80].

Melanoma

Melanoma as a model system

With respect to the myriad of contradictory reports surrounding the concept of CSCs as well as their potential implication in metastasis, we chose human malignant melanoma to address some these open questions. The rational for using melanoma lies in its neoplastic origin, the melanocytes. During development the melanocytic lineage originates from a transient population of highly migratory embryonic stem cells, the neural crest (Figure 13a). Intriguingly, many processes attributed to metastasis formation are reminiscent of embryonic neural crest development, during which neural crest cells migrate from their sites of origin, proliferate, and colonize distant sites in specific locations. Considering these similarities, it is conceivable that its strong propensity to metastasize reflects an intrinsic property of some melanoma cells able to exploit inherent developmental signaling cues. Among these, the most promising relates to the process of EMT, which is not only the initiating event of neural crest delamination from the neural tube, but also a prerequisite for the malignant progression of carcinomas [96]. In view of the, albeit conflictive [70, 106], studies reporting the identification of melanoma stem cells (MSCs) resembling a neural crest stem cells (NCSC) [51, 107], potential parallels between MSCs, Neural Crest development, and metastasis represent the conceptual framework of the project described here.

Melanoma epidemiology

Over the last 6 decades melanoma has shown a dramatic increase in incidence, now ranking among the top 10 cancers in North America, Europe, Australia and New Zealand, the main regions of occurrence [1]. The strongest risk factors

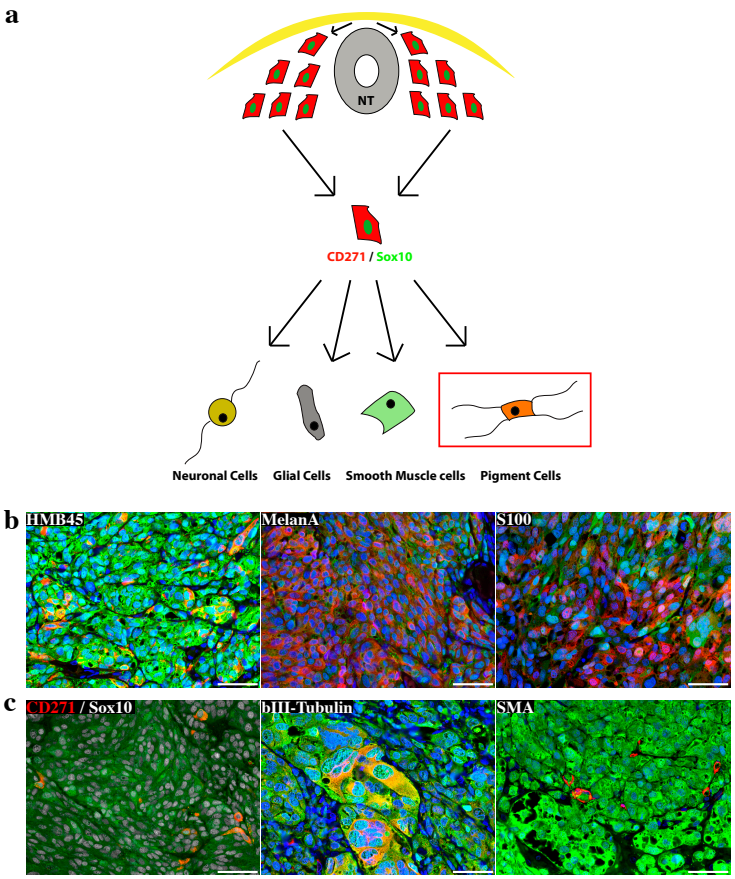

Figure 13. The developmental origin of melanoma. (**a**) Undergoing an archetype EMT, neural crest stem cells delaminate from the dorsal part of the neural tube during early embryonic development. Upon delamination, they migrate along distinct pathways to various sites throughout the embryonic body and differentiate into various cell types like neurons, glia, connective tissue, cartilage, bone, pigment cells and others. Neural crest stem cells express the low-affinity neurotrophin receptor CD271 (also called P75NTR) and the transcription factor Sox10. (**b**) Human melanoma cells express the melanoma associated markers HMB45, MelanA and S100. (**c**) Staining of a human melanoma xenograft for the neural crest stem cell marker CD271 / Sox10 and neural crest derivatives like smooth muscle cells (SMA) or neuronal cells (bIII-tubulin) reveals its close relationship to the neural crest. Counterstaining with GFP excludes that the observed cellular heterogeneity results from infiltrating host cells. Scale bars, 100μm.

to develop melanoma comprise a family history of melanoma, multiple benign or atypical nevi, and a previous melanoma. Additional risk factors include immunosuppression, sun sensitivity, and exposure to ultraviolet radiation [108]. Interestingly, the hazardous effect of ultraviolet radiation, the main etiological factor for the induction of melanoma, appears to be dose-dependent. As such melanoma occurs most frequently in individuals with sporadic intense exposure and heavy sunburns. The underlying reason for this has been proposed to result from genetic damage invoked by intense exposure as compared to DNA damage protection induced by chronic or low-grade exposure [109].

Melanoma classification

Melanoma progression

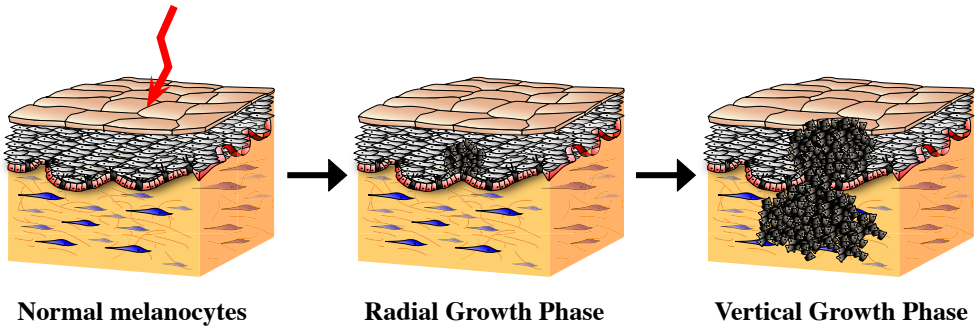

Figure 14. Melanoma progression. Melanoma progression follows a well described sequential pattern. Upon transformation normal melanocytes start to proliferate within the confines of the epidermis (Radial Growth Phase). Accumulating aggressive traits the cells acquire the ability to penetrate the underlying basement membrane and start to invade the dermal compartment and surrounding vasculature (Vertical Growth Phase).

Histopathologically melanoma develops in a multistep fashion first described by the dermatologist Wallace H. Clark jr. in 1984 [110]. Starting with normal

melanocytes or a benign nevus, the begin of neoplastic transformation first manifests as a dysplastic nevus with structural atypia. Accumulating further mutations, these dysplastic nevi then pogress to radial growth phase (RGP) melanoma, typically characterized by a lateral growth pattern confined to the epidermis. During RGP, the cells acquire invasive traits and progress to the last step, the vertical growth phase (VGP). During the vertical growth phase expansive nodules of malignant cells penetrate the basement membrane and start to invade the underlying dermal tissue and surrounding vasculature [108] (Figure 14).

Tumor-Node-Metastasis (TNM) staging

This well documented sequential pattern of disease progression has been implemented into the clinical routine to define treatment and estimate prognosis. Staging of cutaneous melanoma follows the American Joint Committee on Cancer (AJCC) tumor-node-metastasis (TNM) classification [111]. The keystones of these guidelines are the primary tumor thickness (T), the number of infiltrated regional lymphatic nodes (N), and detectable distant metastatic lesions (M). Further sub-classification include non-ulcerated (a) and ulcerated tumors (b), size of nodal metastases, location of distant metastases, and elevated serum lactate-dehydrogenase (LDH) levels (Figure 15a). Based on these criteria patients are separated into 4 groups with decreasing survival estimates [111] (Figure 15b,c).

The main treatment for melanoma is surgical resection of the primary tumor with an increasing margin of surrounding skin depending on the tumor thickness. While this approach proves effective for patients with small localized tumors, the options for the treatment of metastatic disease are limited. As traditional cytotoxic chemotherapeutics have not proved effective [112], the main

a TNM staging categories

Classification	Thickness (mm)	Ulceration Status/Mitoses
T		
Tis	NA	NA
T1	≤ 1.00	a: Without ulceration and mitosis < 1/mm^2 b: With ulceration or mitoses ≥ 1/mm^2
T2	1.01-2.00	a: Without ulceration b: With ulceration
T3	2.01-4.00	a: Without ulceration b: With ulceration
T4	> 4.00	a: Without ulceration b: With ulceration
N	No. of Metastatic Nodes	Nodal Metastatic Burden
N0	0	NA
N1	1	a: Micrometastasis* b: Macrometastasis†
N2	2-3	a: Micrometastasis* b: Macrometastasis† c: In transit metastases/satellites without metastatic nodes
N3	4+ metastatic nodes, or matted nodes, or in transit metastases/satellites with metastatic nodes	
M	Site	Serum LDH
M0	No distant metastases	NA
M1a	Distant skin, subcutaneous, or nodal metastases	Normal
M1b	Lung metastases	Normal
M1c	All other visceral metastases	Normal
	Any distant metastasis	Elevated

b Anatomic stage grouping

	Clinical Staging*				Pathologic Staging†		
	T	N	M		T	N	M
0	Tis	N0	M0	0	Tis	N0	M0
IA	T1a	N0	M0	IA	T1a	N0	M0
IB	T1b	N0	M0	IB	T1b	N0	M0
	T2a	N0	M0		T2a	N0	M0
IIA	T2b	N0	M0	IIA	T2b	N0	M0
	T3a	N0	M0		T3a	N0	M0
IIB	T3b	N0	M0	IIB	T3b	N0	M0
	T4a	N0	M0		T4a	N0	M0
IIC	T4b	N0	M0	IIC	T4b	N0	M0
III	Any T	N > N0	M0	IIIA	T1-4a	N1a	M0
					T1-4a	N2a	M0
				IIIB	T1-4b	N1a	M0
					T1-4b	N2a	M0
					T1-4a	N1b	M0
					T1-4a	N2b	M0
					T1-4a	N2c	M0
				IIIC	T1-4b	N1b	M0
					T1-4b	N2b	M0
					T1-4b	N2c	M0
					Any T	N3	M0
IV	Any T	Any N	M1	IV	Any T	Any N	M1

c

	5-year survival	10-year survival
Stage I (primary tumour ≤ 1mm)	93%	85%
Stage II (primary tumour >1mm)	68%	55%
Stage III (regional node metastasis)	45%	36%
Stage IV (systemic metastasis)	11%	6%

Figure 15. Melanoma staging. (**a**) TNM staging categories according to the American Joint Committee on Cancer (AJCC). (**b**) Based on the TNM staging patients are subdivided into the stages I-IV. (**c**) Survival estimate in relation to the anatomic staging [111].

adjuvant therapies are high dose of Interferon-α for stage III and Interleukin-2 treatment for Stage IV disease, both of which have shown limited efficacy in clinical trials [112]. This lack of effective treatment has to be considered the main reason for the poor prognosis for patients facing metastatic disease (Figure 15c). Thus, in order to improve patient survival, new treatment strategies based on a better understanding of the mechanisms underlying melanoma progression are needed.

Melanoma initiation

Skin-color and melanoma susceptibility

The body's main defensive measure against ultraviolet radiation is the tanning response. Induced by signaling from α-melanocyte-stimulating hormone (α-MSH) binding its receptor, the melanocortin receptor 1 (MC1R), ultraviolet light triggers the expression of the microphthalmia-associated transcription factor (MITF). MITF in turn induces pigmentation by transcriptionally activating the genes underlying melanin synthesis: tyrosinase-related protein 1 (TRP1) and dopachrome tautomerase (DCT) [113]. The subsequent transfer of melanin to keratinocytes protects the skin from sun induces damages by absorbing and dissipating ultraviolet energy [108]. Interestingly, reflecting their increased melanoma susceptibility [114], light-skinned and redheaded people often carry a germ-line polymorphisms reducing the activity of MC1R [115].

Genetic events underlying melanoma genesis

While detrimental alterations of the sun protective system might facilitate melanoma development, they do not constitute the underlying events driving neoplastic transformation. The most prominent pathway mutated in melanoma is the mitogen-activated protein kinase (MAPK) signaling pathway, the main function of which is to relay cell-cycle progression and proliferation signals of numerous growth factor receptors. Activating mutations can be conferred by either a leucine or lysine for glutamine substitution at position 61 (Q61L/K) in N-Ras [116] or a glutamic acid for valine substitution at position 600 (V600E) in B-Raf [117] (Figure 16a). With a penetrance of over 70%, constitutive activation of the MAPK pathway represents the most frequent somatic mutation in melanoma and is considered a crucial event in the neo-

plastic transformation of melanocytes. However, based on the high frequency of B-Raf mutations also in benign and dysplastic nevi [118], it has been suggested that mutational activation of the MAPK pathway is a prerequisite, but in itself not sufficient for melanoma initiation. The reason for this has been mostly attributed to the effect of oncogene-induced cell senescence [119], a protective mechanism active in melanocytes, which prevents the progression of nevi to cancer [119].

Thus, in order to accomplish full malignancy additional cooperating genetic events need to be introduced on top of the MAPK pathway [121, 122]. The first potential candidate was identified by linkage-analysis studies of families with a high incidence of melanoma. These studies revealed a high prevalence of germline mutations in the CDKN2A locus in these families [123]. Located on chromosome 9p21, CDKN2A encodes two distinct tumor-suppressor proteins involved in the regulation of the cell cycle, INK4A (also p16) and ARF (also p14 or p19 in mice) (Figure 16b). INK4A blocks the transition of the cell cycle from G1 to S phase by inhibiting CDK4/6. In this function it is considered a main regulatory element suppressing the proliferation of cells with damaged DNA or activated oncogenes [120, 113] (Figure 16c). The second splice variant of the CDKN2A locus, ARF, participates in the core regulatory function controlling p53 levels. By inhibiting MDM2-mediated ubiquitylation and degradation of p53, it stabilizes and enhances intra-cellular p53 levels. In response to a damaged genome, this accumulation of p53 triggers cell cycle arres, which allows for subsequent DNA damage repair or the induction of apoptosis [120, 113, 108] (Figure 16c).
Based on this cell-cycle regulatory function of the CDKN2A locus products, it was proposed that the escape from growth inhibition in response to over-

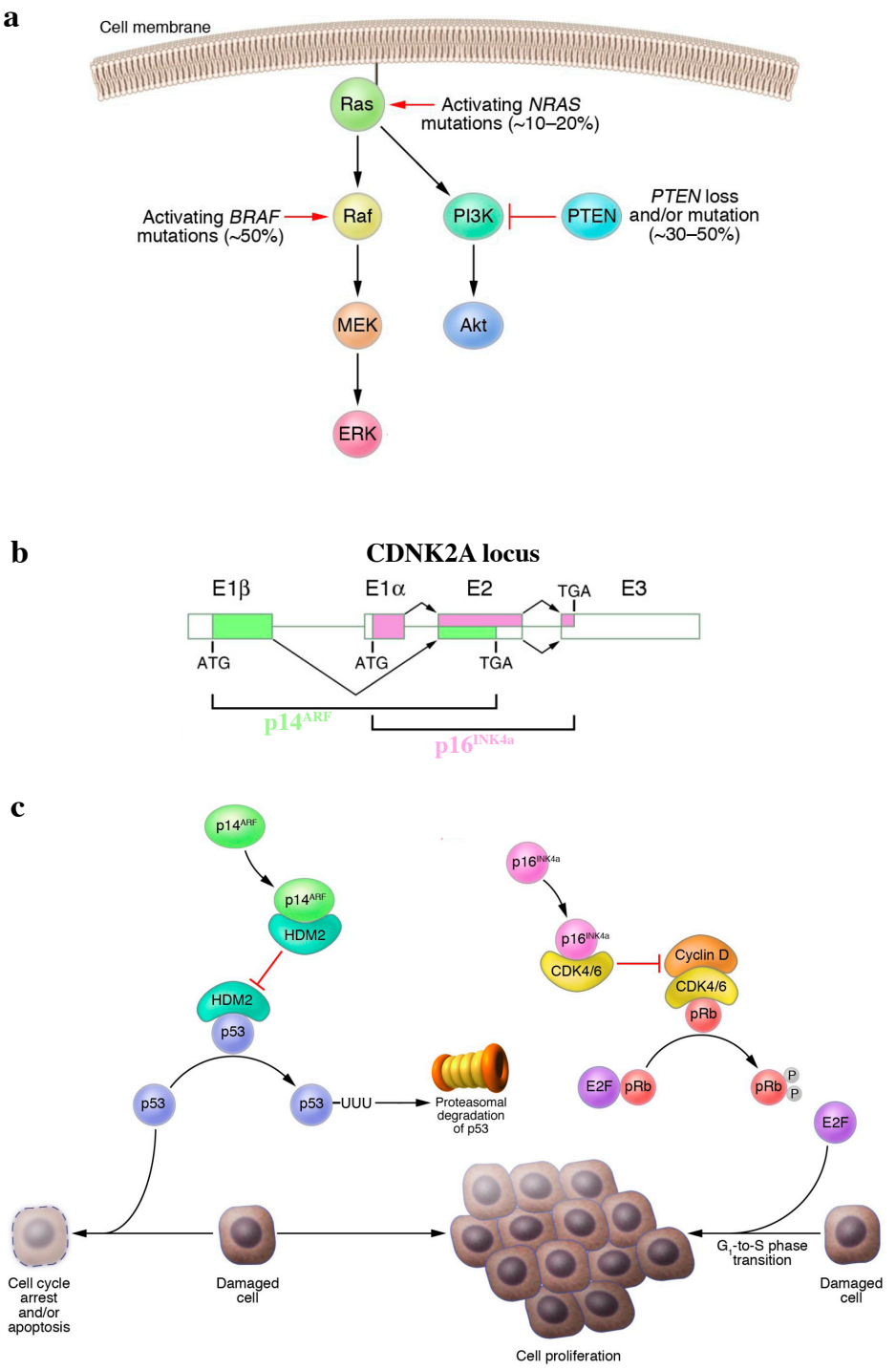
a
Cell membrane
Ras
Activating NRAS mutations (~10–20%)
Activating BRAF mutations (~50%)
Raf
PI3K
PTEN
PTEN loss and/or mutation (~30–50%)
MEK
Akt
ERK
b
CDNK2A locus
E1β
E1α
E2
TGA
E3
ATG
ATG
TGA
p14ARF
p16INK4a
c
p14ARF
p14ARF
HDM2
HDM2
p53
p53
p53
UUU
Proteasomal degradation of p53
p16INK4a
p16INK4a
CDK4/6
Cyclin D
CDK4/6
pRb
E2F
pRb
pRb
P
P
E2F
Cell cycle arrest and/or apoptosis
Damaged cell
Cell proliferation
G1-to-S phase transition
Damaged cell

Figure 16

Caption Figure 16. Key pathways driving the neoplastic transformation of melanocytes. (**a**) The most prominent pathway mutated in melanoma is the MAPK pathway. Constitutive activation is mostly achieved by either an activating N-Ras of B-Raf mutation. Another frequently found mutation inactivates the phosphatase PTEN leading to augmented AKT signaling (**b**) Based on alternative splicing the CDKN2A locus on chromosome 9p21 encodes two tumor-suppressor proteins, INK4A and ARF. (**c**) Both splicing variants are involved in the regulation of cell cycle progression [120].

active MAPK signaling could be achieved by deregulating cell cycle control mechanism. Validating this hypothesis, the functional relationship between enhanced proliferation and loss of cell cycle control in melanoma pathogenesis has been demonstrated in a variety of studies. In several genetic mouse models constitutive active MAPK signaling in conjunction with loss of either INK4A or ARF activity has been shown to induce melanoma growth [124]. Furthermore, in human melanocytes the expression of B-Raf^{V600E} was found to induce cell senescence by upregulating INK4A [119], while loss of INK4A or ARF in combination with activated N-Ras or B-Raf resulted in the development of invasive melanoma [125].

However, mutations of CDKN2A occur in only a portion of familial and sporadic melanoma. A second homozygous deletion frequently found in melanoma relates to the PTEN locus on chromosome 10 [126]. Phosphatase and tensin homolog deleted from chromosome ten (PTEN) encodes a tumor suppressor phosphatase, which attenuates signaling from a variety of growth factor receptors depending on phosphatidylinositol phosphate (PIP_3) as a docking site for downstream effector proteins. In response to a stimulus, the phosphorylation of PIP_2 to PIP_3 activate the protein kinase B (PBK or Akt), which in turn acts as a master regulator promoting proliferation and survival. Counteract-

ing these growth and survival effects, PTEN blocks the activation of Akt by dephosphorlyating PIP_3 (Figure 16a). Loss of PTEN function, therefore, leads to an enhanced survival and proliferation potential of transformed cells and, in conjunction with activated B-Raf^{V600E}, has been shown to induce metastatic melanoma in genetic mouse models [127].

Targeting B-raf and N-ras with specific inhibitors

Given the high penetrance of B-Raf and N-Ras mutations in melanoma, great hopes for therapy lie in specifically targeting these mutant proteins. Based on the failure of unspecific N-Ras and B-Raf inhibitors in clinical phase II trails [128], novel inhibitors specifically targeting the most common mutations in N-Ras and B-Raf are currently developed. The most promising candidate is Zelboraf ®(vemurafenib), a drug designed to specifically block the activity of mutant B-Raf^{V600E}. It has recently been granted market approval by the american Food and Drug Administration (FDA) based on its encouraging results in patients with metastatic melanoma carrying a B-Raf^{V600E} mutation [112, 129].

However, despite these promising results, there remains a fundamental discrepancy between a transient clinical remission and stable cure. Based on some cases showing relapse, a recent study confirmed that melanoma cells can acquire resistance to B-Raf^{V600E} inhibition by up-regulating Receptor Tyrosine Kinases or N-Ras activity [130]. Thus, a major focus in melanoma research has to remain the elimination of all residual disease. At present, however, there is a discordance on how this should be achieved best. While melanoma stem cells (MSC) offer the best explanation for the therapy resistance of melanoma, their existence has been questioned by several conflicting reports [70].

Melanoma stem cells

The eclectic nature of MSCs

While the cancer stem cell model has been accepted for several solid tumors [131], the data regarding the nature and existence of MSCs is contradictory [70]. Following the identification of MSCs based on the heterogeneous expression of a variety of cell surface proteins including CD20 [132], CD133 [133], MDR1 [134], and ABCB5 [135], two seminal studies performed in Sean Morrison's lab gave reason to challenge the entire cancer stem cell paradigm [50, 49]. This relates to the fact that the frequency of human melanoma initiating cells originally was anticipated to be very low (0.0001%) [135, 49]. However, traditionally all these studies haven been performed in NOD/SCID recipient mice, which have impaired T and B cell lymphocyte development but retain natural killer (NK) cell activity. Based on the observation that normal hematopoietic cells engraft more efficiently in NOD/SCID mice also lacking NK cells, NOD/SCID/IL2rγ^{null} (NSG) mice, these two studies showed that also the engraftment efficiency of human melanoma cells was contingent on the residual immuno-competency of the employed recipient animals [50, 49]. Showing a tumor initiating capacity of up to 1 in 4 cells in NSG mice, these studies called the dogma of a rare population of tumor initiating cells in melanoma into question. Furthermore, no correlation between tumor initiating capacity and expression of the previously published MSC markers could be established, which raised the possibility that all the previous findings might be artefacts of their respective model systems.

A developmental approach

These contradictory findings started a debate on the relevance of the model systems and technical procedures used to identify MSCs, which has not been resolved yet [48]. However, considering that a CSC is not only defined by its ability to initiate *de-novo* tumor growth, but also by its potential to self-renew *in-vivo* and re-establish the cellular composition of its parental tumor [36] (Figure 7b), assessing the tumor induction capacity as the only measure of a putative CSC is not entirely accurate. Taking into account that the definition of CSCs was originally inspired by a frequent intra-tumoral heterogeneity, a fundamental property of a CSC has to include the ability to phenotypically recapitulate its original patient tumor. Addressing this issue, a recent study compared melanoma xenografts in NOD/SCID and NSG mice with respect to their cellular composition [51]. Based on the assumption that a putative MSC resembles a neural crest stem cell, from which the melanocytic lineage originates during embryonic development (Figure 13a), all parental tumors and derived xenografts were assessed for their expression of neural crest related markers [51] (Figure 13c). Intriguingly, analysis of 19 independent patient metastases revealed a stable expression pattern for various neural crest derivatives as well as the NCSC marker CD271 and Sox10 [136, 137]. Providing the experimental basis, this robust pattern of cellular heterogeneity was used to analyzed potential differences in xenografts propagated in either NOD/SCID or NSG recipient mice. Strikingly, whereas xenografts growing in NOD/SCID mice faithfully recapitulated the cellular heterogeneity of their respective patient tumors, xenografts arising in NSG mice revealed discrepancies in their phenotypical composition. Based on these findings, the influence of the employed host animals on a putative MSC population was assessed. To this end

human melanoma cells were separated on the basis of CD271 expression, a controversially discussed MSC marker [107, 50, 49]. Following subcutaneous injection into either NOD/SCID or NSG mice the tumor induction capacity, the self-renewal capacity *in-vivo*, and the cellular composition of the resulting xenografts induced by $CD271^{Pos}$ and $CD271^{Neg}$ melanoma cells were analyzed. Interestingly, in line with previous findings [50, 49] NSG mice provided a host environment permissive for tumor induction independent of CD271 expression. But strikingly, the resulting xenografts lacked the ability to self-renew and faithfully recapitulate the cellular heterogeneity of their parental tumors [51]. In contrast, using NOD/SCID mice, $CD271^{Pos}$ melanoma cells showed all attributes expected of a MSC such as exclusive tumor induction potential, self-renewal capacity *in-vivo*, and the ability to recapitulate their parental tumors [51]. Taken together with an independent study corroboration the highly increased tumorigenic potential of $CD271^{Pos}$ melanoma cells [107], it appears likely that melanoma cells positive for CD271, nevertheless, represent a genuine MSC population.

Melanoma metastasis

Using microarray technologies to study melanoma metastasis

Facing extremely poor prognosis, metastatic disease is the most fearsome aspect for patients diagnosed with melanoma (Figure 15c) [111]. Thus, great hope for a better understanding of the pathways underlying melanoma progression has been placed in the rapidly advancing microarray technologies. However, although several comparative analyses of human nevi, VGP, RGP and metastatic melanoma samples have revealed a multitude of differentially

regulated genes involved in cell-cycle control, cell-cell and cell-matrix interactions, cytoskeletal organization, and cell surface receptor signaling pathways [138], they all have failed in producing reliable results with respect to future treatment [139, 140, 141, 142, 139, 143, 144] (see also section 'Technical considerations studying metastasis'). Therefore, in order to improve our understanding of the mechanisms rendering melanoma one of the most aggressive forms of cancer, new approaches need to be established.

Metastatic propensity

In principle two distinct molecular mechanisms could explain the proclivity of melanoma to metastasize. First, a strong genetic instability could render melanoma cells highly susceptible to alterations driving metastatic dissemination. Or second, melanoma cells could generally be equipped with an intrinsic predisposition to metastasize. Although both mechanisms appear equally feasible, it is the latter model that offers the more promising concept. This follows from the developmental origin of the melanocytic lineage. As a progeny of highly migratory neural crest stem cells (Figure 13a), the implication would be that elements of the molecular neural crest migratory circuit could be re-activated during melanoma progression. Taken together with the recent identification of MSCs showing NCSC-like features [107, 51], the possibility that melanoma progression indeed reflects its developmental origin appears feasible. This is further supported by several studies associating the MSC-marker CD271 with enhanced invasion and metastasis [145, 146, 147, 148, 149, 107, 51]. However, among these studies only one directly correlated MSCs to metastatic disease. In this study, using human tissue microarrays, the frequency of CD271/Sox10-positive MSCs in primary tumors was found to be inversely related to survival

[51] (Figure 17).

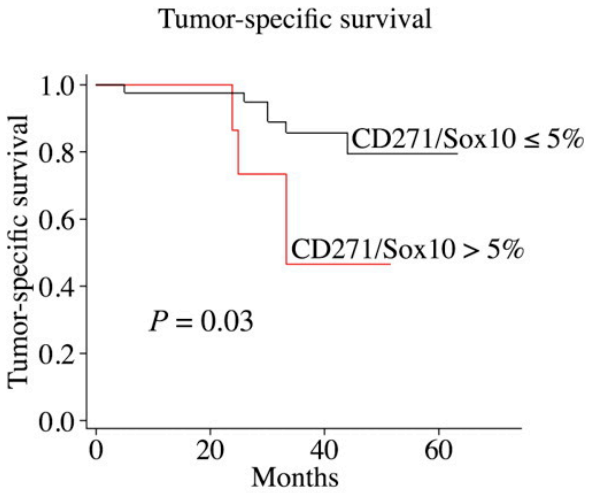

Figure 17. The effect of melanoma stem cells on survival. The frequency of MSCs expressing CD271/Sox10 correlates with metastatic potential and, consequently, decreased survival in patients [51].

The embryonic neural crest and melanoma metastasis

Neural crest EMT and melanoma metastasis

Given the robust, neural crest associated phenotypical heterogeneity identified in several primary patient tumors as well as metastases [51], these findings are difficult to reconcile with the idea of stochastic genetic alterations driving melanoma metastasis. It rather points towards a directed process, which involves stringent cellular programs that are able to induce a consistent morphological phenotype across a wide variety of patients. Intriguingly, the most prominent candidate for such an underlying program is, yet again, conceptually derived from embryonic neural crest development. As such, key processes of metastasis formation are reminiscent of neural crest EMT, which governs the delamination of neural crest cells from the neural tube. Upon EMT, neural crest cells adopt a remarkable migratory capacity, which allows the cells to disseminate

throughout the embryonic tissue and to colonize even distant sites, where they differentiate into specialized cells types. Based on the striking similarities to the metastatic process, it has been suggested that the aggressive nature of melanoma reflects the ability to recapitulate elements of the molecular network underlying neural crest EMT [150, 151]. With respect to the circumstantial evidence suggesting a hierarchical organization of melanoma, this could imply that the strong propensity to metastasize is a consequence of few 'metastatic' MSCs able to exploit inherent developmental signaling cues. However, whether in this scenario the ability to undergo EMT is an exclusive trait inherent to a putative MSC fraction or a causative factor inducing stem cell behavior in response to microenvironmental cues remains to be addressed (for detailed discussion see section 'Tumor cell plasticity and epigenetic stability').

The induction of the neural crest EMT

Considering the potential implication of neural crest EMT pathways underlying melanoma metastasis, novel insights might be gained by considering the role of known EMT pathways in the context of melanoma progression (Figure 18). The induction of EMT in neural crest cells is controlled by BMP4, which activates the canonical Wnt pathway leading to Cyclin D1 expression, G1/S transition, and neural crest delamination [152]. The onset of neural crest specification and migration is controlled by a gradient of the BMP inhibitor Noggin, which has also been shown to block invasive growth of a murine melanoma cell line upon transplantation into the optic cup of a chick embryo [153]. Consistent with these findings, BMP4 and BMP7 were shown to be overexpressed in primary metastatic melanoma [154]. Interestingly, inhibition of BMP 4 and 7 resulted in reduced in vitro invasiveness suggesting that a tumor microenvironment mimicking the dorsal neural tube might drive tumor

cell dissemination by inducing EMT. Furthermore, Wnt signaling, a key regulator of development and cancer [155] links the BMP/Noggin signaling axis to regulation of another group of crucial EMT regulatory elements: the calcium-dependent intercellular adhesion molecules of the cadherin super-family [156].

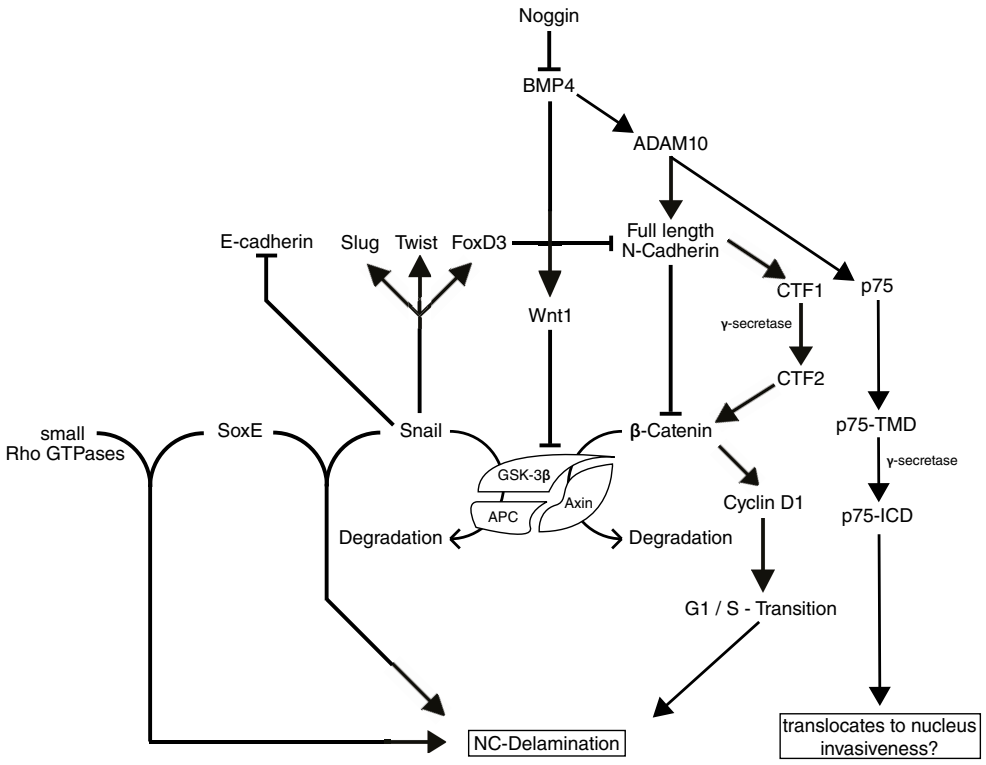

Figure 18. Neural crest EMT pathways. Known molecular pathways controlling the delamination of neural crest cells from the neural tube.

The role of N-Cadherin

One of the most important cadherin implicated in neural crest development is N-cadherin. Initially expressed in the entire neural tube, it is lost upon EMT of neural crest cells [157]. Interestingly, full length N-cadherin inhibits the onset of neural crest EMT by sequestering β-catenin and, thus, block-

ing Wnt signaling [158]. However, extracellular cleavage of N-Cadherin by the BMP4-activated metalloproteinase ADAM10 generates an intracellular C-terminal fragment (CTF1), which is further processed by a γ-secretase to yield the active signaling compound CTF2 [159]. This attributes a dual function to N-cadherin in promoting EMT: cleavage of the extracellular domain reduces cell-cell adhesion, while translocation of the resulting CTF2 to the nucleus stimulates cyclin D1 transcription and neural crest delamination [158]. Signaling elicited by CTF2 also leads to increased β-catenin expression, adding another level of complexity to the crosstalk between Wnt/β-catenin and N-cadherin signaling.

The role of E-Cadherin

Although not crucial for neural crest EMT, E-cadherin is considered the main determinant of progression in epithelial carcinomas [160]. Its expression is directly controlled by the zinc-finger transcription factor Snail, which itself is an important mediator of metastasis [161]. Interestingly, Snail is among the earliest markers observed in prospective neural crest cells upon induction by BMP4/Wnt [152]. Moreover, inherent β-catenin-like canonical motifs places it under the control of the Wnt dependent GSK-3β degradation pathway suggesting that stabilization of Snail, either through mutation in the degradation pathway or constitutively active Wnt signaling, might trigger disease progression [162]. Consistent with this idea, Snail was found to induce the neural crest markers Slug, Twist and Fox3D [163], all of which have been linked to neural crest EMT and migration [152] as well as melanoma progression [164, 139]. Finally, another Wnt-dependent pathway involving Wnt5A acting through Protein Kinase C rather than β-catenin has been associated with in-

creased Snail expression and melanoma cell motility [165].

The role of Snail and SoxE transcription factors

During embryonic neural crest development, Slug/Snail is able to induce EMT only in conjunction with a member of the SoxE transcription factor superfamily [166], pointing to a possible role of SoxE factors in driving tumor progression in melanoma, as shown for Sox9 in prostate cancer [167]. Similarly, SoxE transcription factors are able to induce neural crest delamination upon concomitant activation of small RhoGTPases, suggesting also alternative molecular pathways promoting neural crest EMT. In line with this hypothesis, the small RhoGTPases Cdc42 and Rac1 have been implicated in membrane protrusion formation associated with invasiveness of a human melanoma cell line [168].

The role of the low affinity neurotrophin receptor CD271

Although widely used as a marker for NCSCs, the functional role of of the low-affinity neurotrophin receptor CD271 (or P75NTR) is not well characterized. As a member of the tumor necrosis factor (TNF) receptor family, it has mainly been associated with mediating neuronal cell death. However, based on some idiosyncratic structural and behavioral features, CD271 is considered to have multiple functions [169]. As such it acts as a cooperative facilitator of TrkA signaling, the nerve growth factor (NGF) receptor. In conjunction with TrkA, CD271 builds a high affinity binding site for NGF [170], which has been implicated in regulating cell survival [170]. In addition, CD271 was shown to play a role in several cellular pathways regulating survival, apoptosis and axonal

outgrowth [171, 172, 173]. However, missing an active kinase domain, it is not entirely clear how CD271 affects these processes. While signaling has been suggested to occur largely through association with cytoplasmic adaptor proteins [172], CD271 has also been shown to undergo regulated intramembrane proteolysis [174]. During this process, similar to the N-Cadherin intracellular signaling pathway, the CD271 receptor is cleaved twice, first by ADAM10/17 and then by γ-secretase. This yields an intracellular signaling domain (p75-ICD), which is thought to directly regulate transcription [175, 174, 176]. Considering these versatile functions, it is not surprising that CD271 has been implicated in various human pathologies like Alzheimer, Schizophrenia, Asthma [170] as well as in melanoma brain-metastasis [177] and invasion [147, 178]. However, the exact functional contribution of CD271 to these various effects remains to be elucidated.

In sum, there is multiple evidence for common mechanisms underlying neural crest delamination and melanoma metastasis. However, to what extend MSCs and neural crest migratory pathways are involved in the metastatic process remains to be determined.

Model systems to study melanoma metastasis

Considering the multiple evidence for common mechanisms underlying neural crest delamination and melanoma metastasis, their experimental validation might yield novel insights into the mechanisms driving melanoma dissemination. However, to investigate the functional contribution of neural crest EMT pathways on melanoma progression, novel experimental model systems need to be established first. This is particularly relevant considering the crucial contributions of the microenvironment to the metastatic process [66, 70, 48](see

section 'Metastatic disease'). As a consequence, the development of fully humanized orthotopic systems has been deemed crucial, because such systems would allow the investigation of central processes of human melanoma formation in their original tissue context [70, 103, 53]. However, for melanoma this is technically challenging. Whereas orthotopic *in-vitro* model systems have emerged using organotypic skin reconstructs [179, 180, 181, 182, 183, 184], fully orthotopic, humanized *in-vivo* models are still missing. As such neither subcutaneous injection into immunocompromised mice [50, 49, 135] nor more recent advances, including intradermal injections into human foreskin grafts [107, 185] or skin reconstructs using human devitalized dermal substrate [125], provide the structural context equivalent to the site of human tumor formation. On the one hand, subcutaneous or intradermal injections, even into a human skin graft [107, 185], cannot recapitulate the important early steps of invasion from the epidermal compartment through the basement membrane into the dermis. On the other hand, the use of a de-vitalized dermal substrate [125] creates an unfavorable chimeric environment, as the graft gets populated with recipient fibroblasts rather than with human stromal cells [103, 186, 187, 188, 189]. Thus, in order to recapitulate human melanoma progression in a humanized environment *in-vivo*, entirely new approaches have to be developed.

Specific Aims

The overall aim of this thesis was to investigate the aggressive nature of melanoma with respect to its developmental origin, the neural crest. Along this line the goal was to establish a potential link between MSCs, known neural crest EMT signaling pathways, and the metastatic process. However, lacking an appropriate model systems to study melanoma progression in an autochthonous environment *in-vivo*, a humanized model system recapitulating all steps of melanoma progression had to be established first. Based on this dichotomous approach, the scope of this thesis comprised two major parts:

1. Development of a fully orthotopic, humanized *in-vivo* model for melanoma progression
2. Investigate the role of MSCs and neural crest EMT pathways in melanoma progression on the basis of the developed model

Part 1. In order to place human melanoma cells into their orthotpic environment at the dermis-epidermis boarder, we took advantage of recently established human dermo-epidermal skin substitutes. Upon transplantation onto the back of immuno-compromized rats, these substitutes mature into skin

grafts closely resembling the human skin architecture. Using this approach we explored the possibility to engineer melanoma progression in humanized skin grafts.

Part 2. By establishing standard flow-cytometric isolation protocols, different *in-vivo* models, retroviral over-expression and knock-down systems, as well as immunohistochemical analysis, this project established the experimental basis to address the role of MSCs and EMT pathways in melanoma progression.

Results

Published results

Engineering melanoma progression in a humanized environment *in-vivo*

Gregor Kiowski, Thomas Biedermann, Daniel S. Widmer, Gianluca Civenni, Charlotte Burger, Reinhard Dummer, Lukas Sommer & Ernst Reichmann

Author Contributions:
G.K and T.B contributed equally to this work. G.K. performed and designed research, analyzed data, and wrote the paper. T.B. performed research and analyzed data, D.S.W, G.C., and R.D. contributed vital reagents and assessed the histopathologies; G.C. and C.B. provided technical support, L.S. and E.R. designed research, analyzed data, and wrote the paper.

Melanoma development in engineered human skin substitutes

Aiming at the orthotopic positioning of human melanoma cells into an epidermal stratum basale of human origin, we took advantage of human dermo-epidermal skin substitutes [190, 191] (Figure 19). These substitutes were engineered from freshly isolated human keratinocytes that were plated onto high

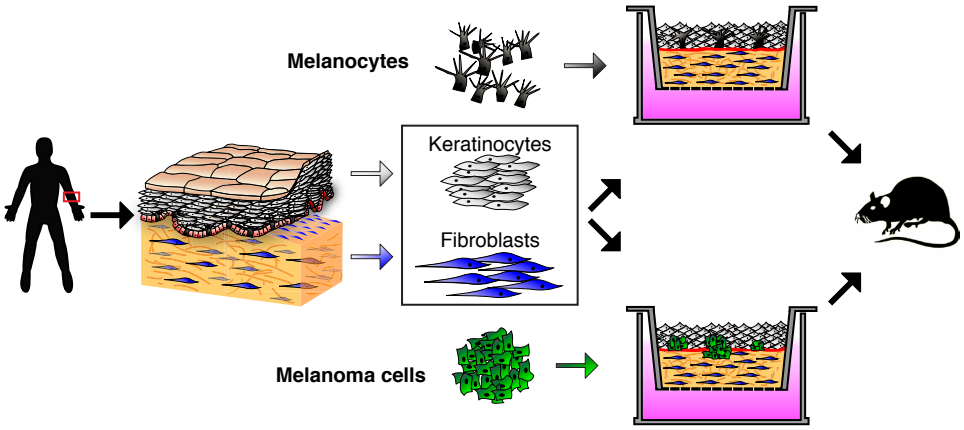

Figure 19. Experimental approach. Scheme illustrating the experimental approach using human organotypic skin substitutes as the basis for a humanized *in-vivo* melanoma model. The two main components, keratinocytes and dermal fibroblasts, are enzymatically isolated from human neonatal foreskin samples. A two step approach, during which the isolated keratinocytes are seeded onto high density type-I collagen hydrogels containing human dermal fibroblasts, allows the engineering of a human dermo-epidermal skin equivalent suitable for transplantation. Addition of human melanocytes or melanoma cells results in their orthotopic incorporation into the skin composites.

density type-I collagen hydrogels containing primary human dermal fibroblasts. In such composites, melanocytes have been shown to incorporate into their orthotopic location *in-vitro* [182]. To assess their incorporation *in-vivo* we transplanted dermo-epidermal skin substitutes into full thickness wounds on the back of immuno-compromized rats [190, 191] (Figure 20a), potentially allowing to create tumors with extensions closely representing those of patients' tumors. Using polypropylene rings to shelter the grafts from the surrounding rat skin prevented wound healing through recipient-derived cells and resulted in the maturation of the skin substitutes to a state macroscopically resembling human skin (Figure 20b). The epidermal compartment revealed normal stratification (Figure 20c) and a laminin-10 (Lam10)-positive basement membrane tightly anchoring the cytokeratin-10 (K10)-expressing epidermis to

the dermal compartment (Figure 20d). Staining of the skin grafts for the rat-specific endothelial marker CD31 (rCD31) revealed a fully vascularized dermal compartment indicating good acceptance of the graft (Figure 20e). The integrity of the humanized dermal compartment (Figure 20e, white dotted line), marked by the human fibroblast-specific antibody CD90 (Thy1) (hCD90), was maintained for at least 12 weeks, the latest time point analyzed. Moreover, Ki67-positive proliferating cells in the stratum basale, in conjunction with the expression of the wound-specific cytokeratin 16 (K16), indicated sustained homeostasis of the epidermal tissue (Figure 20f). Importantly, the addition of human melanocytes resulted in their recruitment to the stratum basale (Figure 20g) where they fully differentiated into dendritic pigment-producing melanocytes (Figure 20h).

Given the functional integration of melanocytes into their physiological surroundings, we sought to determine the behavior of human melanoma cells in this experimental set-up (for detailed information about all samples used, see Table S1). To this end, we replaced the melanocyte fraction with human melanoma cells expressing green fluorescent protein (GFP). Six weeks after transplantation multiple large tumors pushing through an otherwise well developed epidermis were observed (Figure 20i). Macroscopically, these tumors showed partial pigmentation (Figure 20i, black arrowhead) and a prominent vasculature that readily ruptured upon touching, leading to excessive bleeding (Figure 20i, white arrowhead). Macroscopic GFP expression confirmed that the tumors originated from the seeded melanoma cells (Figure 20j). Histological analyses further revealed large, densely growing, non-necrotic GFP-positive tumors, expressing the two commonly used melanoma markers MelanA and S100 (Figure 20k-n).

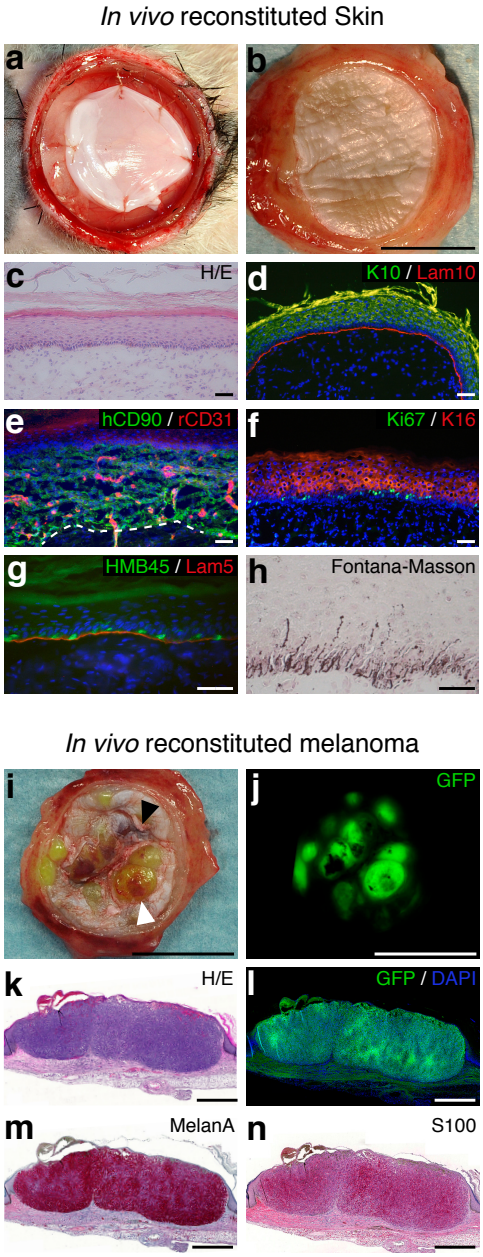

Figure 20. Transplantation of human skin substitutes containing either melanocytes or melanoma cells. Transplantation of a human dermo-epidermal skin substitute (**a**) drives its maturation within 3 weeks (**b**). Scale bar, 1cm. Analysis of the resulting skin by (**c**) H/E, (**d**) Lam10 and K10, (**e**) hCD90 and rCD31, and (**f**) Ki67 and K16 stainings reveals typical skin histology and sustained homeostasis. Scale bars, 50μm. (**g**) Addition of human melanocytes (HMB45) results in their orthotopic incorporation into the stratum basale contacting the underlying basement membrane (Lam5) *in-vivo*. (**h**) This leads to fully differentiated dendritic, pigment producing melanocytes (Fontana-Masson). Scale bars, 20μmm. (**i** and **j**) Replacing the melanocytes with GFP-expressing human melanoma cells (ID4286) results in ulcerated, bleeding (white arrowhead), partially pigmented (black arrowhead), GFP-expressing tumors. Scale bars, 1cm. (**k-n**) Analysis reveals a dense lesion uniformly expressing GFP, MelanA and S100. Scale bars, 1mm.

Engineering human melanoma progression *in-vivo*

To analyze the steps of melanoma progression, we added human GFP-expressing primary melanoma cells in the physiological ratio of melanocytes to keratinocytes into the skin substitutes. Following tumor development over 42 days *in-vivo* revealed the typical stages of melanoma progression (Figure 21a-c). At the day of transplantation, the tumor cells were already uniformly integrated into the thin epidermis (Figure 21a). Importantly, the in vitro generated skin substitute did not reveal any melanoma cells in the dermal compartment (Figure 21a). This was crucial to our model, as inclusion of tumor cells into the dermis would have compromised the experimental set-up, in which dermal tumor growth needs to be established as a part of disease progression. 28 days after transplantation, the graft was fully integrated and epidermal maturation became evident by the appearance of distinct keratinocyte layers (Figure 21b, middle panel). At this time point, the tumor cells had integrated into their natural surrounding in the basal layer of the epidermis, where the presence of melanomas in situ already marked the onset of radial, lentiginous tumor growth (Figure 21b, right panel). After 42 days, tumor cell nests had become vascularized (Figure 21c, arrowheads) and progressed to invasive tumors disintegrating the epidermis and penetrating the dermis (Figure 21c, middle and right panel). Histopathologically, the resulting reconstituted tumors showed strong resemblance to the original patient tumor from which the cells had been derived (Figure 21d,e). Although the reconstituted tumor was smaller at the time point analyzed, both lesions showed a similar nodular growth pattern featuring lentiginous nests, a similar overall cell morphology, epithelial spread of single cells (Figure 21d,e, insets 1) and dermal invasion (Figure 21d,e, insets 2). Strikingly, both parental and reconstituted tumors substantially interfer-

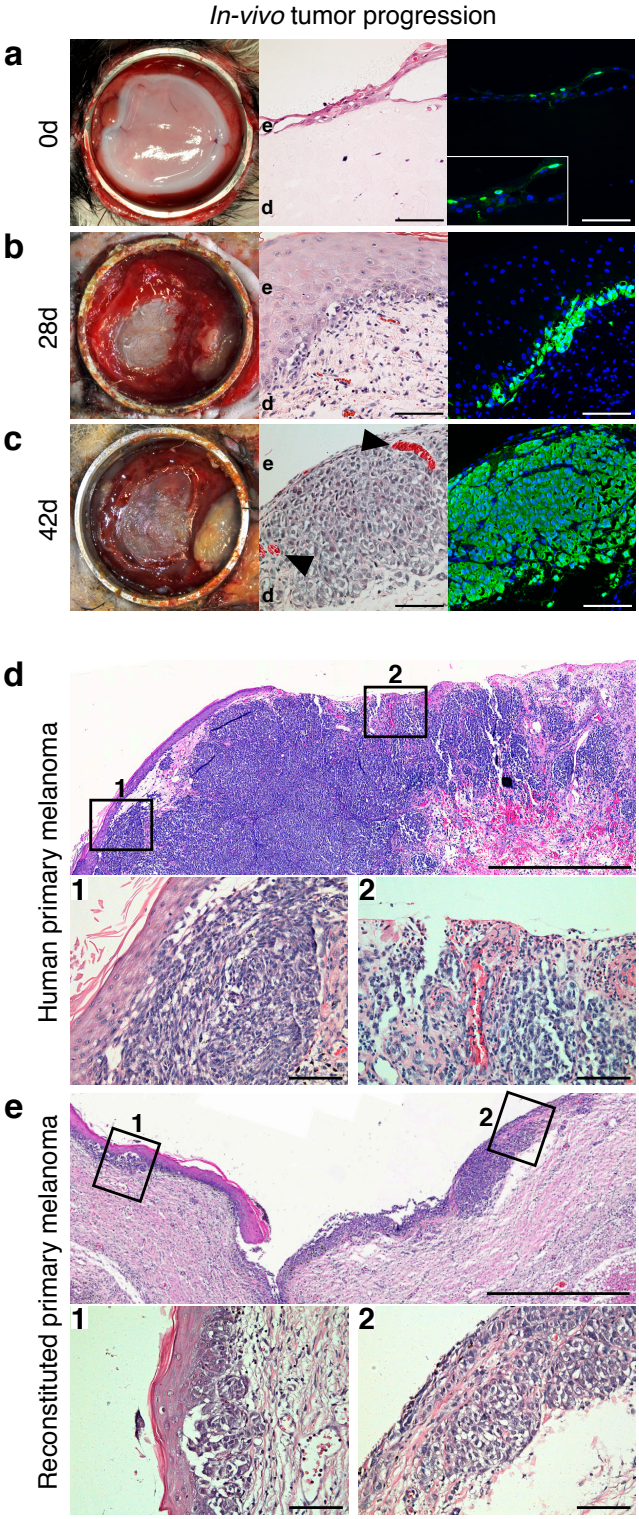
In-vivo tumor progression
a
0d
e
d
b
28d
e
d
c
42d
e
d
d
Human primary melanoma
1
2
1
2
e
Reconstituted primary melanoma
1
2
1
2

Figure 21

Caption Figure 21. Human melanoma induction and progression in engineered skin substitutes *in-vivo*. (**a-c**) Growth kinetics of GFP-expressing human primary melanoma cells (ID12741) upon transplantation. The left panels show the macroscopic maturation of the transplants while the middle and left panels show a magnified view of consecutive H/E and GFP stained transversal sections (e, epidermis; d, dermis). Scale bars, 100μm. (**d,e**) Histological comparison of the reconstituted tumor (ID12741) and the corresponding primary patient tumor (ID12741). Apart from the differences in size, both lesions show a similar nodular growth pattern featuring lentiginous nests and epithelial spread of single cells (insets 1), dermal invasion and ulceration (insets 2), vascularization and a similar overall cell morphology. Overview scale bars, 1mm, insets scale bars, 100μm.

ed with the epidermal integrity (Figure 21d and e), which presumably correlated with ulceration, a clinically significant prognostic feature [192]. These data demonstrate that reconstitution of a primary melanoma in a humanized environment not only recapitulates the onset of human disease *in-vivo*, but also gives rise to tumors histologically resembling their original human counterparts.

However, while primary melanoma biopsies are rarely accessible, a plethora of metastasis samples and cell lines are available for research. Therefore, we explored the potential of cells derived from human metastasis samples to assume primary tumor characteristics if exposed to the appropriate microenvironment. Intriguingly, metastasis-derived melanoma cells recapitulated the key events of early disease progression, indicating a remarkable context dependent plasticity [193, 71]. Strikingly, cells derived from an axillary skin metastasis not only adopted a progression pattern similar to transplanted primary melanoma cells, but were also found to recapitulate many histopathological characteristics of the primary patient tumor, from which the metastasis had originated (Figure 22a,b and Figure S1). Tumor growth started at the dermo-epidermal junction

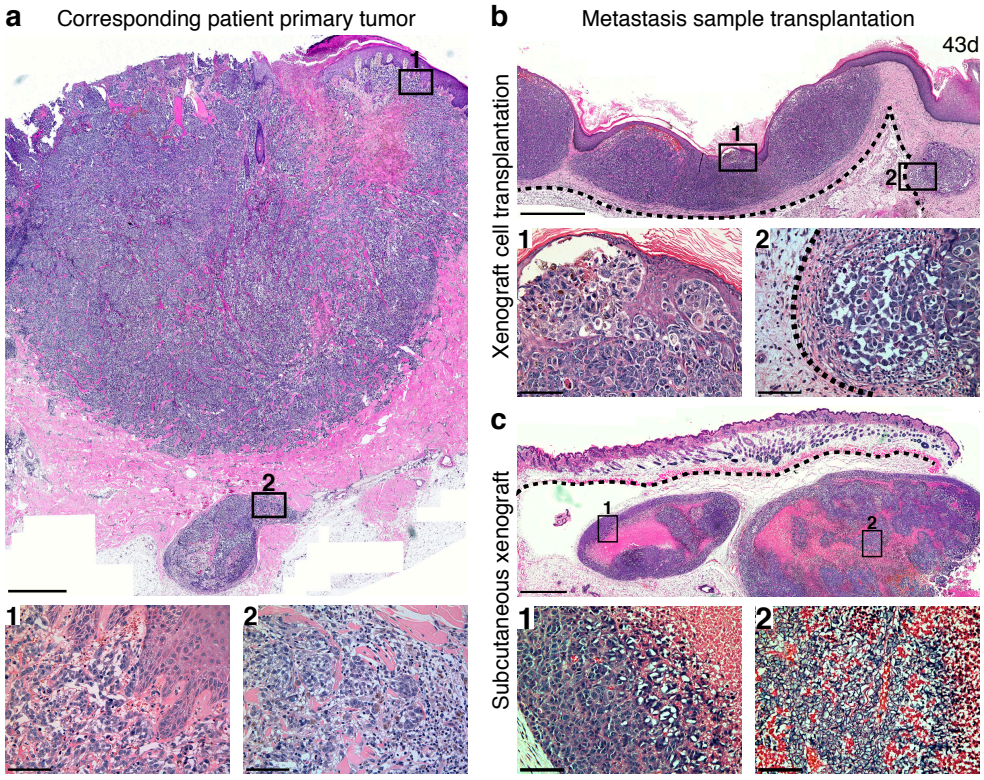

Figure 22. Reconstitution of a primary melanoma from an axillary skin metastasis sample. (**a**) Patient-matched primary tumor (ID11928) that gave rise to the metastasis used for reconstitution. (**b**) Tumor reconstituted from cells originally isolated from the corresponding axillary skin metastasis (ID4286). The resulting tumors show identical growth characteristics as the original primary tumor (insets). Note the barrier presented by the distinct human-rat tissue border (dotted lines) restricting tumor growth to the humanized dermal compartment. (**c**) Matched subcutaneous xenograft (ID4286) in a Swiss nude mouse. Subcutaneous inoculation results in highly necrotic (inset 1), encapsulated tumors growing in the subdermal fat tissue without epithelial involvement (inset 2). Dotted line, border between murine skin and subdermal fat tissue. Overview scale bars, 1mm, inset scale bars, 100μm.

giving rise to tumors mirroring the original tumor cell morphology, nodular growth pattern, ulceration, as well as dermal and epidermal invasion (Figure 22a,b, insets 1). Furthermore, 50% of all reconstituted tumors (6/12) derived from this axillary skin metastasis sample gave rise to satellite metastases in the

skin, similar to those found in the corresponding primary tumor (Figure 22a,b, insets 2 and Figure S1, inset 2). Intriguingly, these features were recapitulated irrespective of whether the cells had been maintained as xenografts in mice (Figure 22b) or as sphere cultures in vitro (Figure S1). Moreover, analysis of the most commonly used clinical melanoma markers S100, MelanA, HMB45, as well as the clinically relevant prognostic factor Ki67 [111] further confirmed the close resemblance between reconstituted tumors and their patient-matched counterparts (Figure S2). This showed that even melanoma cells isolated from metastases harbor the potential to recapitulate original primary tumor growth if placed in the appropriate tissue context.

Subcutaneous xenotransplantation into immunocompromized mice represents the most widely used method for the analysis of human melanoma formation [194, 103]. Therefore, we compared the histology of the reconstituted tumor (Figure 22b) to a matched subcutaneous xenograft (Figure 22c), revealing an advantageous effect of the humanized environment on tumor growth. Whereas the humanized model system (Figure 22b) allowed the generation of large, non-necrotic lesions closely resembling human melanoma histopathology (Figure 22a), subcutaneous inoculation resulted in highly necrotic tumors that lacked any epidermal involvement (Figure 22c and Figure S3). Despite the abundant vascularization (Figure S3d), higher magnification revealed only a small rim of healthy (Figure 22c, inset 1), proliferating (Figure S3e) cells on the periphery of the tumor facing necrotic areas inside the tumor (inset 2). This suggests that additional influences from the microenvironment are required to sustain tumor growth and progression independent of the vasculature. In addition, none of the reconstituted tumors (N=19 tumors derived from 3 different patient samples), including their occasionally arising dermal metastases, ever invaded the underlying rat tissue (Figure 22b and Figure S1,

dotted lines). Taken together, this indicates a favorable effect of the engineered human stroma on human melanoma cell growth and progression [187, 189], highlighting the paramount importance of a fully humanized environment in studying melanoma progression.

Vascularization and hypoxia in reconstituted melanoma

A crucial step during tumor progression and a promising target for drug development is neoangiogenesis. A key-parameter guiding this process is hypoxia resulting from the imbalance of oxygen supply and consumption in a growing tumor mass [195, 196]. To validate the potential use of reconstituted melanoma in studying neoangiogenesis, we immunohistochemically assessed vascularization and hypoxia in reconstituted skin and tumors. The dermal compartment of skin substitutes transplanted without melanoma cells displayed hypoxia and vascularization similar to the dermis of normal skin (Figure 23a,b, arrowheads). In contrast, in reconstituted melanoma samples, we observed a correlation between pronounced hypoxia and tumor vessel ingrowth (Figure 23c-e). GFP-tracking of melanoma cells revealed that tumor vessels were predominantly host derived (data not shown), in agreement with previous reports [51]. Both in an early stage patient sample and the reconstituted tumor after 25 days, blood vessel ingrowth was found along highly hypoxic regions (Figure 23c,d, arrowheads). This onset of hypoxia-guided blood vessel ingrowth most likely set the basis for the subsequent rapid progression to the highly vascularized, non-necrotic lesions observed after 42 days *in-vivo* (Figure 23e,f).

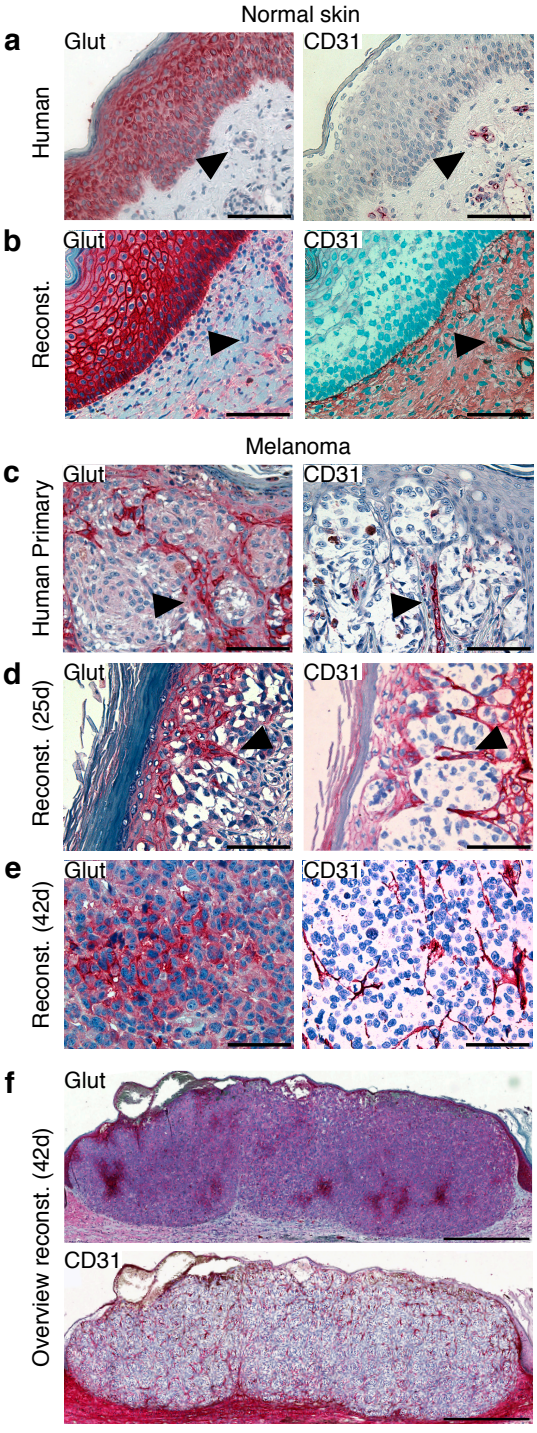
Normal skin
a
Glut
CD31
Human
b
Glut
CD31
Reconst.
Melanoma
c
Glut
CD31
Human Primary
d
Glut
CD31
Reconst. (25d)
e
Glut
CD31
Reconst. (42d)
f
Glut
CD31
Overview reconst. (42d)

Figure 23

Caption Figure 23. Vascularization and hypoxia in the reconstituted tumors. (**a,b**) Immunohistochemical analysis of vascularization (CD31) and the hypoxia-associated glucose transporter-1 (Glut) (arrowheads) in adjacent histological sections of human skin and reconstituted dermal epidermal skin substitute. (**c,d**) Comparison of an early stage patient sample (ID 16754) and a reconstituted tumor (ID 4286) after 25 days indicates blood vessel ingrowth along a highly hypoxic region (arrowheads). (**e**) After 42 days *in-vivo* the reconstituted tumors (ID 4286) are highly vascularized and contain only few small hypoxic regions. Scale bars, 100μm. (**f**) Overview over hypoxia and the intricate capillary network observed in the reconstituted tumor after 42 days *in-vivo*. Scale bars, 1mm.

Reconstituting the switch from radial to vertical growth in melanoma

As malignant disease remains the central challenge in melanoma therapy, we further investigated the potential of the system to faithfully recapitulate the early phases of human tumor progression. The first step towards malignant disease is the switch from radial to vertical tumor growth. Radial growth is restricted to the epidermal compartment, whereas vertical growth extends through the basement membrane into the dermis. Thus, we analyzed the functional integrity of the basement membrane in reconstituted tumors at different progression stages (Figure 24a). Starting with an intact, fully functional basement membrane, initial radial growth progressively reduced the underlying basement membrane until complete loss ensued.

A key-event driving this malignant progression is thought to be a process reminiscent of epithelial-to-mesenchymal transition (EMT) that is associated with the acquisition of an invasive, mesenchymal phenotype in epithelial tumor cells [96]. Although not an epithelial tumor, human melanoma express E-cadherin [197], the loss of which has been functionally implicated in EMT and tumor cell dissemination in some tumor types [96]. This makes E-cadherin an

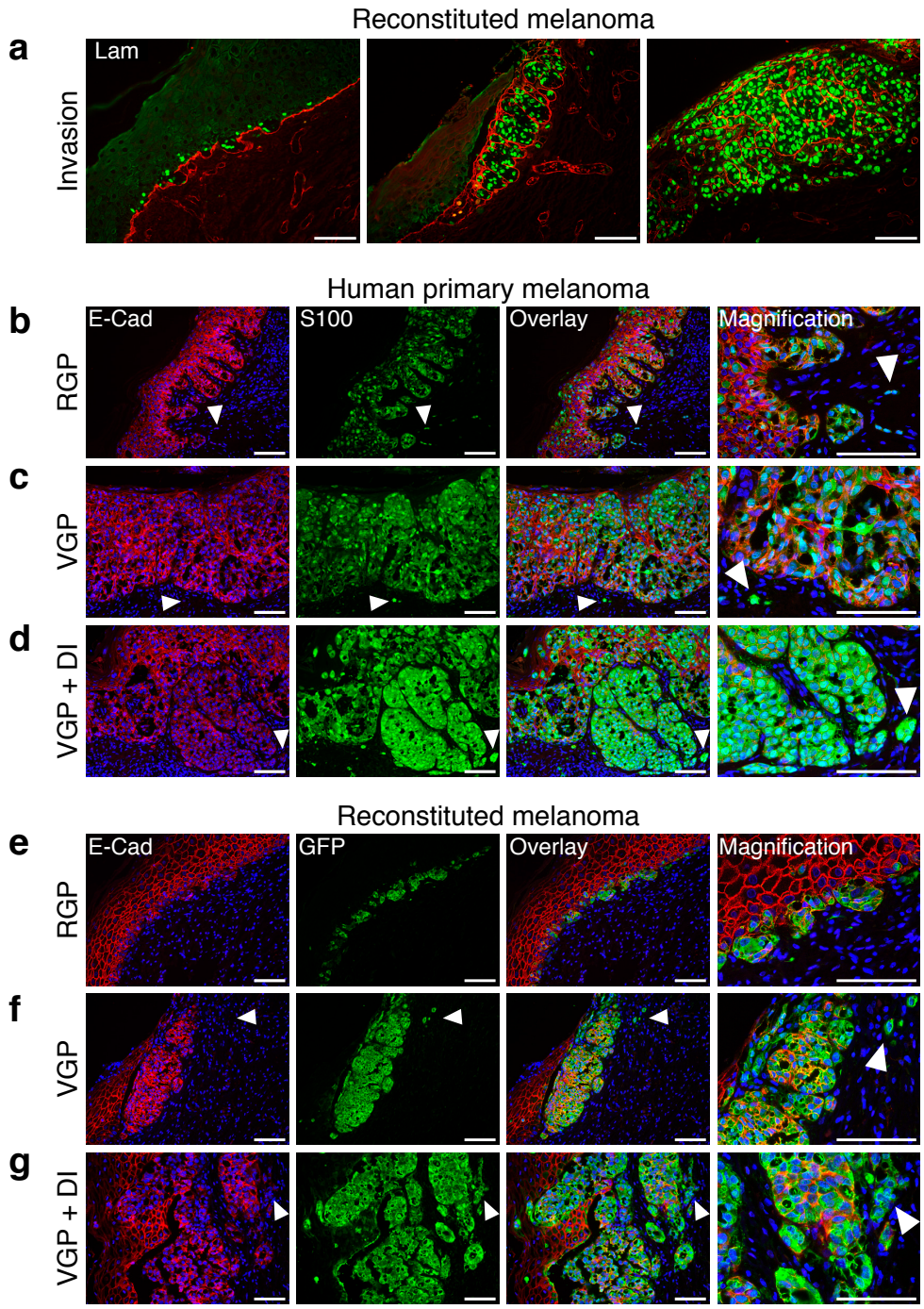
Reconstituted melanoma
a
Lam
Invasion
Human primary melanoma
b
E-Cad
S100
Overlay
Magnification
RGP
c
VGP
d
VGP + DI
Reconstituted melanoma
e
E-Cad
GFP
Overlay
Magnification
RGP
f
VGP
g
VGP + DI

Figure 24

Caption Figure 24. Reconstituting the switch from radial to vertical growth in melanoma. (**a**) Staining for the basement membrane marker Laminin-5 (Lam5) reveals successive degradation of the basement membrane in a reconstituted melanoma (ID12741). The final loss of the basement membrane marks the onset of vertical tumor growth. Scale bars, 100μm. (b-g) Comparison of E-cadherin (E-cad) expression in progressing stages of human primary (**b-d**) and reconstituted melanoma (**e-g**). (b) Radially growing human primary tumor (ID12826), (**c,d**) Vertically growing human primary tumor (ID16754) with and without dermal infiltrates (DI). (**e-g**) Corresponding stages of a reconstituted tumor using human primary melanoma cells (ID12741). Arrowheads indicate cells negative for E-cadherin without contact to their parental tumors. To visualize the tumor borders, the patient samples were counterstained with S100 and the reconstituted tumors with GFP (RGP, radial growth phase; VGP, vertical growth phase). Scale bars, 100μm

interesting candidate to investigate potential EMT-like processes underlying melanoma cell dissemination. Therefore, we compared the expression pattern of E-cadherin on histological samples of primary patient (N=4) and reconstituted melanoma (N=9 tumors derived from 3 different patient samples) (Figure 24b-g). During the early stages of tumor development (radial growth phase, RGP) none of the primary human tumors analyzed nor of the reconstituted tumors showed an overt downregulation of E-cadherin, which was strongly expressed in epidermal lesions extending from the epidermis (Figure 24b and e). Strikingly, E-cadherin expression was even retained in bigger lesions showing distinct vertical growth phase (VGP) characteristics (Figure 24c and f). In contrast, both in the reconstituted tumors and the patient samples, substantial downregulation of E-cadherin was only observed in dermal tumor cell infiltrates (DI) that had lost all contacts to the epidermis (Figure 24d and g). In addition, in 12 out of 13 samples analyzed (N=4 patient samples and 9 reconstituted tumors), E-cadherin-negative cells were observed that appeared to move away from the parental tumor (Figure 24b-g, arrowheads). Taken

together, our data show that even complex events like dermal invasion, the induction of neoangiogenesis, and early tumor cell dissemination were faithfully recapitulated using our humanized melanoma reconstitution approach.

Supplementary Figures

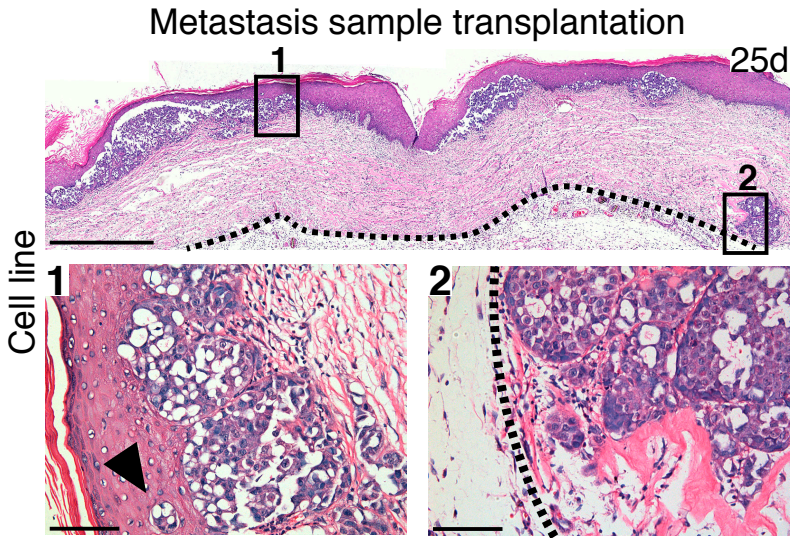

Figure S 1. Reconstitution of a melanoma from an axillary skin metastasis sample maintained as sphere culture. 25 days after transplantation of the sphere culture-derived cells (ID 4286), typical pathological features of aggressive melanoma start to be recapitulated. Mark tumor induction in the basal layer of the epidermis, dermal and epidermal invasion including pagetoid spread (inset 1, arrowhead) and a developing satellite metastasis (inset 2). Note the barrier presented by the distinct human-rat tissue border (dotted lines). Overview scale bars, 1mm, inset scale bars, 100μm.

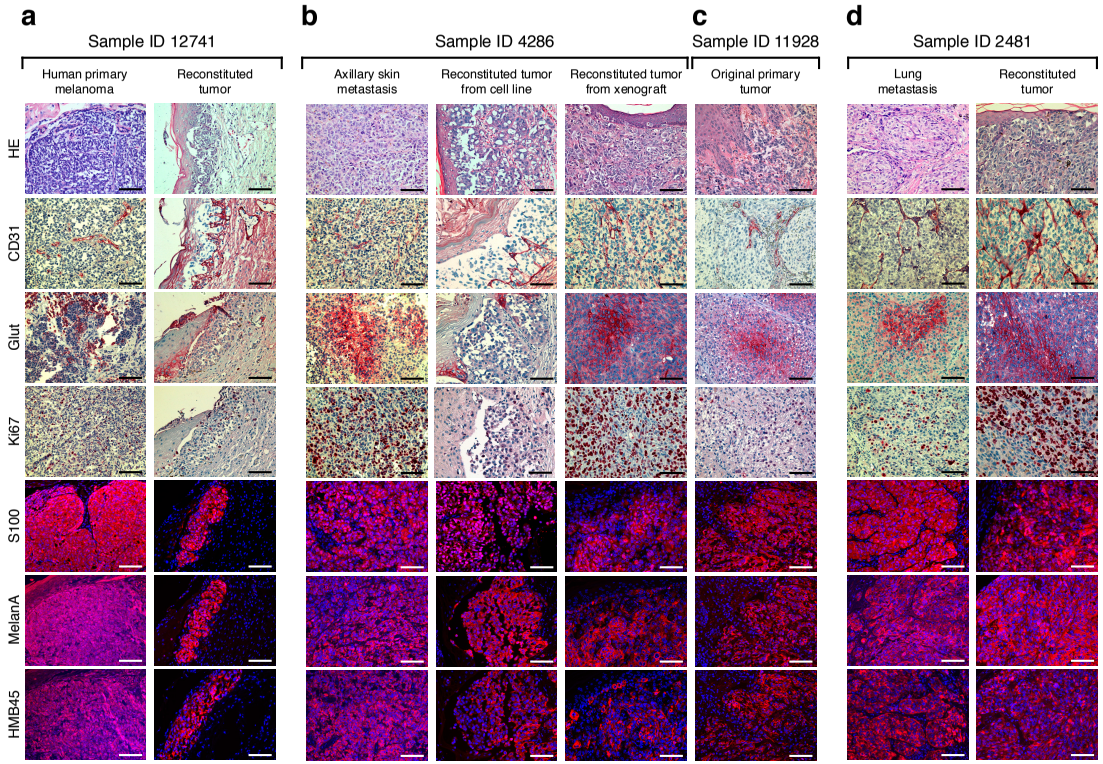

Figure S 2. Representative pictures of all tumors reconstituted during this study, including their matched patient material. (**a**) Reconstituted tumor resulting from transplantation of cells isolated from the shown human primary tumor. (**b**) Reconstituted tumors established from the depicted axillary skin metastasis maintained as cell line or xenograft. (**c**) Corresponding original primary tumor that gave rise to the axillary skin metastasis used for reconstitution. (**d**) Reconstituted tumor derived from a lung metastasis. For sample information see Supplementary Table 1. All scale bars, 100μm.

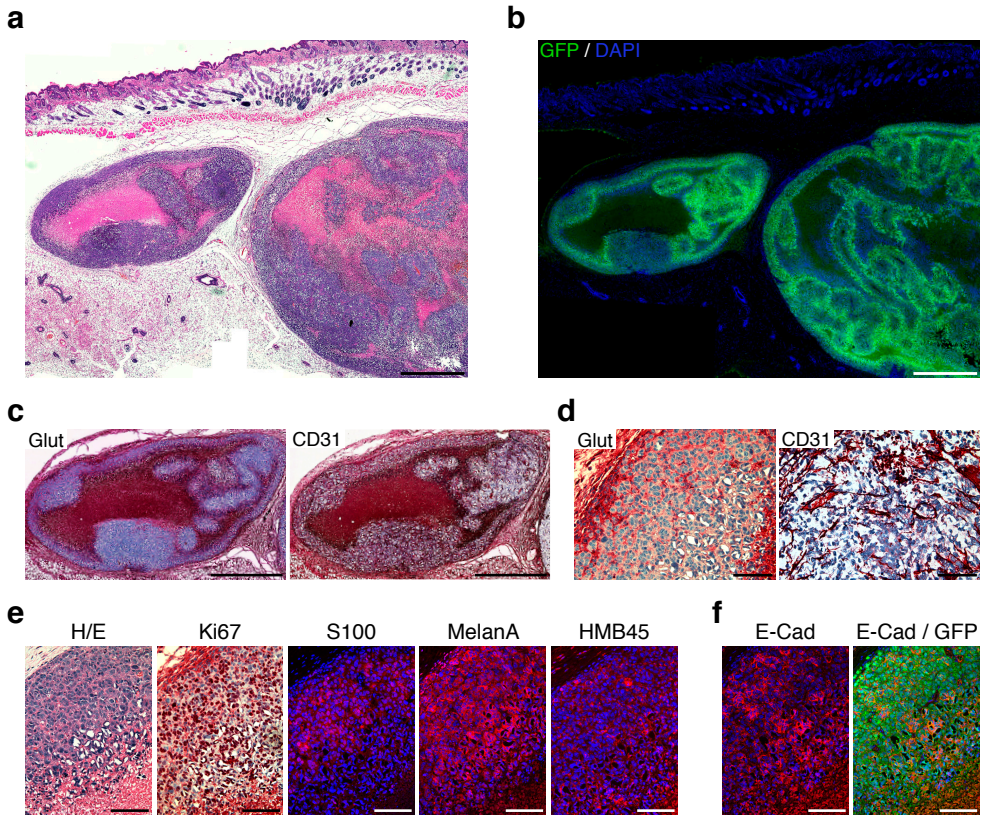

Figure S 3. Analysis of a human melanoma subcutaneous xenograft. (**a**) Tumor histology upon injection of the melanoma sample used in Figure 22 (ID4286) into the subcutaneous space of a Swiss nude mouse. (**b**) GFP expression confirms that the tumors originated from the injected cells. (**c**) Immunohistochemical analysis of the vasculature (CD31) and hypoxia (Glut). (**d**) Although generally highly vascularized, the magnified view reveals that the tumor cells are still subjected to highly hypoxic conditions. (**e**) Although histologically (H/E) not resembling a human primary melanoma, the expression of the most commonly used melanoma markers Ki67, S100, MelanA and HMB45 is retained (**f**) Double staining for E-cadherin and GFP shows overall strong E-cadherin expression. Scale bars a-c, 1mm. Other scale bars, 100μm.

Characteristics of melanoma samples used in this study

	Type	Sample ID	Gender/age, years	Primary tumor type	Breslow (mm)	Clark	TNM stage	Location	Used in figure
	Primary	12741	M/80	Non classifiable	6.0	V	T4bN2bM0	Upper right arm	Fig. 3d; Supple 2a
	Primary	12826	F/94	Non classifiable	Unknown	Unknown	T1bN0M0	Unknown	Fig. 6b
	Primary	16754	M/35	SSM	0.5	IV	T2aN0M0	Middle lower back	Fig. 5c; Fig. 6c,d
Matched Sample	Primary	11928	M/35	NMM	10.0	IV-V	T4bN3M0	Back skin	Fig. 4a; Suppl 2c
Matched Sample	Metastasis	4286	M/35	NMM	10.0	IV-V	pT4bN3M0	Skin axillary	Suppl 2b
	Metastasis	2481	F/63	Unknown	Unknown	Unknown	pTxN3M1c	Lung	Suppl 2d

Characteristics of melanoma samples used for reconstitution

Type	Sample ID	Tumors/Transpl.	Efficiency	Growth as melanomaspheres	Tumors/Transpl., melanomaspheres	Used in figure
Primary	12741	3 / 5	60%	yes	N.d.	Fig. 3a-c, e; Fig. 6a, e-g; Suppl 2a
Metastasis	4286	12 / 12	100%	yes	3 / 3	Fig. 2i-n; Fig. 4b; Fig. 5d-f; Suppl 1, 2b
Metastasis	2481	2 / 2	100%	yes	N.d.	Suppl 2d

Table S 1. Patient information and characteristics of the used human melanoma samples. Characteristics of all melanoma samples used in the study. The upper panel describes all biopsies used, the lower panel shows all samples employed in this study for reconstitution. The type (primary tumor or metastasis), patient's ID, age, gender, primary tumor type, Breslow thickness, Clark level, TNM (tumor-node-metastasis) stage, location, and transplantation efficiency are listed. NMM, nodular malignant melanoma; SSM, superficially spreading melanoma, Suppl., supplementary figure; N.d., Not done)

Additional results

The role of CD271 positive MSCs in tumor progression

CD271 expression *in vivo*

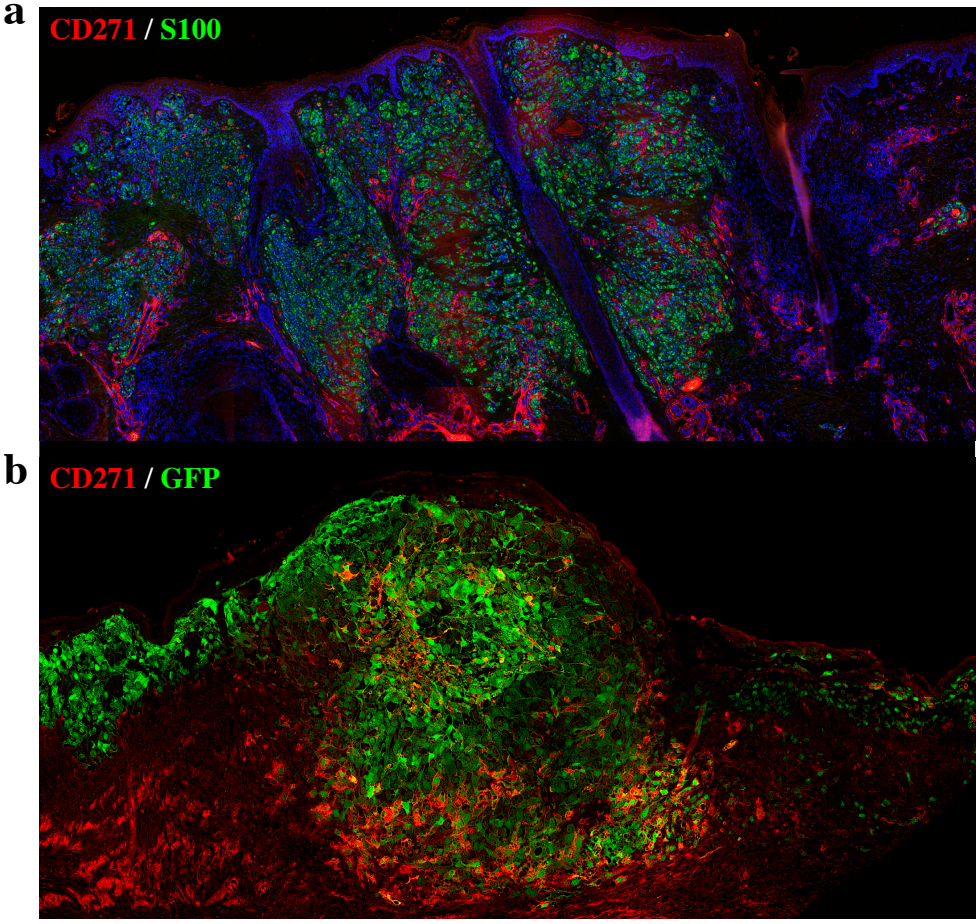

Figure 25. CD271 expression in a patient and reconstituted melanoma. (**a**) Overview over a human primary melanoma sample stained for CD271 and S100. Whereas only few tumor cells are positive for CD271, other cell types like nerves and glia cells strongly express CD271. (**b**) CD271 staining in a reconstituted melanoma. Based on the GFP expression all tumor cells can be easily identified. CD271 appears to be preferentially expressed at the invasive front.

Following its experimental validation, we took advantage our newly developed

model system to address the potential implication of CD271 positive neural crest-like MSCs [107, 51] in tumor progression. Comparison of the CD271 expression pattern between a human primary tumor and a reconstituted melanoma revealed the advantage of the system for functional analyses (Figure 25). Different from the patient sample (Figure 25a), all tumor cells in the reconstituted sample could be unequivocally visualized based on their expression of GFP (Figure 25b). The importance of this became clear following the immunohistochemical analysis of CD271 expression on a histological patient section (Figure 25a). Although counterstained with the melanoma marker S100, in some cases it was impossible to differentiate between tumor cells and other structures positive for CD271 like nerves, glia cells and potentially others. Taken together with the possibility that not all tumor cells necessarily express S100, this approach did not allow any conclusion with regard to the abundance and location of CD271 positive tumor cells in patient samples. In contrast, immunohistochemical analysis of a reconstituted tumor counterstained with GFP allowed a precise analysis of the CD271 expression pattern in all tumor cells, including single cells dispersed in the dermal compartment (Figure 25b). Based on this approach, CD271 expression was found to be preferentially located at the invasive front indicating a potential implication of neural crest-like melanoma cells in the invasive process.

Tumor initiating potential of CD271 positive melanoma cells *in-vivo*

To assess whether these invasive CD271 positive cells showed properties of MSCs, we fractionated a subcutaneous xenograft on the basis of CD271 using fluorescent activated cell sorting (FACS) (Figure 26a). Following the transplantation of dermo-epidermal skin substitutes containing either 50'000 $CD271^{Pos}$, $CD271^{Neg}$ or unsorted control cells, tumor growth was assessed

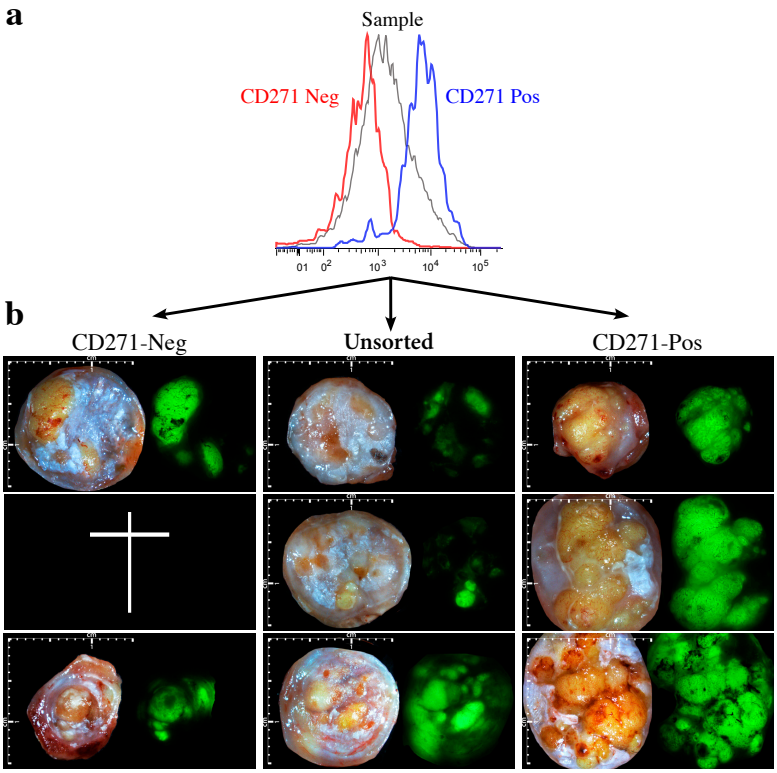

Figure 26. Transplantation of CD271 sorted cells. (**a**) Human CD271-positive and CD271-negative melanoma cells were isolated from a subcutaneous xenograft by FACS. The unsorted cells served as control. (**b**) 42 days after transplantation all fractions gave rise to macroscopic tumors. The strong GFP expression proves that all tumors were derived from the transplanted cells. The indicated animal succumbed to an infection 4 weeks after transplantation.

after 42 days *in-vivo* (Figure 26b). Surprisingly, in contrast to previously published results [107, 51], all fractions gave rise to macroscopic, ulcerated tumors (Fig. 26b, the indicated animal died of an infection, but also revealed tumor growth upon histological analysis (data not shown)). In support of the reports questioning CD271 as a genuine MSC marker [49, 50], this showed that also in a humanized environment CD271 expression does not correlate with an exclusive tumor induction potential.

Melanoma Cell Plasticity

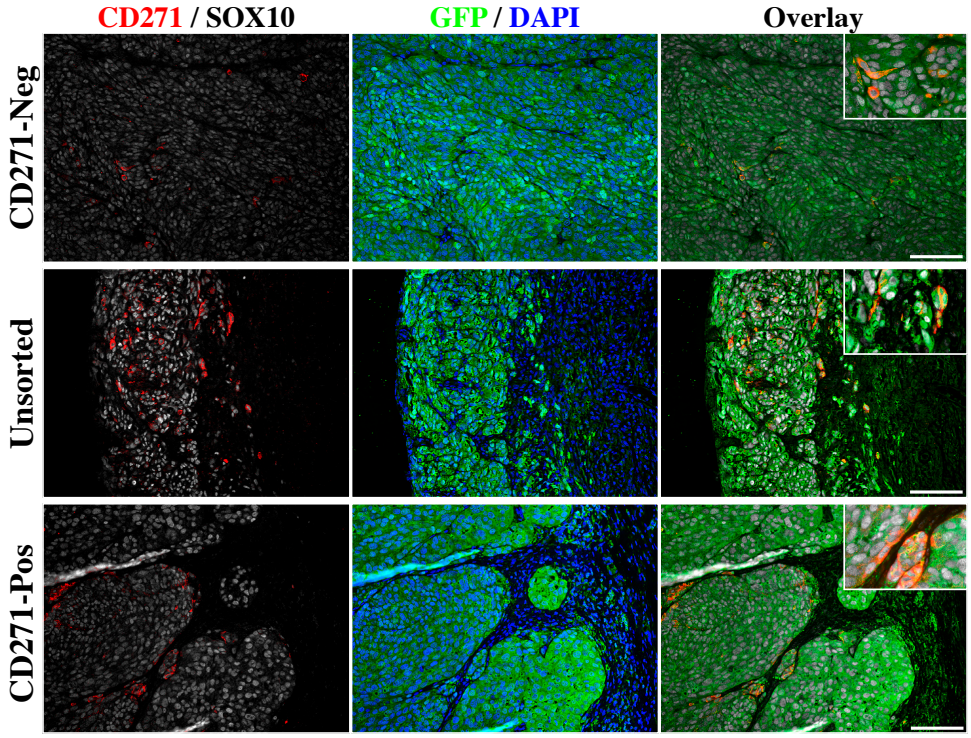

Figure 27. CD271/Sox10 double staining in CD271-sorted samples Double staining for CD271 and Sox10 on reconstituted tumors induced by CD271-positive, CD271-negative and unsorted human melanoma cells reveals that all samples contain double positive cells. Correlation to the GFP-positive tumor cells excludes a potential contamination from infiltrating cell types.

However, considering the growing body of evidence that tumor stem cells represent plastic entities [66, 48, 71], we addressed the question whether also CD271 positive cells could arise as a consequence of tumor cell plasticity. Intriguingly, in support of this theory, immunohistochemical analysis revealed that all tumors, independent of the fraction they originated from, contained cells positive for the MSC-associated NCSC marker CD271 and Sox10 [51] (Figure 27).

Intrigued by this finding, we developed a novel time-lapse imaging technique

to address whether MSCs can be dynamically regulated (Figure 28). To this end we created a migration assay that retained the cellular integrity and immediate microenvironment of the cells prior to their emigration by using whole

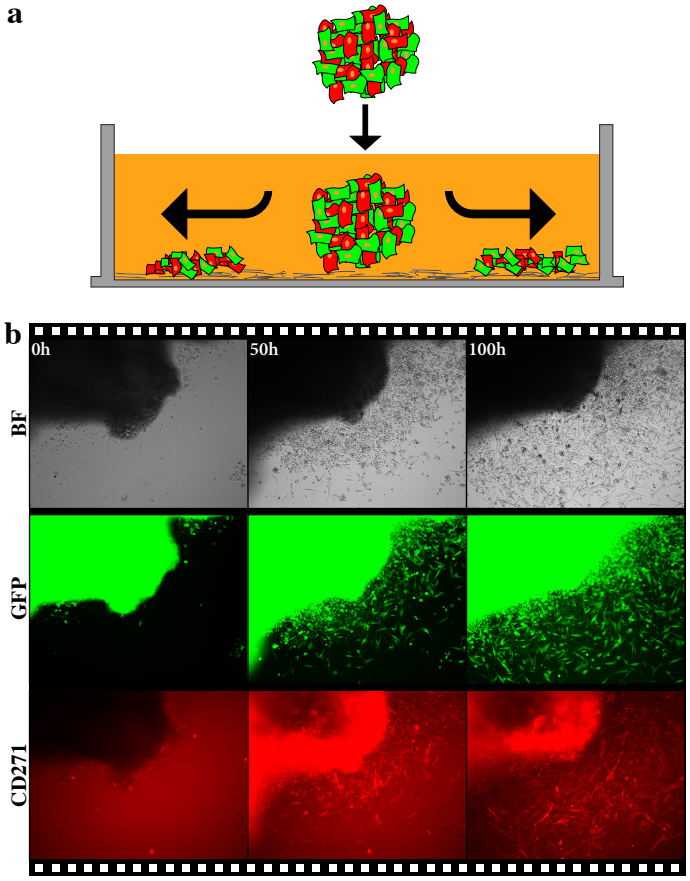

Figure 28. Tumor emigration model. (**a**) Schematic overview of the experimental approach. Approximately 1mm^3 large tumor pieces are microdissected from a subcutaneous xenograft. Coating with Fibronectin and Matrigel provides the structural stability for the tumor pieces to adhere to a cell culture dish. Following incubation in serum containing growth medium tumor cells start to emigrate in the range of 4-6 days. (**b**) Using an automated microscope equipped with an incubation chamber allows to image the emigrating cells. Tumor cells can be differentiated from emigrating mesenchymal cells by their fluorescent tag. Adding a fluorochrome-coupled CD271 antibody allows to follow CD271 expression on emigration tumor cells with high temporal resolution.

tumor pieces (Figure 28a). This was achieved by microdissecting approximately 1mm^3 large pieces of a GFP expressing subcutaneous xenografts and plating them into a cell culture dish. Coating with Fibronectin and Matrigel provided the structural stability for the pieces to adhere to the dishes. Incubation at 37°C in serum containing growth medium resulted in the emigration of tumor cells in the range of 4-6 days. In combination with an automated microscopy system equipped with an incubation chamber set to 5 minutes picture intervals, this approach allowed us to follow emigrating cells with high temporal resolution. Furthermore, addition of a directly fluorochrome-coupled anti-CD271 antibody into the growth medium enabled us to follow expression of CD271 in emigrating tumor cells (Figure 28b). Thus, based on this system potential dynamic changes in CD271 expression were assessed by imaging individual cells at high magnification (Figure 29). Interestingly, this revealed that some emigrating tumor cells indeed showed the ability to become CD271 positive over a time range of 600 minutes (Fig. 29a). Moreover, after 6 days in culture the CD271 expressing cells were located mainly at the outer periphery of the emigrated cells (Fig. 29b). These findings demonstrated that a dynamic regulation of CD271 in melanoma cells can occur, which provided the first experimental evidence for a potential plasticity inherent to migrating melanoma cells. However, whether the acquired expression of CD271 really reflected an acquired stem cell potential could not be determined using this approach.

The functional role of CD271 *in-vivo*

Thus, to address the functional role of CD271 in melanoma progression, a lentiviral overexpression system was constructed (Figure 30a). To allow the unequivocal identification of infected cells in all subsequent analyses, a system

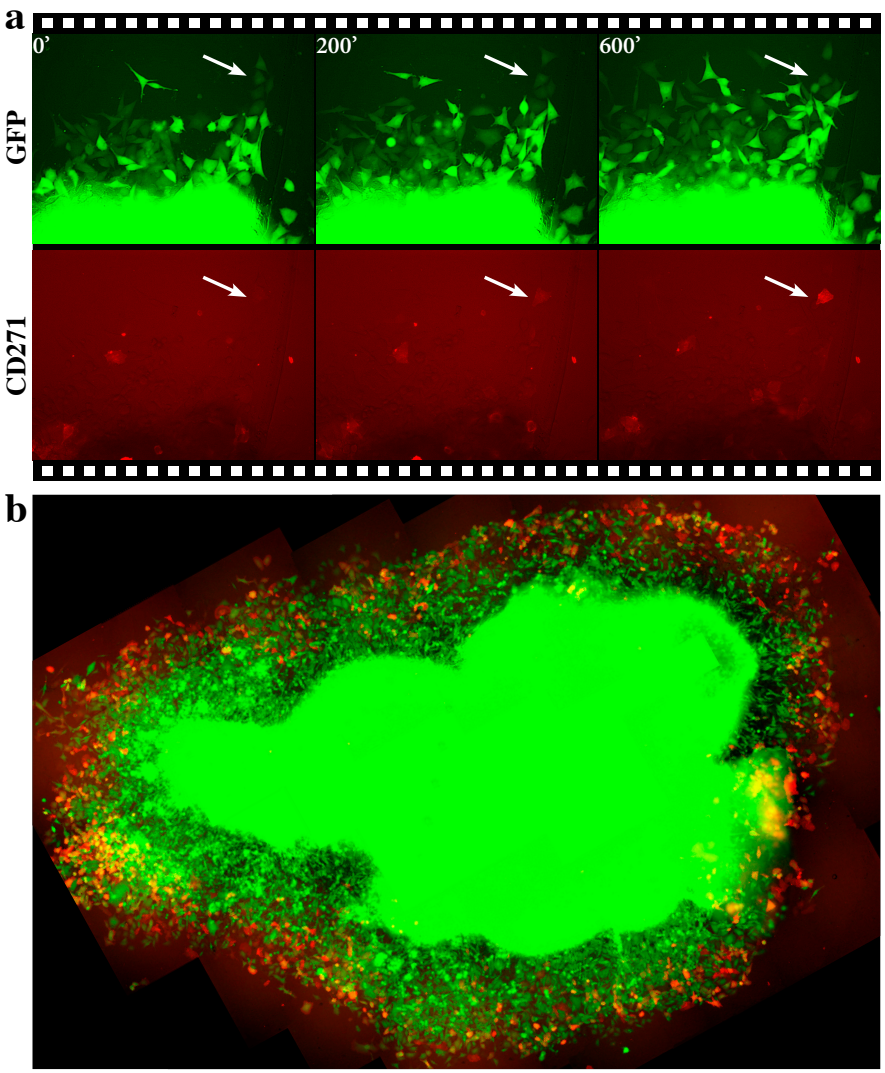

Figure 29. CD271 expression in emigrating melanoma cells. (**a**) Imaging cell emigration at 20x magnification reveals that some tumor cells are able to induce CD271 expression over a time range of 600 minutes (arrows). (**b**) Overview over the emigrated cells after 6 days. CD271 positive cells are mainly located at the outermost boarder.

concomitantly expressing GFP from an internal ribosome entry site (IRES) was chosen. Infection of human melanoma cells with this construct resulted in a high efficiency of approximately 90% and a more than 2-fold upregulation of CD271 expression after 5 days in culture (Figure 12b).

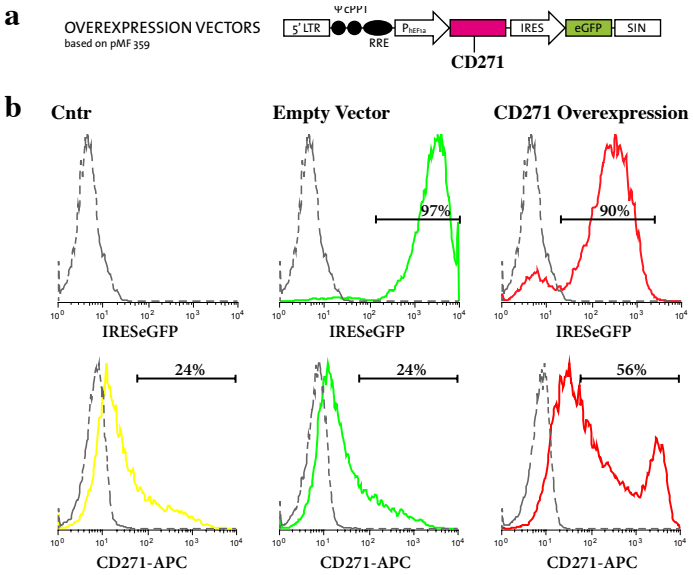

Figure 30. Lentiviral CD271 overexpression. (**a**) Lentiviral overexpression vector used in this study. Using an internal ribosome entry site (IRES) allows the concomitant expression of CD271 and GFP. (**b**). Flow cytometric analysis reveals CD271 expression to be induced by more than 2-fold in human melanoma cells 5 days after infection.

Based on this lentivrial vector, we subsequently addressed the effect of CD271 overexpression on tumor growth and progression *in-vivo*. To this end cells overexpressing CD271 and cells containing the empty control vector were seeded into skin substitutes (N=2 animals per group). However, histological analysis revealed no striking difference with respect to tumor size and morphology after 42 days *in-vivo* (Figure 31). But interestingly, while this questioned the functional implication of CD271 overexpression in tumor induction and growth, a striking effect with respect to the metastatic potential was observed (Figure 31). Comparison of several section throughout the control (Figure 31a) and CD271 overexpressing tumors (Figure 31b) indicated an enhanced ability to form satellite metastases in the sub-dermal rat tissue in response

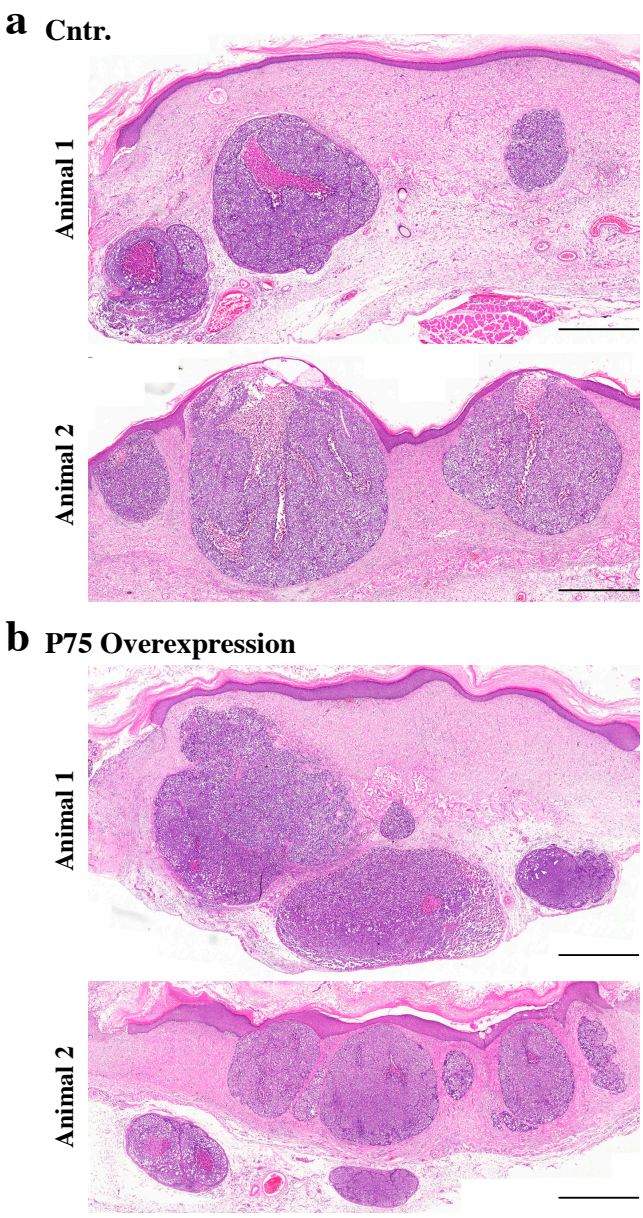

Figure 31. CD271 overexpression *in-vivo*. (**a**) Transplantation of cells carrying an empty control vector gives rise to large, invasive tumors that are mostly confined to the humanized dermal compartment. (**b**) Although similar in size and morphology, cells overexpressing CD271 give rise to tumors with an enhanced proclivity to seed multiple satellite metastases in the subdermal rat tissue. Scale bars, 1mm.

to CD271 overexpression. This is of particular interest considering that sub-dermal metastases have not been observed in this model system before (see section 'Engineering melanoma progression in a humanized environment *in-vivo*'), which suggested an increased ability of CD271 expressing cells to adapt to a hostile microenvironment. To exclude that the similar growth rate of the primary tumors were induced by a downregulation of ectopic CD271 expression *in-vivo*, we immunohistochemically assessed the CD271 expression pattern on whole transversal sections (Figure 32). As expected, the tumors arising from the control cells only revealed a moderate amount of CD271 expression (Figure 32a). The only exception constituted a small population of scattered cells showing strong invasive growth (Figure 32a, inset). Surprisingly, although showing uniform GFP expression, not all tumors carrying the overexpression vector also revealed detectable CD271 expression (Figure 32b). But the underlying reason for this remains to be addressed. Along this line the used construct or cell intrinsic or extrinsic regulatory mechanism could offer conceivable explanations. Nevertheless, already the fact that in the same graft no differences in tumor size with respect to CD271 levels were observed excluded a direct effect of CD271 expression on tumor induction and growth. But importantly, CD271 expression was detected in the sub-dermal metastasis as well as in a strongly invasive population of cells (Figure 32b, inset). Taken together, these findings indicate that primary tumor growth is not directly affected by the level of CD271 expression in human melanoma cells. However, strong expression on the dermal metastasis and on highly invasive cells in the control points to a potential implication of CD271 positive cells in invasion *in-vivo*.

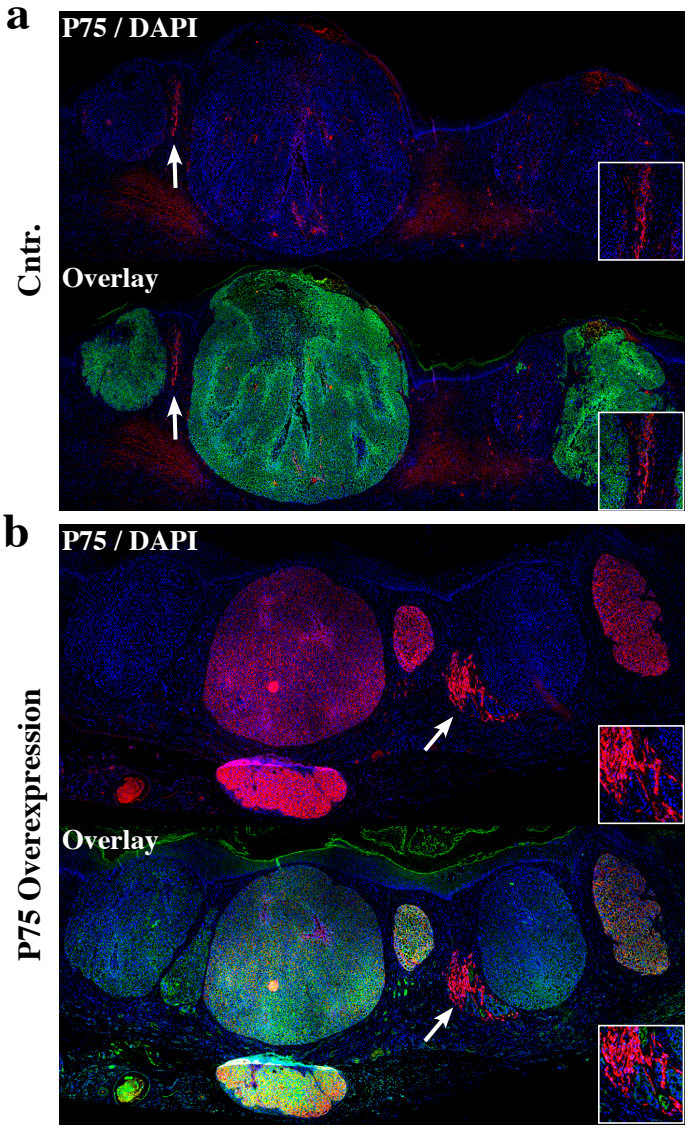

Figure 32. Analysis of CD271 overexpression levels *in-vivo*. (**a**) Analysis of CD271/GFP expression in a control tumor carrying an empty vector. Whereas the large tumors only contain few cells positive for CD271, a strong increase is observed in a small population of highly invasive cells (inset). (**b**) Despite positive for GFP, not all tumors derived from CD271 overexpressing cells reveal detectable CD271 levels. Strong expression is found in some primary tumors, the sub-dermal metastasis as well as some single, invasive cells.

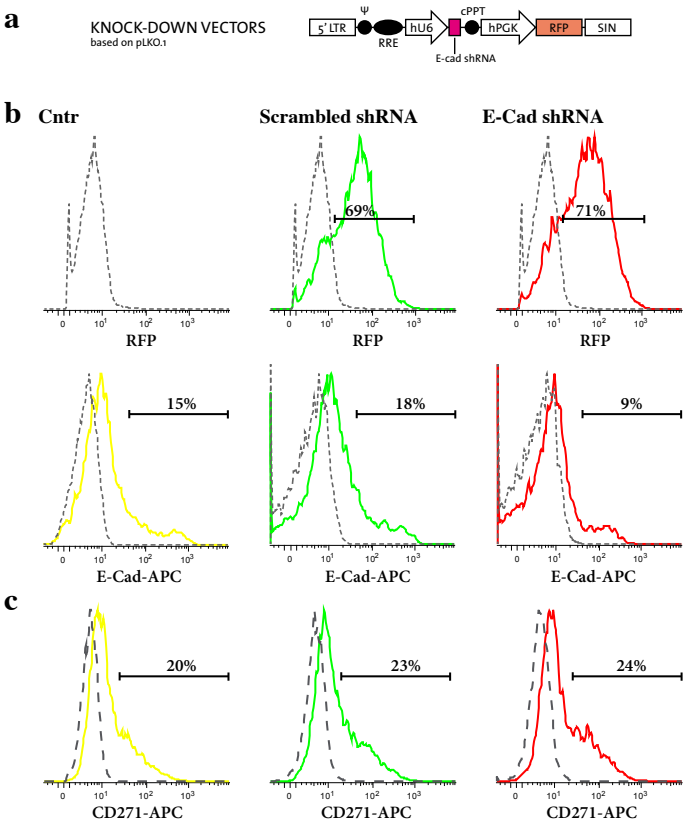

Figure 33. Lentiviral E-cadherin knock-down. (**a**) Lentiviral knock-down vector used in this study. Ablation is achieved by expressing E-cadherin shRNA from a constitutive active hU6 promoter. Red fluorescent protein (RFP) is expressed from an independent promoter and serves as fluorescent marker. As a control the same vector carrying a scrambled shRNA sequence was used. (**b**) Flow cytometric analysis shows a 2-fold reduction of E-cadherin levels in human melanoma cells 5 days after infection. (**c**) CD271 expression is not altered upon E-Cadherin ablation.

Analysis of E-cadherin knock-down *in-vivo*

Given the potential implication of CD271 positive cells in invasion and the dynamic regulation of CD271 expression in emigrating melanoma cells, we addressed the possibility that invasive CD271 positive cells arise as a consequence of an EMT process. Based on the findings implicating the loss of E-cadherin, the main determinant of EMT in epithelial carcinomas [160], in melanoma

invasion (Figure 24), we addressed to what extend loss of E-cadherin might be involved in inducing MSC features in human melanoma cells. To this end we constructed a shRNA-based lentiviral E-cadherin knock-down vector. To dif-

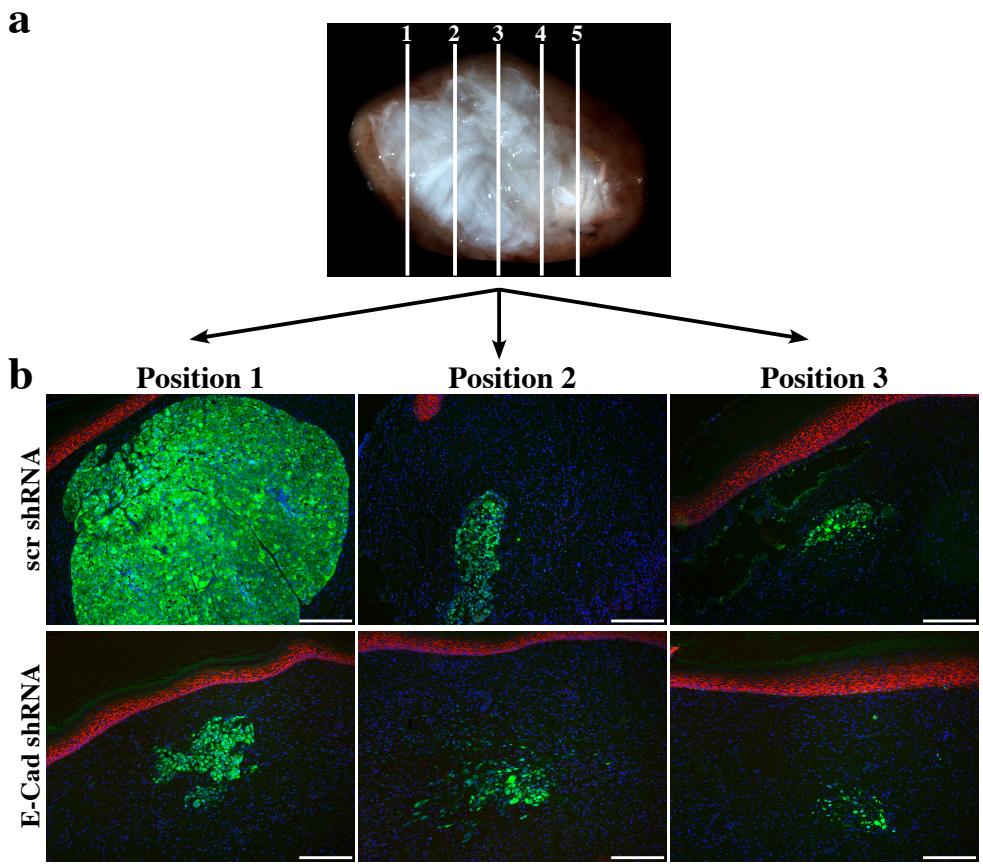

Figure 34. E-cadherin knock-down *in-vivo*. (**a**) Skin graft containing E-cadherin knock-down cells after 35 days *in-vivo*. Given the lack of macroscopic tumor growth, analysis was based on the histological evaluation of 5 independent positions throughout the sample. (**b**) Representative pictures of 3 of the 5 analyzed positions of a control (scr shRNA) and E-cadherin knock-down (E-cad shRNA) sample. Compared to the control, loss of E-cadherin results in loose cell aggregates missing any higher structure. Scale bars, 50μm.

ferentiate between between infected cells and non-infected cells, a fluorescent marker was introduced by replacing the antibiotic resistance with Red Fluorescent Protein (RFP) driven from an independent promoter (Figure 33a).

As a control vector the same construct carrying a scrambled shRNA sequence was used. Infection of human melanoma cells resulted in an approximately 2-fold reduction of E-cadherin expression within 5 days (Figure 33b). However, contradicting a direct relationship between loss of E-cadherin and induction of MSC features, ablation of E-cadherin was not found to induce CD271 expression *in-vitro* (Figure 33c). But considering that there is no direct evidence proving that the loss of E-cadherin is an underlying cause of melanoma invasion, the relevance of this finding was unclear. Thus, we embarked to determine whether loss of E-cadherin is a causative factor of melanoma progression or only a result thereof. To address this question we transplanted skin substitutes containing melanoma cells carrying either the E-cadherin knock-down or the scrambled control vector (Figure 34) (N=2 animals per group). Because no macroscopic tumor growth was observed after 35 days in *in-vivo*, each sample was histologically analyzed at 5 independent positions (Figure 34a). Representative pictures of 3 of these 5 positions are shown in Figure 34, 35 and 36.

Intriguingly, in comparison to the control sample loss of E-cadherin revealed a striking effect on tumor shape *in-vivo*. Whereas the control cells were found to form dense, coherent tumors, loss of E-cadherin resulted in loose aggregates of cells missing any discernible structure (Figure 34b). Furthermore, detailed analysis of E-cadherin and CD271 expression on adjacent histological sections revealed a correlation between loss of E-cadherin, CD271 expression, and disseminated single cells. Strikingly, although E-cadherin expression was generally weak in the control sample, expression of CD271 and E-cadherin was found to be mutually exclusive (Figure 35). Whereas this effect was not so prominent in the big lesion analyzed, it became significant in the dermal parts of two tumors where the expression of CD271 was drastically upregulated in single, E-cadherin negative cells moving away from the primary tumor

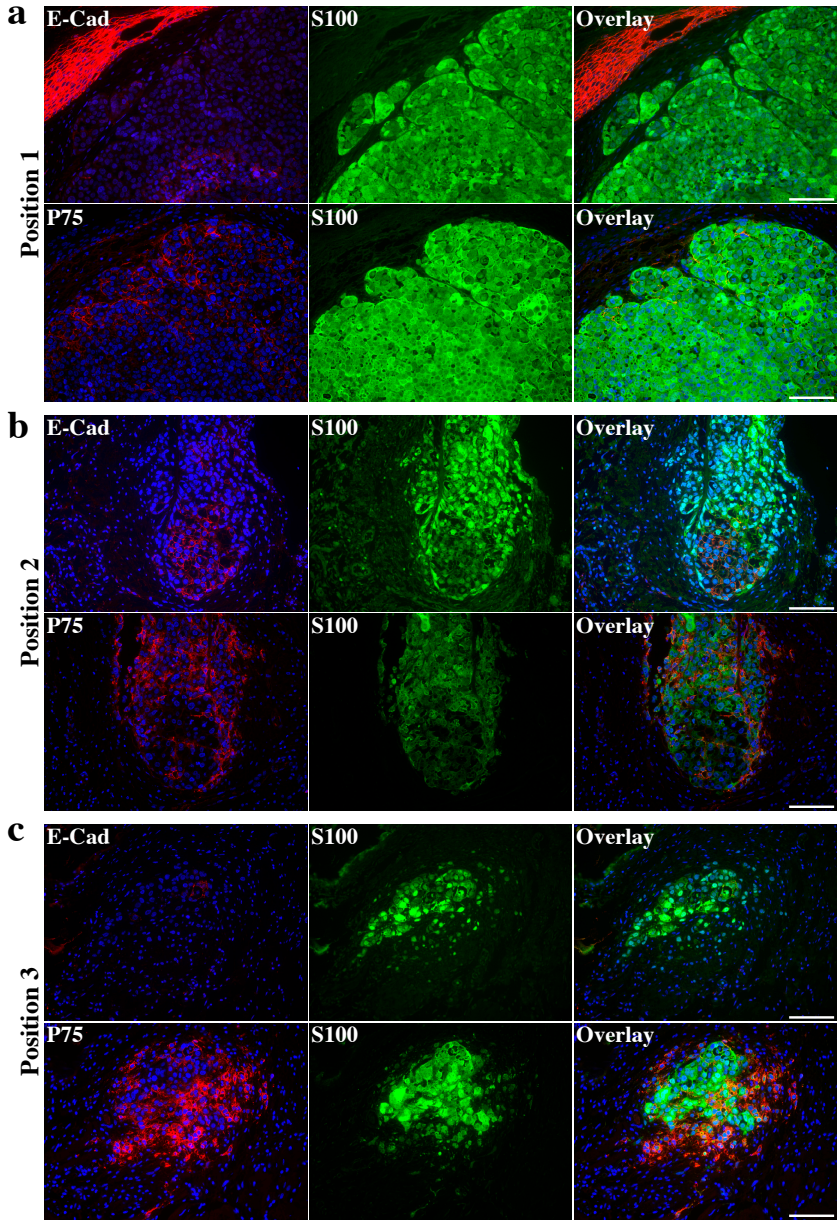

Figure 35. Analysis scrambled shRNA control *in-vivo*. Immunohistochemical analysis of CD271 and E-cadherin expression on consecutive sections at 3 independent positions. (**a**) Despite weak in this big lesion, E-cadherin expression does not overlap with CD271 expression. (**b,c**) CD271 expression becomes progressively stronger in single, E-cadherin negative cells moving away from their primary tumor. Scale bars, 100μm.

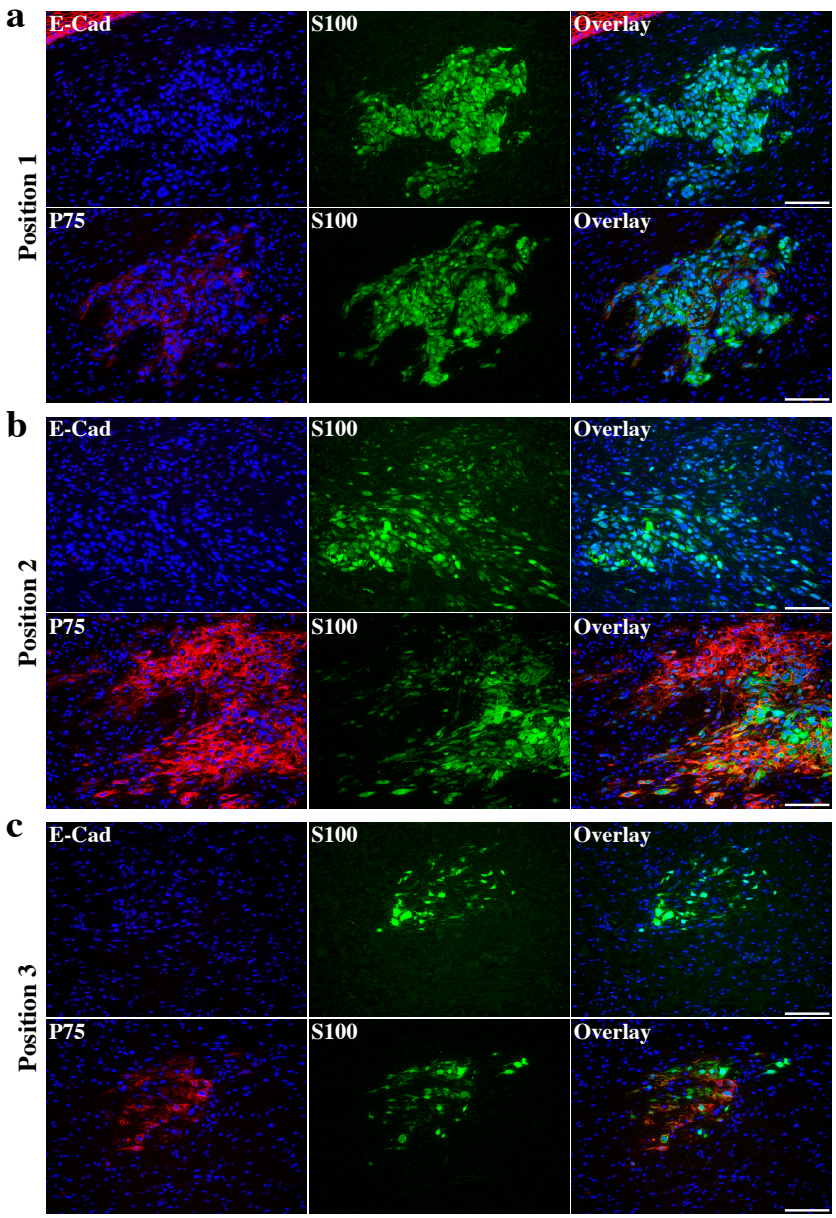

Figure 36. Analysis of E-cadherin knock-down *in-vivo*. Immunohistochemical analysis of CD271 and E-cadherin expression on consecutive sections at 3 independent positions. (**a**) Although almost entirely positive for CD271, expression is weaker in this more dense aggregate of tumor cells. (**b,c**) In the invasive, more scattered cell aggregates CD271 is ubiquitously expressed. Scale bars, 100μm.

(Figure 35b,c). Interestingly, this effect became even more prominent in the tumors lacking E-cadherin expression (Figure 36). Although weak in a larger aggregate of cells (Figure 36a), the smaller, more scattered lesion induced by E-cadherin ablation showed a strong, uniform expression of CD271 (Figure 36b,c). Taken together, these results provide the first direct evidence that the loss of E-cadherin can act as a determinant of melanoma invasion *in-vivo*. Furthermore, considering the preliminary findings that invasive melanoma cells appear to upregulate the MSC-associated marker CD271, these results present a promising start for future projects.

Materials and Methods

Melanoma reconstitution model

Isolation of human skin cells

This study was conducted according to the Declaration of Helsinki Principles. Human foreskin samples were obtained from patients after permission by the ethic commission of the Canton Zurich and after informed consent given by parents or patients. Keratinocytes and fibroblasts were isolated as described previously [190, 191]. In brief, human foreskin samples were digested in 12 U/ml dispase in Hank's buffered salt solution containing 5 μg/ml gentamycin overnight at 4 °C. This allowed the subsequent separation of the epidermis and dermis using forceps. In order to isolate the desired cell types from the respective compartments, the dermis and epidermis were separately processed after separation. To isolate keratinocytes or melanocytes the epidermis was further digested in 1% trypsin, 5 mM EDTA for 5 minutes at 37 °C and the digested epidermal cells were cultured in serum-free keratinocyte medium containing 25 μg/ml bovine pituitary extract, 0.2 ng/ml EGF, and 5 μg/ml gentamycin or in melanocyte growth medium containing 1 ng/ml bFGF, 10 ng/ml PMA, 5 μg/ml insulin, 0.5 μg/ml hydrocortisone, 2 ml bovine pituitary extract (all from PromoCell) and 5 μg/ml gentamycin, respectively. To

establish primary dermal fibroblast cultures the dermal tissue was digested in 2 mg/ml collagenase for 60 minutes at 37 °C followed by culturing in DMEM supplemented with 10% fetal calf serum, 4 mM L-alanyl-L-glutamine, 1 mM sodium pyruvate, and 5 μg/ml gentamycin. Collagenase was from Sigma, all other compounds were from Invitrogen.

Construction of human organotypic skin cultures

Organotypic cultures were prepared using a previously established transwell system consisting of 6 well cell culture inserts containing a porous membrane (3.0 μm pore-size, BD Falcon) [190, 191]. The membranes were covered with collagen type I hydrogels containing human dermal fibroblasts prepared according to the protocol of Costea et al. [198]. Briefly, 0.7 ml rat tail collagen type I (3.2- 3.4 mg/ml, BD Biosciences), was added to 0.2 ml chilled neutralization buffer containing 0.15 M NaOH and 1x10^5 fibroblasts. After polymerization (10 min at room temperature and 20 min at 37°C) these dermal equivalents were grown in DMEM supplemented with 10% FCS for 5 days. Corresponding to the physiological ratio of melanocytes to keratinocytes (approx. 1:5), 5x10^4 melanocytes or melanoma cells were mixed with 2-2.5x10^5 keratinocytes and seeded onto each dermal equivalent. To avoid dispersion the cells were pippeted into siliconized polypropylene rings of 5 mm diameter. After 12 h the rings were removed, 1 ml keratinocyte/melanocyte medium (ratio 5:1) was added in the upper chamber, and 2 ml was added to the lower chamber. Culturing for 1 week with regular medium changes gave rise to the dermo- epidermal skin substitues used for transplantation.

Transplantation of human organotypic skin substitutes

The study protocol was approved by the local Committee for Experimental Animal Research (permission number 135/2010). The surgical procedure was performed as described previously [199, 190, 191]. In short, a fully thickness skin defect was surgically created on the back of 10 weeks old, female athymic Nu/Nu rats (Harlan, Netherlands). To prevent wound closure from the surrounding skin, metal rings (27mm in diameter, made to order from stainless steel at the ETH Zurich) were sutured into the skin defects using non-absorbable polyester sutures (Ethibond®, Ethicon). The dermo-epidermal skin substitutes were placed into the rings, fixed with 4-6 stiches, and covered with a silicone foil (Silon-SES, BMS). The rings were then covered with 5 cm x 5 cm polyurethane sponges (Ligasano®, Ligamed) and medical strip. Sedation and anesthesia was performed as follows. All animals were sedated with 15mg/kg ketamine s.c. (Pfizer) prior to surgery. Anesthesia was induced and maintained using isofluorane (Abbott), post-operative analgesia was provided by 0.5 mg/kg buprenorphine s.c. (Temgesic®, Essex). Animals were sacrificed at the indicated time points with carbon dioxide. The grafts were excised and prepared for immunohistchemical processing.

Tumor cell isolation and xenograft inoculation

All patients enrolled in the study were treated at the Dermatology Department of the University Hospital of Zurich. The biobank project including the establishment of cell cultures was approved by the local IRB (EK647 and EK800) (ethics committee of canton Zurich) and all patients gave written informed consent. The patient samples used for transplantation were derived from one primary tumor and two metastases (see Supplementary Table S1).

After surgical resection, the solid, metastatic lesions were immediately dissociated into single-cell suspensions using HBSS (without Ca^{2+} and Mg^{2+}, Invitrogen) containing Collagenase III (1mg/ml, Worthington Bioch.) and Dispase (0.5 mg/ml, Roche) [200]. Incubation for 1h at 37°C with concurrent mincing allowed for complete digestion. The resulting cell suspension was filtered through a 40 μm nylon mesh and single cells were harvested and re-suspended in 200μl Matrigel matrix (BD Biosciences) 1:1 diluted with RPMI-1640 (Invitrogen). Subcutaneous (s.c) injections using a 1- ml syringe with a 25-gauge hypodermic needle in the flank of BALB/c-Swiss nude (CAnN.Cg-Foxn1nu/Crl, Harlan) mice established the initial xenograft cultures, which were maintained using the same routine for re-injection.

GFP infection

The GFP-expressing lentivirus was produced as described [201]. Lentivirus-containing supernatants were collected 48 hours after transfection, filtered through a 0.22 μm membrane and transferred to target cells freshly isolated from mouse xenografts. During transfection cells were maintained under sphere conditions as described below. After one week the cells were reinjected s.c. into Swiss nude mice. The resulting tumors were dissociated as described above and the GFP-positive cells were purified by FACS-sorting. Re-injection resulted in purified GFP-positive xenografts. For all further passages GFP-expression was regularly analyzed by FACS and, if deemed necessary, purified again.

Cell culture

Melanoma cells in vitro were maintained in sphere cultures as previously described for neural stem cells [202]. Briefly, single cells were plated in flasks

(Nunc) coated with Poly(2-hydroxyethylmethacrylate) (Poly- Hema, Sigma) at a density of 20,000 viable cells/ml in DMEM-F12 1:1 media (Gibco) containing 1x B-27 supplement (Invitrogen), 20 ng/ml FGF2 (PeproTech), 10 ng/ml EGF (PeproTech), 5% Pen/Strep (Invitrogen). The resulting spheres were collected after 7-10 days by gentle centrifugation (800 rpm), dissociated using PBS containing 2 mM EDTA and replated into Poly- Hema coated culture flasks. Passage three sphere cells were used for transplantation.

Immunohistochemistry

All tissue used for immunohistochemistry was fixed in 4% paraformaldehyde and embedded in parafin. Sections were deparaffinized in xylene and rehydrated. Epitope retrieval was performed in Tris-EDTA pH9 for Glut1, in Tris pH6 for Ki67 and S100, and with proteinase K for CD31. Staining was performed using the according Dako REAL kit 5005 with the following primary antibodies at the indicated dilutions: Melan-A (clone A103, 1:60, Novacastra), CD31 (clone JC70A, 1:40, Dako), Glut-1 (AB1341, 1:1000, Chemicon), S100 (L-S100P, 1:200, Novacastra). Melanin was visualized using the Masson-Fontana technique with nuclear fast red as counterstain (Eichhoff et al., 2010).

Immunofluorescence

Immunofluorescence was performed on either cryo or parafin sections. For cryo processing tissue samples were embedded in OCT compound (Sakura Finetek/Digitana AG) and frozen at -20°C. Cryosections were fixed and permeabilized in acetone for 5 min at -20°C, air dried, washed 3x in PBS and blocked in PBS containing 2% BSA (Sigma) for 30 minutes. Following primary antibodies were incubation in blocking buffer for 1 hour at room temperature : K10 (clone DE-K10, 1:100, Dako), laminin 10 (clone 4C7, 1:25,

Dako), human melanosome (clone HMB45, 1:50, Dako), K16 (clone LL025, 1:100, Millipore), Ki-67 (clone B56, 1:200, BD Pharmingen), anti-rat CD31 (PCAM-1, clone TDL-3A12, 1:50, BD Pharmingen), laminin 5 (clone P3H9-2, 1:100, Labforce), human fibroblasts (clone AS02, anti-CD90 (Thy-1), 1:100, Dianova). After washing the sections were incubated with FITC-conjugated goat anti-mouse (Dako) secondary antibodies for 1h at room temperature. Parafin sections were deparaifinized as described above. Antigen-retrieval was performed in 10 mM trisodium citrate buffer at pH 6.0 and a Microwave Histoprocessor (Milestone). Sections were incubated over-night at 4°C with the following primary antiobodies: MelanA (clone A103, 1:100, Abcam), S100P (Z0311, 1:400, DAKO), human melanosome (clone HMB45, 1:100, DAKO), E-cadherin (C20820, 1:200, Translab), GFP (ab290, 1:400, Abcam). Sections were subsequently incubated with the according secondary antibody for 1 h at room temperature: Cy2-conjugated goat anti-rabbit (1:250, Jackson ImmunoResearch) or Alexa 546-conjugated goat anti-mouse (1:500, Invitrogen). All slides were counterstained with Hoechst 33342 (Invitrogen).

Image acquistion

Microscopy pictures were taken using a Leica DMI6000 microscope equipped with a fluorescent lamp, a high sensitivity black and white camera (Leica DFC350 LX) for immunofluorescent images and a color camera (Leica DFC420c) for immunohistochemistry images. All macroscopic tissue pictures were taken using a Leica MZ16 stereo-loupe equipped with a fluorescence lamp. The histological overview pictures were taken using a Zeiss Mirax Midi Slide Scanner. Fluorescent overview pictures were taken using the tile scan function included in the Leica DMI6000 microscope software.

Additional material and methods

Patient samples

All patients enrolled in the study were treated at the Dermatology Department of the University Hospital of Zurich. The biobank project including the establishment of cell cultures was approved by the local IRB (EK647 and EK800) (ethics committee of canton Zurich) and all patients gave written informed consent. Characteristics of the used biopsies are listed according to their figure contribution: Fig. 25: (a) ID12826, F/94, primary, location unknown, T1bN0M0 (b) ID4286, M/35, metastasis, skin axillary, pT4bN3M0; Fig. 26,27: ID4286, M/35, metastasis, skin axillary, pT4bN3M0; Fig. 28: ID12741,M/80, primary, upper right arm, T4bN2bM0; Fig. 29: ID2481, F/63, metastasis, Lung, pTxN3M1c; Fig. 30-36: ID25126, F/76, metastasis, lymphnode left groin, T3N3M1a.

Immunofluorescence

Immunofluorescence was performed on parafin sections. Sections were deparaffinized in xylene and rehydrated. For E-cadherin, Sox10 and S100 stainings antigen-retrieval was performed with 10 mM trisodium citrate buffer at pH 6.0 in a Microwave Histoprocessor (Milestone). For CD271 staining antigen-retrieval was performed with proteinase K for 10min at RT. Following antigen-retrieval the section were incubated in blocking buffer consisting of PBS supplemented with 10% goat serum and 0.2% Triton-X for 15min at RT. After blocking, sections were incubated over-night at 4°C with the following primary antibodies: E-cadherin (C20820, 1:200, Translab), GFP (ab290, 1:400, Abcam), S100P (Z0311, 1:400, DAKO), CD271 (130-091-884, 1:100, Miltenyi Biotec), Sox10 (MAB2864, 1:400, R&D). Sections were subsequently incu-

bated with the according secondary antibody for 1 h at room temperature: Cy2-conjugated goat anti-rabbit (1:250, Jackson ImmunoResearch) or Alexa 546-conjugated goat anti-mouse (1:500, Invitrogen). All slides were counterstained with Hoechst 33342 (Invitrogen). All pictures were taken on a Leica DMI6000 microscope. Overviews were created from individual pictures using the automated stitching function of Photoshop CS4 (Adobe).

Flow cytometry and FACS-sorting

Sorting and analysis were performed as described before [51]. In short, all steps for flow cytometry were performed in DMEM supplemented with 10% FCS (Invitrogen), 1% Pen/Strep (Invitrogen) and 2mM EDTA. For sorting or analysis, single cell tumor samples were stained with anti-human CD271 (1:100, FITC-conjugated: 130-091-917, or APC-conjugated: 130-091-884, Miltenyi Biotec) and anti-human E-Cadherin (1:100, APC-conjugated: 130-095-412, Miltenyi Biotec) for 30min at 4°C. Samples were measured with a FACScanto II (BD Biosciences) an analyzed with Flowjo software. Sorting was performed with a FACSAria (BD Biosciences).

Tumor emigration

Mice carrying subcutaneous, GFP expressing xenografts were sacrificed in CO_2 and tumors were resected. Using micro-dissection tools $1mm^3$ large pieces were dissected and washed in PBS. To achieve enough stability for the pieces to adhere, the wells of a 48 well plate (NUNC) were coated with Fibronectin (Sigma). Placing the tumor pieces into the coated wells, also the tumor pieces themselves were coated with Fibronectin and incubated for 30min at 37°C. Following incubation, the pieces were additionally coated with cold Matrigel (BD Biosciences) diluted 1:5 in DMEM medium (GIBCO) and again incubated

for 30min at 37°C. After incubation 1ml pre-warmed growth medium (DMEM supplemented with 10%FCS and 1% P/S) was carefully added to each piece. For the live imaging CD271 antibody (APC-conjugated: 130-091-884, Miltenyi Biotec) was directly diluted 1:100 in the growth medium. Time-lapse imaging was performed with a Leica DMI6000 microscope equipped with an incubation chamber set to 5min picture intervals. Single pictures were combined to movies using ImageJ.

Virus production

The GFP-expressing lentivirus was produced as described [201]. All other constructs were produced by L. Habegger in the range of his master thesis. Lentiviral particles were produced in HEK293T cells following calcium phosphate transfection. Supernatant was collected 3x every 12h, pooled and concentrated 100x using a Beckman Ti70 rotor at 25'200RPM. Cells were infected in a final concentration of 20x under sphere conditions as described above. Infection efficiency was checked 5 days after infection using FACScanto II (BD Biosciences) flow-cytometer.

In-vivo experiments

All experiments were performed as described above. Independent of the employed cell types, 50'000 cells were used for all tumor reconstitutions. For the functional analyses, 2 animals per group (CD271 overexpression, CD271 control, E-cadherin shRNA, E-cadherin scrambled control) were transplanted. All animals were sacrificed at the indicated time points using CO_2, grafts were resected, fixed in 4% Pfa, embedded in Parafin and analyzed as described above.

Discussion

Using human skin substitutes to model melanoma progression *in-vivo*

Conclusion

By using human skin substitutes we were able to develop a fully humanized *in-vivo* system faithfully recapitulating all initial steps of human melanoma progression. In one and the same system radial growth including pagetoid spread, vertical growth, marker expression, angiogenesis, ulceration, and hypoxia were validated in direct comparison to patient-matched tumor samples (Figure 19 - Figure 24). Interestingly, all these traits were re-established upon tumor reconstitution with samples derived from both primary melanomas and the more abundant metastases biopsies. This demonstrates the potential of cancer cells to adapt to the local environment, making our system amenable to a wide range of human melanoma samples. This concurs with recently described dynamic processes mediating tumor initiation and maintenance [72, 71]. Along this line it will be interesting to assess how environmental cues override the intrinsic differences between primary and metastatic tumor cells.

Efficiency

A crucial point to consider for every model system is its efficiency and reproducibility. Achieving an overall reconstitution efficiency of about 90% (17 tumors out of 19 transplantations using 3 individual patient samples), the method described here provides a reliable and repeatable experimental set-up. Importantly, irrespective of the cells' origin or of previous expansion *in-vivo* or *in-vitro*, the different samples did not exhibit any discernible differences with respect to the key events of disease progression. This makes our model a valuable tool for pre-clinical drug testing in an experimental set-up reminiscent of the patient situation. For *in-vitro* tumor cell expansion, we have purposely employed melanomasphere cultures rather than adherent cell cultures. This is because such cultures contain higher numbers of tumor-initiating cells than adherent cell cultures and are able to establish a cellular heterogeneity closely resembling that of patients' tumors [51, 132, 203]. Because melanomaspheres can readily be generated both from fresh tumor biopsies and cell lines passaged as adherent cultures, this method is applicable to a large variety of samples.

Metastasis

Most patients die of metastatic disease and not of primary tumor growth [204]. Therefore, we also assessed systemic metastatic spread upon transplantation by checking all animals for metastatic lesions in the inguinal and axillary lymph nodes, lung, intestine and liver. Unfortunately, no macroscopic visceral metastases were found in the range of this study. Considering that metastatic disease is a rare event, which in humans can take decades to evolve [204], we did not expect to find distant metastases already after 42 days *in-vivo*. How-

ever, whether single tumor cells are already present in the internal organs at the time point analyzed could not concludingly be determined and is subject to further investigations.

The effect of a humanized environment

In contrast to previously described model systems [107, 125, 185], we use organotypic skin substitutes as the basis for an orthotopic *in-vivo* model. This approach offers the advantage to reconstruct skin grafts from distinct cellular components, allowing the engineering of a fully humanized organotypic environment. Moreover, all cell types used for melanoma reconstruction can be manipulated, including the melanoma cells, the keratinocytes, and the dermal fibroblasts. This, for the first time, will allow *in-vivo* studies addressing the influence of a human microenvironment on tumor progression in a defined experimental set-up. The significance of such studies becomes apparent by our observation that the humanized dermal compartment clearly exerted a favorable effect on tumor growth as compared to the neighboring rat tissue. Given the known influence of stromal fibroblast on tumor growth and progression [187, 188, 189], the use of a fully humanized dermal compartment containing human fibroblasts is therefore favorable over a chimeric dermal compartment that results from the repopulation of devitalized human dermal substrate with recipient animal fibroblasts [125, 103, 186].

The influence of the microenvironment has to be considered in particular when studying tumorigenesis in subcutaneous xenografts [50, 49, 135]. Subcutaneous injections are placed into the subdermal compartment, which according to our findings represents an unphysiological environment for tumor growth

and is associated with extensive necrosis in the transplanted tumor tissue. Thus, recent controversial findings regarding the nature of melanoma-initiating cells [50, 49, 135, 107, 106, 71] may indeed partly be attributed to the use of subcutaneous xenografts in some of these studies [70]. Moreover, apart from creating an unphysiological environment, subcutaneous xenografts do not recapitulate the invasive behavior of melanoma [103], and thus, should not be considered an orthotopic model system. As a result, it has been suggested that studies performed with human samples should be validated in a humanized *in-vivo* environment [53]. A recent report has used intradermal injections into human foreskin grafts [107]. However, like subcutaneous injections, intradermal inoculation cannot entirely reproduce the early stages of tumor progression. This is because the initial influence of the microenvironment and the crucial switch from radial to vertical growth are sidestepped upon dermal seeding of melanoma cells. Thus, even if applied into the context of a human skin graft, also intradermal injections do not represent a fully orthotopic model system.

The immune system

Even though our model closely mimics human disease progression, the use of immunocompromized recipient animals for transplantation creates the inherent problem of an incomplete immune system. As the immune system is considered to have an important impact on growth and progression of tumors, including human melanoma [51, 205, 206, 207], this aspect falls short in every model system using human cells. Indeed, only few host macrophages and NK cells were found close to or within the reconstituted human tumors in our model system (data not shown). Despite this limitation, we feel that the use

of human patient samples remains crucial for the development of therapeutics targeting human cancer cells. This is particularly relevant given the dramatically different architecture of human and rodent skin, with human melanocytes mainly residing in the interfollicular epidermis and rodent melanocytes being mostly confined to hair follicles [103]. Therefore, although crucial for the identification of molecular processes involved in tumorigenesis, genetic mouse melanoma models only approximate the human disease [194] impeding their direct translation to the clinic.

Advantages for future studies

In contrast to other approaches, the model system described here allows the faithful recapitulation of the central steps of human melanoma growth and progression in a physiological, humanized environment *in-vivo*. This in turn will help to translate basic research into a clinically more relevant context by providing the opportunity to devise and test therapeutics in a model system closely resembling the human disease. Furthermore, it retains the possibility to experimentally influence every single cell type in the system, which will allow manifold strategies to study the interactions between the tumor cells and the surrounding microenvironment. As a proof of principle we addressed the functional role of E-cadherin in melanoma progression. Whereas in subcutaneous xenografts no difference upon loss of E-cadherin was observed (data not shown), using the same samples in a reconstitution approach induced a dramatic effect on tumor integrity (Figure 34). This clearly shows the advantage of an orthotopic model in studying tumor progression. Especially if considering that, although the loss of E-cadherin has been implicated in melanoma progression for over a decade [182, 197], this is the first evidence validating

these findings *in-vivo*. Thus, given these promising results, we are convinced that the model system developed in the range of this thesis harbors a great potential for future studies.

Limitations

Nevertheless, there remain some technical limitations that have to be taken into consideration. Originally developed as a preclinical model for human skin grafts, the surgical procedure and the resulting animal care is cumbersome. This fact limits the amount of animals available for studies dramatically, making functional analyses difficult and time consuming to realize. Whereas it remains feasible to investigate few targets at a time, the system will not prove suitable for larger screening approaches. However, considering the original incentive underlying its development, namely to study the implication of multiple EMT target genes in the metastatic process, this represents a sever limitation. Therefore, with respect to future screening approaches, additionally establishing the same procedure in a mouse model should be considered. Given similar approaches using human foreskin grafts [107, 185] or devitalized skin substrates [125] in mice, a transfer should be technically feasible. With regard to that, a major advantage would be gained by establishing an alternative to the used metal rings. Being delicate and labor intensive, establishing a more practical solution, for examples using silicon Boyden chambers, could significantly facilitate subsequent animal care.

The role of melanoma stem cells in metastasis

Melanoma stem cells in the reconstituted skin model

Following the conflicting reports surrounding the hierarchical organization of melanoma [50, 49, 135, 107, 106, 71, 66], it was suggested that studies performed with human samples should be validated in a humanized *in-vivo* environment [53, 48]. To follow up on this suggestion, we chose to test the previously described MSC marker CD271 [51, 107] in our skin reconstitution model. To this end we assessed the tumor induction potential of $CD271^{Pos}$, $CD271^{Neg}$, or unsorted melanoma cells in transplanted skin substitutes. However, in contrast to the reports affirming CD271 as a MSC marker [51, 107], no difference regarding their tumor induction potential was observed (Figure 26b). Although we cannot entirely exclude a potential contamination of the negative fraction with $CD271^{Pos}$ cells, it appears an unlikely explanation for the observed result. This is because, even in case of a contamination, still comparatively few cells would be present in the negative fraction given their flow-cytometric profile (Figure 26a). Considering that in this case the negative cells exceed the contaminating positive cells by several orders of magnitude, one would expect this imbalance to manifest in a slower growth kinetic. As this was not found to be the case, it appears that in this experimental system CD271 does not discriminate cells with an exclusive tumor induction potential. However, whether this lack of hierarchical organization has to be considered a direct effect of the orthotopic environment or simply reflects the use of a 'wrong' MSC marker remains to be determined.

Melanoma cell plasticity

In line with the theory suggesting that tumors are not static entities [53, 48, 66], we found some preliminary evidence pointing to a potential dynamic regulation of MSCs. The first evidence came from the finding that all tumors, irrespective of whether they originated from a $CD271^{Pos}$, $CD271^{Neg}$ or unsorted population, contained cells positive for the MSC markers CD271 and Sox10 (Figure 27). Even though the most logic interpretation for this simply points to an alternative MSC population heterogeneously expressing CD271, two convincing arguments contradict this conclusion. First, the robust neural crest phenotype consistently found across several patients [51] points to the implication of a neural crest stem cell-like cell in melanoma growth. Given the identification of such a population on the basis of the neural crest marker CD271 in two independent studies [51, 107], CD271 represents the most plausible candidate. And second, CD271/Sox10 expression was shown to be directly correlated with survival and metastasis in patients [51] (Figure 17). If these arguments are considered in the context of a potential dynamic regulation of the MSC population, an interesting concept evolves. Similar to the findings in breast cancer [72, 73], in this model extrinsic cues could be able to govern metastatic dissemination of melanoma cells by inducing stem-cell traits. Intriguingly, the ramifications of this hypothesis would allow to reconcile many disparate findings surrounding the nature and abundance of melanoma stem cells. As such the stem-cell characteristics found in a particular sample would be dependent on the origin of the sample (primary vs. metastasis), the stage of the tumor, the amount of disseminated cells, the used model system etc.

Thus, to test whether CD271 can be dynamically expressed in human mel-

anoma, we established a novel time-lapse technique. Using whole pieces of subcutaneous xenografts allowed us to follow single cells leaving their intact tumor microenvironment with high temporal resolution (Figure 28). Based on this technique, we were able to confirm a dynamic expression of CD271 in some emigrating melanoma cells (Figure 29). However, although these findings show that CD271 expression can be upregulated in human melanoma cells, it could not be determined whether these cells also acquired stem-cell features in the process. To test this, some means allowing the prospective isolation of cell acquiring CD271 expression would have to be implemented into the experimental set-up, which proved technically not feasible in the range of this study.

Neural crest EMT signaling pathways in melanoma metastasis

Supported by recent findings in breast cancer [72, 73], a process reminiscent of neural crest EMT presently appears to be the most promising candidate able to induce the potential acquisition of stem-cell characteristics in melanoma. Intriguingly, taking into account that EMT is also considered a determinant of malignant progression, validation of this theory would establish a direct link between the acquisition of stem-cell traits and metastasis. Strikingly, in favor of this theory, several studies have implicated CD271 in melanoma invasion and metastasis [145, 146, 147, 148, 149, 107, 51].

Thus, to address a potential link between CD271 expression, EMT, and invasion, we assessed CD271 expression in reconstituted tumors. Whereas it was found to be sporadically upregulated at the invasive front in some samples (Figure 25b), the most prominent effect was observed in response to loss of E-cadherin. Showing highly invasive, scattered tumors, CD271 was strongly

expressed throughout all samples analyzed (N=2 animals) (Figure 36). Interestingly, the same expression pattern was also found in invasive tumors of the control sample (Figure 35), which substantiated the implication of CD271 positive cells in invasion. However, although these preliminary findings point to a correlation between EMT, loss of E-cadherin, gain of CD271, and invasion, loss of E-cadherin was not found to directly induce CD271 expression *in-vitro* (Figure 33b,c). And moreover, whether the observed invasive cells positive for CD271 represent true stem-cells in the sense of self-renewal and differentiation capacity also remains to be addressed.

The functional role of CD271

Given the preliminary findings suggesting a role for CD271 positive cells in invasion, we addressed whether CD271 in its function as a TNF receptor family member directly influences the invasive behavior of melanoma cells *in-vivo*. But questioning a prominent function of CD271, no striking differences in terms of tumor size and morphology was found upon transplantation of cells overexpression CD271 (Figure 31). Nevertheless, the samples overexpressing CD271 (N=2 animals) showed an increased ability to seed satellite metastases in the subdermal rat tissue, an effect not observed before. However, to what extend this reflected an enhanced invasive or survival potential in response to CD271 expression needs to be validated in additional experiments. Along this line, especially the functional ablation of CD271 expression would yield more relevant information with respect to the functionality of CD271.

In conclusion, the results obtained in the range of this thesis point to the functional implication of neural crest pathways in melanoma metastasis. As such loss of E-cadherin was shown to induce invasive growth *in-vivo*, whereas

expression of CD271 was found to be highly expressed on invasive cells. Although most of these functional results are preliminary, they clearly show the potential of the developed model system to study melanoma progression. Taken together with the construction of several lentiviral vectors targeting neural crest EMT pathways, this project presents a first step towards a better understanding of the most deadly form of skin cancer.

Outlook

Neural crest EMT signaling pathways in melanoma metastasis

With respect to the functional contribution of neural crest EMT pathways in the metastatic process, a variety of lentiviral vectors have been constructed in the range of this study (Figure 31). Testing these on the basis of the reconstituted skin model will yield further insights into their implication in the metastatic process.

Given the promising results with respect to loss of E-cadherin, these findings have to validated in statistic relevant numbers using different patient samples. Along this line, to confirm the role of E-cadherin as a determinant of melanoma invasion also the effect of E-cadherin gain-of-function experiments should be assessed.

Considering the unclear results obtained by overexpressing CD271, loss-of-function experiments might prove the more promising approach to elucidate the functional role of CD271 in melanoma growth and progression.

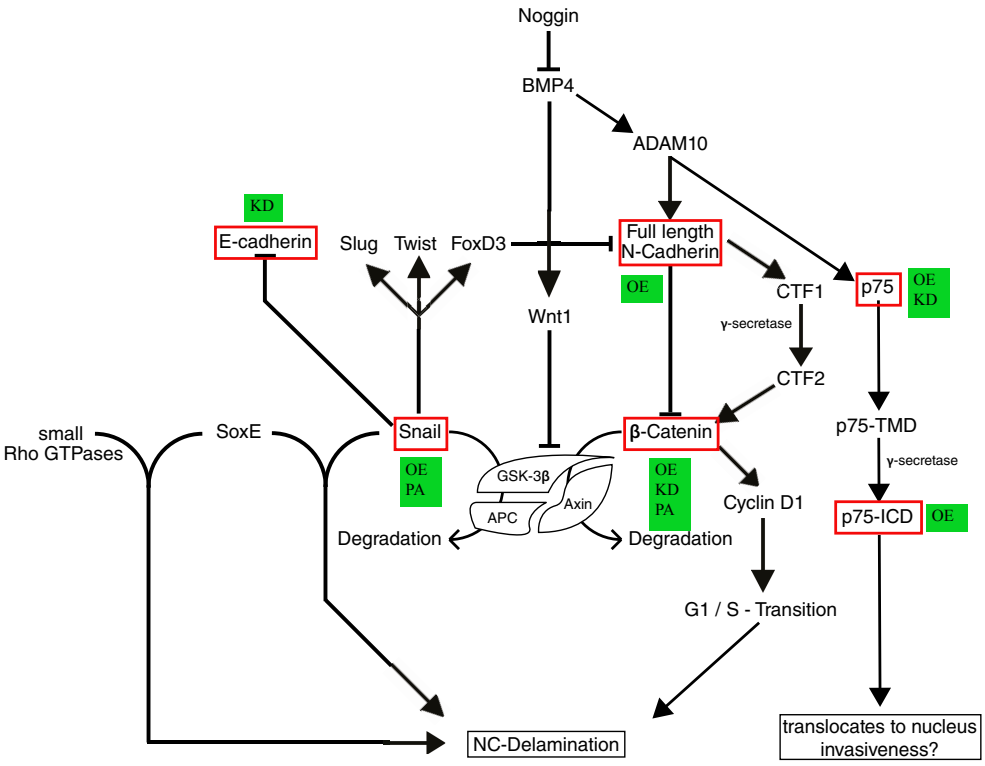

Figure 37. Neural crest EMT vectors. Neural crest EMT target vectors that have been constructed in the range of this study (green). Using these vectors will allow to assess the functional contribution of key neural crest EMT pathways to melanoma progression *in-vivo*. OE, overexpression, PA, promoter activity, KD, knock-down.

Microarray analysis

Considering the preliminary findings implicating the loss of E-cadherin and an upregulation of CD271 in melanoma invasion, it would be interesting to assess to what extend these populations are intrinsically different from each other. However, given the lack of suitable *in-vivo* model systems for melanoma progression, addressing these differences has not been possible so far. Thus, based on our reconstitution approach we currently conduct a study to address the nature of $CD271^{Pos}$ and $E\text{-}cad^{Neg}$ cells *in-vivo*. To this end we

take advantage of the fact that our model not only recapitulates disease progression, but also allows the unequivocal isolation of GFP expressing tumor cells. This will allow us to fractionate a reconstituted tumor in GFP/CD271^{Pos} vs. GFP/CD271^{Neg} and GFP/E-cad^{Pos} vs. GFP/E-cad^{Neg} populations using FACS. Subjecting the resulting fractions to microarray analysis will allow us to address central questions regarding E-cadherin as a determinant of EMT and CD271 as a MSC marker. Along this line it will be especially interesting to assess whether E-cad^{Neg} cells show a mesenchymal expression profile as compared to E-cad^{Pos} cells and whether the CD271^{Pos} expression pattern can be correlated to that of neural crest stem cells.

Acknowledgments

First of all I would like to thank my supervisor, Lukas Sommer, for giving me the chance to conduct this study in his lab. Without his limitless fascination for science and his great enthusiasm, I would probably not be writing these lines right now. During these 4 years I have learned a lot, not only about Biology, but also personally. I appreciated the chance to think and work independently, a possibility that I might not come to enjoy soon again. In all, my PhD proved a challenging, yet rewarding experience that I will never forget. Thanks!

I would also like to thank my PhD committee members, Burkhard Becher and Alex Hajnal, for their support throughout the project. I valued the lively discussion we had during our meetings and the good input you provided. Thanks!

Furthermore, I would also like to thank all our lab members. You guys always provided a nice work environment that made life considerably easier. Along this line a special thanks goes to Gainluca Civenni (aka 'THE Gianneluca') for providing me with samples, viruses, vectors, mice and a variety of other things one eventually needs during a PhD. But mostly I appreciated the possibility to laugh or complain at all times, both of which are basic needs during any

PhD. Another special thanks goes to Iris, our lab manger, without whom the lab simply would not function. Thanks!

I would also like to thank all my collaborators. Without them this project would never have come to where it stands now. Thus, although it did not work out as planned, I would like to thank Johannes Vomberg for his support during my first year. My gratitude also goes to Reinhard Dummer, who helped me out with tumor histology and to Daniel Widmer for organized a multitude of stainings. And of course I would like to especially thank Ernst Reichmann and Thomas Biedermann, without whom the reconstituted melanoma model would never have been developed. Along this line I am very grateful to Ernst, who agreed to go down a new road and allowed me to use his resources to develop this new model system. But most of all I would like to thank Thomas Biedermann. Only based on his enthusiasm for the project and the willingness to take care of all the surgical procedures and animal care, we were able to make this project work. Thanks!

Finally, I would also like to thank my parents Monika and Wolfgang for their generous support during these 4 years. You always supported my decision to go down this road and for this I am grateful. This made many dark hours a lot easier to endure. At this point, I would also like to thank my brother Peter. Although always complaining that I am wasting his tax money, I am sure that he secretly enjoyed cross-funding this work. Thanks!

But above all I would like to thank my lovely wife, Celine. Without her support this journey into science would not have been the same. Although it was not always an easy path, you always stood at my side sharing the good as well

as the bad parts of it. That is all I could have asked for. Thanks!

Bibliography

[1] Boyle P, Levin B. Who cancer report. International Agency for Research on Cancer 2008;1–260. Global statistics 16-section 1.

[2] Parkin DM, Bray F, Ferlay J, Pisani P. Global cancer statistics, 2002. CA Cancer J Clin 2005;55:74–108.

[3] Jemal A, Siegel R, Ward E, Hao Y, Xu J, Murray T. Cancer statistics, 2008. CA: A Cancer Journal for Clinicians 2008;.

[4] Siegel R, Ward E, Brawley O, Jemal A. Cancer statistics, 2011: the impact of eliminating socioeconomic and racial disparities on premature cancer deaths. CA: A Cancer Journal for Clinicians 2011;61:212–36.

[5] Soria JC, Blay JY, Spano JP, Pivot X, Coscas Y, Khayat D. Added value of molecular targeted agents in oncology. Annals of oncology : official journal of the European Society for Medical Oncology / ESMO 2011;22:1703–16.

[6] Peterson C. Drug therapy of cancer. Eur J Clin Pharmacol 2011;67:437–47.

[7] Rothenberg ML, Carbone DP, Johnson DH. Improving the evaluation of new cancer treatments: challenges and opportunities. Nat Rev Cancer 2003;3:303–9.

[8] Hanahan D, Weinberg RA. The hallmarks of cancer. Cell 2000;100:57–70.

[9] Hanahan D, Weinberg RA. Hallmarks of cancer: the next generation. Cell 2011; 144:646–74.

[10] Knudson AG. Two genetic hits (more or less) to cancer. Nat Rev Cancer 2001; 1:157–62.

[11] Kroemer G, Pouyssegur J. Tumor cell metabolism: cancer's achilles' heel. Cancer Cell 2008;13:472–82.

[12] Jones RG, Thompson CB. Tumor suppressors and cell metabolism: a recipe for cancer growth. Genes Dev 2009;23:537–48.

[13] Luo J, Solimini NL, Elledge SJ. Principles of cancer therapy: oncogene and non-oncogene addiction. Cell 2009;136:823–37.

[14] Merlo LMF, Pepper JW, Reid BJ, Maley CC. Cancer as an evolutionary and ecological process. Nat Rev Cancer 2006;6:924–35.

[15] Negrini S, Gorgoulis VG, Halazonetis TD. Genomic instability–an evolving hallmark of cancer. Nat Rev Mol Cell Biol 2010;11:220–8.

[16] Colotta F, Allavena P, Sica A, Garlanda C, Mantovani A. Cancer-related inflammation, the seventh hallmark of cancer: links to genetic instability. Carcinogenesis 2009; 30:1073–81.

[17] Greaves M. Cancer stem cells: back to darwin? Semin Cancer Biol 2010;20:65–70.

[18] Nowell PC. The clonal evolution of tumor cell populations. Science 1976;194:23–8.

[19] Campbell PJ, Pleasance ED, Stephens PJ, et al. Subclonal phylogenetic structures in cancer revealed by ultra-deep sequencing. Proc Natl Acad Sci USA 2008;105:13081–6.

[20] Benetkiewicz M, Piotrowski A, Ståhl TDD, et al. Chromosome 22 array-cgh profiling of breast cancer delimited minimal common regions of genomic imbalances and revealed frequent intra-tumoral genetic heterogeneity. Int J Oncol 2006;29:935–45.

[21] Fujii H, Marsh C, Cairns P, Sidransky D, Gabrielson E. Genetic divergence in the clonal evolution of breast cancer. Cancer Res 1996;56:1493–7.

[22] Glöckner S, Buurman H, Kleeberger W, Lehmann U, Kreipe H. Marked intratumoral heterogeneity of c-myc and cyclind1 but not of c-erbb2 amplification in breast cancer. Lab Invest 2002;82:1419–26.

[23] Shah SP, Morin RD, Khattra J, et al. Mutational evolution in a lobular breast tumour profiled at single nucleotide resolution. Nature 2009;461:809–13.

[24] Torres L, Ribeiro FR, Pandis N, Andersen JA, Heim S, Teixeira MR. Intratumor genomic heterogeneity in breast cancer with clonal divergence between primary carcinomas and lymph node metastases. Breast Cancer Res Treat 2007;102:143–55.

[25] Konishi N, Hiasa Y, Matsuda H, et al. Intratumor cellular heterogeneity and alterations in ras oncogene and p53 tumor suppressor gene in human prostate carcinoma. Am J Pathol 1995;147:1112–22.

[26] Samowitz WS, Slattery ML. Regional reproducibility of microsatellite instability in sporadic colorectal cancer. Genes Chromosomes Cancer 1999;26:106–14.

[27] Mora J, Cheung NK, Gerald WL. Genetic heterogeneity and clonal evolution in neuroblastoma. Br J Cancer 2001;85:182–9.

[28] Sauter G, Moch H, Gasser TC, Mihatsch MJ, Waldman FM. Heterogeneity of chromosome 17 and erbb-2 gene copy number in primary and metastatic bladder cancer. Cytometry 1995;21:40–6.

[29] Dick JE. Stem cell concepts renew cancer research. Blood 2008;112:4793–807.

[30] Marusyk A, Polyak K. Tumor heterogeneity: causes and consequences. Biochim Biophys Acta 2010;1805:105–17.

[31] Salk JJ, Fox EJ, Loeb LA. Mutational heterogeneity in human cancers: origin and consequences. Annu Rev Pathol 2010;5:51–75.

[32] Kobayashi S, Boggon TJ, Dayaram T, et al. Egfr mutation and resistance of non-small-cell lung cancer to gefitinib. N Engl J Med 2005;352:786–92.

[33] Gorre ME, Mohammed M, Ellwood K, et al. Clinical resistance to sti-571 cancer therapy caused by bcr-abl gene mutation or amplification. Science 2001;293:876–80.

[34] Stratton MR. Exploring the genomes of cancer cells: progress and promise. Science 2011;331:1553–8.

[35] Pardal R, Clarke MF, Morrison SJ. Applying the principles of stem-cell biology to cancer. Nat Rev Cancer 2003;3:895–902.

[36] Ward R, Dirks P. Cancer stem cells: At the headwaters of tumor development. Annual review of pathology 2007;2:175–189.

[37] Dalerba P, Cho R, Clarke M. Cancer stem cells: models and concepts. Annu Rev Med 2007;.

[38] Dean M, Fojo T, Bates S. Tumour stem cells and drug resistance. Nat Rev Cancer 2005;5:275–84.

[39] Reya T, Morrison SJ, Clarke MF, Weissman IL. Stem cells, cancer, and cancer stem cells. Nature 2001;414:105–11.

[40] Virchow R. Cellular-pathologie. Virchows Archiv 1855;.

[41] Cohnheim J. Ueber entzündung und eiterung. Virchows Archiv 1867;.

[42] Lapidot T, Sirard C, Vormoor J, et al. A cell initiating human acute myeloid leukaemia after transplantation into scid mice. Nature 1994;367:645–8.

[43] Bonnet D, Dick JE. Human acute myeloid leukemia is organized as a hierarchy that originates from a primitive hematopoietic cell. Nature medicine 1997;3:730–7.

[44] Huntly BJP, Gilliland DG. Leukaemia stem cells and the evolution of cancer-stem-cell research. Nat Rev Cancer 2005;5:311–21.

[45] O'Brien CA, Kreso A, Jamieson CHM. Cancer stem cells and self-renewal. Clin Cancer Res 2010;16:3113–20.

[46] Ailles LE, Weissman IL. Cancer stem cells in solid tumors. Curr Opin Biotechnol 2007;18:460–6.

[47] Visvader JE, Lindeman GJ. Cancer stem cells in solid tumours: accumulating evidence and unresolved questions. Nat Rev Cancer 2008;8:755–68.

[48] Gupta PB, Chaffer CL, Weinberg RA. Cancer stem cells: mirage or reality? Nat Med 2009;15:1010–2.

[49] Quintana E, Shackleton M, Sabel MS, Fullen DR, Johnson TM, Morrison SJ. Efficient tumour formation by single human melanoma cells. Nature 2008;456:593–8.

[50] Quintana E, Shackleton M, Foster HR, et al. Phenotypic heterogeneity among tumorigenic melanoma cells from patients that is reversible and not hierarchically organized. Cancer Cell 2010;18:510–23.

[51] Civenni G, Walter A, Kobert N, et al. Human cd271-positive melanoma stem cells associated with metastasis establish tumor heterogeneity and long-term growth. Cancer Res 2011;.

[52] Shackleton M, Quintana E, Fearon ER, Morrison SJ. Heterogeneity in cancer: cancer stem cells versus clonal evolution. Cell 2009;138:822–9.

[53] Weinberg R, Fisher DE, Rich J. Dynamic and transient cancer stem cells nurture melanoma. Nat Med 2010;16:758.

[54] Zhu L, Gibson P, Currle DS, et al. Prominin 1 marks intestinal stem cells that are susceptible to neoplastic transformation. Nature 2009;457:603–7.

[55] Barker N, Ridgway RA, van Es JH, et al. Crypt stem cells as the cells-of-origin of intestinal cancer. Nature 2009;457:608–11.

[56] Wang X, de Julio MK, Economides KD, et al. A luminal epithelial stem cell that is a cell of origin for prostate cancer. Nature 2009;461:495–500.

[57] Youssef KK, Keymeulen AV, Lapouge G, et al. Identification of the cell lineage at the origin of basal cell carcinoma. Nat Cell Biol 2010;12:299–305.

[58] Wong DJ, Liu H, Ridky TW, Cassarino D, Segal E, Chang HY. Module map of stem cell genes guides creation of epithelial cancer stem cells. Cell Stem Cell 2008;2:333–44.

[59] Jamieson CHM, Ailles LE, Dylla SJ, et al. Granulocyte-macrophage progenitors as candidate leukemic stem cells in blast-crisis cml. N Engl J Med 2004;351:657–67.

[60] Visvader JE. Cells of origin in cancer. Nature 2011;469:314–22.

[61] Park SY, Gönen M, Kim HJ, Michor F, Polyak K. Cellular and genetic diversity in the progression of in situ human breast carcinomas to an invasive phenotype. J Clin Invest 2010;120:636–44.

[62] Shipitsin M, Campbell LL, Argani P, et al. Molecular definition of breast tumor heterogeneity. Cancer Cell 2007;11:259–73.

[63] Tian T, Olson S, Whitacre JM, Harding A. The origins of cancer robustness and evolvability. Integr Biol (Camb) 2011;3:17–30.

[64] Takebe N, Ivy SP. Controversies in cancer stem cells: targeting embryonic signaling pathways. Clin Cancer Res 2010;16:3106–12.

[65] Odoux C, Fohrer H, Hoppo T, et al. A stochastic model for cancer stem cell origin in metastatic colon cancer. Cancer Res 2008;68:6932–41.

[66] Fukunaga-Kalabis M, Roesch A, Herlyn M. From cancer stem cells to tumor maintenance in melanoma. J Invest Dermatol 2011;131:1600–4.

[67] Hendrix MJC, Seftor EA, Seftor REB, Kasemeier-Kulesa J, Kulesa PM, Postovit LM. Reprogramming metastatic tumour cells with embryonic microenvironments. Nat Rev Cancer 2007;7:246–55.

[68] Mintz B, Illmensee K. Normal genetically mosaic mice produced from malignant teratocarcinoma cells. Proc Natl Acad Sci USA 1975;72:3585–9.

[69] Welte Y, Adjaye J, Lehrach HR, Regenbrecht CR. Cancer stem cells in solid tumors: elusive or illusive? Cell Commun Signal 2010;8:6.

[70] Dirks P. Cancer stem cells: Invitation to a second round. Nature 2010;466:40–1.

[71] Roesch A, Fukunaga-Kalabis M, Schmidt EC, et al. A temporarily distinct subpopulation of slow-cycling melanoma cells is required for continuous tumor growth. Cell 2010;141:583–94.

[72] Mani SA, Guo W, Liao MJ, et al. The epithelial-mesenchymal transition generates cells with properties of stem cells. Cell 2008;133:704–15.

[73] Morel AP, Lièvre M, Thomas C, Hinkal G, Ansieau S, Puisieux A. Generation of breast cancer stem cells through epithelial-mesenchymal transition. PLoS ONE 2008; 3:e2888.

[74] Chambers AF, Groom AC, MacDonald IC. Dissemination and growth of cancer cells in metastatic sites. Nat Rev Cancer 2002;2:563–72.

[75] Fidler IJ. The pathogenesis of cancer metastasis: the 'seed and soil' hypothesis revisited. Nat Rev Cancer 2003;3:453–8.

[76] Luzzi KJ, MacDonald IC, Schmidt EE, et al. Multistep nature of metastatic inefficiency: dormancy of solitary cells after successful extravasation and limited survival of early micrometastases. Am J Pathol 1998;153:865–73.

[77] Fidler I. Metastasis, quantitative analysis of distribution and fate of tumor cell emboli labelled with ‚ÇÅ25 1udr. enscientificcommonsorg 1970;.

[78] Paget S. The distribution of secondary growths in cancer of the breast. Lancet 1889;.

[79] Ewing J. Neoplastic diseases. a treatise on tumors. The American Journal of the Medical Sciences 1928;.

[80] Talmadge JE, Fidler IJ. Aacr centennial series: the biology of cancer metastasis: historical perspective. Cancer Res 2010;70:5649–69.

[81] Fidler IJ, Kripke ML. Metastasis results from preexisting variant cells within a malignant tumor. Science 1977;197:893–5.

[82] Chambers A, MacDonald I, Schmidt... E. Clinical targets for anti-metastasis therapy. Advances in cancer ... 2000;.

[83] Liu W, Laitinen S, Khan S, et al. Copy number analysis indicates monoclonal origin of lethal metastatic prostate cancer. Nature medicine 2009;15:559–65.

[84] Ding L, Ellis M, Li S, Larson D, Chen... K. Genome remodelling in a basal-like breast cancer metastasis and xenograft. Nature 2010;.

[85] Pleasance ED, Cheetham RK, Stephens PJ, et al. A comprehensive catalogue of somatic mutations from a human cancer genome. Nature 2010;463:191–6.

[86] Bissig H, Richter J, Desper R, et al. Evaluation of the clonal relationship between primary and metastatic renal cell carcinoma by comparative genomic hybridization. Am J Pathol 1999;155:267–74.

[87] Campbell PJ, Yachida S, Mudie LJ, et al. The patterns and dynamics of genomic instability in metastatic pancreatic cancer. Nature 2010;467:1109–13.

[88] Talmadge J. Evidence that intravenously derived murine pulmonary melanoma metastases can originate from the expansion of a single tumor cell. Cancer Res 1986;.

[89] Jones T, Carr M, Eble J, Wang... M. Clonal origin of lymph node metastases in bladder carcinoma. Cancer 2005;.

[90] Klein CA. Parallel progression of primary tumours and metastases. Nat Rev Cancer 2009;9:302–12.

[91] Kuukasjärvi T, Karhu R, Tanner M, et al. Genetic heterogeneity and clonal evolution underlying development of asynchronous metastasis in human breast cancer. Cancer Res 1997;57:1597–604.

[92] Hüsemann Y, Geigl JB, Schubert F, et al. Systemic spread is an early step in breast cancer. Cancer Cell 2008;13:58–68.

[93] Daskalakis A, Granzow M, Ahr... A. From latent disseminated cells to overt metastasis: genetic analysis of systemic breast cancer progression. Proceedings of the ... 2003;.

[94] Schmidt-Kittler O, Petronio M, Polzer... B. Genetic heterogeneity of single disseminated tumour cells in minimal residual cancer. The Lancet 2002;.

[95] Borovski T, Melo FDSE, Vermeulen L, Medema JP. Cancer stem cell niche: the place to be. Cancer Res 2011;71:634–9.

[96] Thiery JP. Epithelial-mesenchymal transitions in tumour progression. Nat Rev Cancer 2002;2:442–54.

[97] Adhikari AS, Agarwal N, Iwakuma T. Metastatic potential of tumor-initiating cells in solid tumors. Front Biosci 2011;16:1927–38.

[98] Singh A, Settleman J. Emt, cancer stem cells and drug resistance: an emerging axis of evil in the war on cancer. Oncogene 2010;29:4741–51.

[99] Polyak K, Weinberg RA. Transitions between epithelial and mesenchymal states: acquisition of malignant and stem cell traits. Nat Rev Cancer 2009;9:265–73.

[100] Bos PD, Nguyen DX, Massagué J. Modeling metastasis in the mouse. Curr Opin Pharmacol 2010;10:571–7.

[101] MacDonald IC, Groom AC, Chambers AF. Cancer spread and micrometastasis development: quantitative approaches for in vivo models. Bioessays 2002;24:885–93.

[102] Kiowski G, Biedermann T, Widmer DS, et al. Engineering melanoma progression in a humanized environment in vivo. J Invest Dermatol 2011;.

[103] Khavari PA. Modelling cancer in human skin tissue. Nat Rev Cancer 2006;6:270–80.

[104] Welch DR. Technical considerations for studying cancer metastasis in vivo. Clin Exp Metastasis 1997;15:272–306.

[105] Bachtiary B, Boutros PC, Pintilie M, et al. Gene expression profiling in cervical cancer: an exploration of intratumor heterogeneity. Clin Cancer Res 2006;12:5632–40.

[106] Refaeli Y, Bhoumik A, Roop DR, Ronai ZA. Melanoma-initiating cells: a compass needed. EMBO Rep 2009;10:965–72.

[107] Boiko AD, Razorenova OV, van de Rijn M, et al. Human melanoma-initiating cells express neural crest nerve growth factor receptor cd271. Nature 2010;466:133–137.

[108] Miller AJ, Mihm MC. Melanoma. N Engl J Med 2006;355:51–65.

[109] Gilchrest B, Eller M, Geller... A. The pathogenesis of melanoma induced by ultraviolet radiation. The New England journal of ... 1999;.

[110] Jr WC, Elder D, IV DG, Epstein... M. A study of tumor progression: the precursor lesions of superficial spreading and nodular melanoma. Human pathology 1984;.

[111] Balch CM, Gershenwald JE, Soong SJ, et al. Final version of 2009 ajcc melanoma staging and classification. J Clin Oncol 2009;27:6199–206.

[112] Ko JM, Fisher DE. A new era: melanoma genetics and therapeutics. J Pathol 2011; 223:241–50.

[113] Chin L. The genetics of malignant melanoma: lessons from mouse and man. Nat Rev Cancer 2003;3:559–70.

[114] Kennedy C, ter Huurne J, Berkhout M, et al. Melanocortin 1 receptor (mc1r) gene variants are associated with an increased risk for cutaneous melanoma which is largely independent of skin type and hair color. J Invest Dermatol 2001;117:294–300.

[115] Valverde P, Healy E, Jackson I, Rees JL, Thody AJ. Variants of the melanocyte-stimulating hormone receptor gene are associated with red hair and fair skin in humans. Nat Genet 1995;11:328–30.

[116] Albino A, Nanus D, Mentle... I. Analysis of ras oncogenes in malignant melanoma and precursor lesions: correlation of point mutations with differentiation phenotype. Oncogene 1989;.

[117] Davies H, Bignell GR, Cox C, et al. Mutations of the braf gene in human cancer. Nature 2002;417:949–54.

[118] Pollock PM, Harper UL, Hansen KS, et al. High frequency of braf mutations in nevi. Nat Genet 2003;33:19–20.

[119] Michaloglou C, Vredeveld LCW, Soengas MS, et al. Brafe600-associated senescence-like cell cycle arrest of human naevi. Nature 2005;436:720–4.

[120] Chudnovsky Y, Khavari PA, Adams AE. Melanoma genetics and the development of rational therapeutics. J Clin Invest 2005;115:813–24.

[121] Patton EE, Widlund HR, Kutok JL, et al. Braf mutations are sufficient to promote nevi formation and cooperate with p53 in the genesis of melanoma. Curr Biol 2005; 15:249–54.

[122] Larue L, Beermann F. Cutaneous melanoma in genetically modified animals. Pigment Cell Res 2007;20:485–97.

[123] Hussussian CJ, Struewing JP, Goldstein AM, et al. Germline p16 mutations in familial melanoma. Nat Genet 1994;8:15–21.

[124] Sharpless NE, Kannan K, Xu J, Bosenberg MW, Chin L. Both products of the mouse ink4a/arf locus suppress melanoma formation in vivo. Oncogene 2003;22:5055–9.

[125] Chudnovsky Y, Adams AE, Robbins PB, Lin Q, Khavari PA. Use of human tissue to assess the oncogenic activity of melanoma-associated mutations. Nat Genet 2005; 37:745–9.

[126] Guldberg P, thor Straten P, Birck A, Ahrenkiel V, Kirkin AF, Zeuthen J. Disruption of the mmac1/pten gene by deletion or mutation is a frequent event in malignant melanoma. Cancer Res 1997;57:3660–3.

[127] Dankort D, Curley D, Cartlidge R, et al. Braf(v600e) cooperates with pten loss to induce metastatic melanoma. Nat Genet 2009;.

[128] Gray-Schopfer V, Wellbrock C, Marais R. Melanoma biology and new targeted therapy. Nature 2007;445:851–7.

[129] McDermott U, Downing JR, Stratton MR. Genomics and the continuum of cancer care. N Engl J Med 2011;364:340–50.

[130] Nazarian R, Shi H, Wang Q, et al. Melanomas acquire resistance to b-raf(v600e) inhibition by rtk or n-ras upregulation. Nature 2010;468:973–7.

[131] Cho RW, Clarke MF. Recent advances in cancer stem cells. Curr Opin Genet Dev 2008;18:48–53.

[132] Fang D, Nguyen TK, Leishear K, et al. A tumorigenic subpopulation with stem cell properties in melanomas. Cancer Res 2005;65:9328–37.

[133] Monzani E, Facchetti F, Galmozzi E, et al. Melanoma contains cd133 and abcg2 positive cells with enhanced tumourigenic potential. Eur J Cancer 2007;43:935–46.

[134] Keshet G, Goldstein I, Yitzhaki O, et al. Mdr1 expression identifies human melanoma stem cells. Biochem Biophys Res Commun 2008;.

[135] Schatton T, Murphy GF, Frank NY, et al. Identification of cells initiating human melanomas. Nature 2008;451:345–9.

[136] Paratore C, Goerich DE, Suter U, Wegner M, Sommer L. Survival and glial fate acquisition of neural crest cells are regulated by an interplay between the transcription factor sox10 and extrinsic combinatorial signaling. Development 2001;128:3949–61.

[137] Stemple DL, Anderson DJ. Isolation of a stem cell for neurons and glia from the mammalian neural crest. Cell 1992;71:973–85.

[138] Smith AP, Hoek K, Becker D. Whole-genome expression profiling of the melanoma progression pathway reveals marked molecular differences between nevi/melanoma in situ and advanced-stage melanomas. Cancer Biol Ther 2005;4:1018–29.

[139] Hoek K, Rimm DL, Williams KR, et al. Expression profiling reveals novel pathways in the transformation of melanocytes to melanomas. Cancer Res 2004;64:5270–82.

[140] Koh SS, Opel ML, Wei JPJ, et al. Molecular classification of melanomas and nevi using gene expression microarray signatures and formalin-fixed and paraffin-embedded tissue. Mod Pathol 2009;22:538–46.

[141] Jaeger J, Koczan D, Thiesen HJ, et al. Gene expression signatures for tumor progression, tumor subtype, and tumor thickness in laser-microdissected melanoma tissues. Clin Cancer Res 2007;13:806–15.

[142] Haqq C, Nosrati M, Sudilovsky D, et al. The gene expression signatures of melanoma progression. Proc Natl Acad Sci USA 2005;102:6092–7.

[143] Bittner M, Meltzer P, Chen Y, et al. Molecular classification of cutaneous malignant melanoma by gene expression profiling. Nature 2000;406:536–40.

[144] Seykora JT, Jih D, Elenitsas R, Horng WH, Elder DE. Gene expression profiling of melanocytic lesions. Am J Dermatopathol 2003;25:6–11.

[145] Iwamoto S, Odland PB, Piepkorn M, Bothwell M. Evidence that the p75 neurotrophin receptor mediates perineural spread of desmoplastic melanoma. J Am Acad Dermatol 1996;35:725–31.

[146] Denkins Y, Reiland J, Roy M, et al. Brain metastases in melanoma: roles of neurotrophins. Neuro-oncology 2004;6:154–65.

[147] Marchetti D, Menter D, Jin L, Nakajima M, Nicolson GL. Nerve growth factor effects on human and mouse melanoma cell invasion and heparanase production. Int J Cancer 1993;55:692–9.

[148] Walch ET, Albino AP, Marchetti D. Correlation of overexpression of the low-affinity p75 neurotrophin receptor with augmented invasion and heparanase production in human malignant melanoma cells. Int J Cancer 1999;82:112–20.

[149] Truzzi F, Marconi A, Lotti R, et al. Neurotrophins and their receptors stimulate melanoma cell proliferation and migration. J Invest Dermatol 2008;128:2031–40.

[150] Gupta PB, Kuperwasser C, Brunet JP, et al. The melanocyte differentiation program predisposes to metastasis after neoplastic transformation. Nat Genet 2005;37:1047–54.

[151] Alonso SR, Tracey L, Ortiz P, et al. A high-throughput study in melanoma identifies epithelial-mesenchymal transition as a major determinant of metastasis. Cancer Res 2007;67:3450–60.

[152] Burstyn-Cohen T, Stanleigh J, Sela-Donenfeld D, Kalcheim C. Canonical wnt activity regulates trunk neural crest delamination linking bmp/noggin signaling with g1/s transition. Development 2004;131:5327–39.

[153] Busch C, Drews U, Eisele SR, Garbe C, Oppitz M. Noggin blocks invasive growth of murine b16-f1 melanoma cells in the optic cup of the chick embryo. Int J Cancer 2008; 122:526–33.

[154] Rothhammer T, Poser I, Soncin F, Bataille F, Moser M, Bosserhoff AK. Bone morphogenic proteins are overexpressed in malignant melanoma and promote cell invasion and migration. Cancer Res 2005;65:448–56.

[155] Klaus A, Birchmeier W. Wnt signalling and its impact on development and cancer. Nat Rev Cancer 2008;8:387–98.

[156] Gumbiner BM. Regulation of cadherin-mediated adhesion in morphogenesis. Nat Rev Mol Cell Biol 2005;6:622–34.

[157] Akitaya T, Bronner-Fraser M. Expression of cell adhesion molecules during initiation and cessation of neural crest cell migration. Dev Dyn 1992;194:12–20.

[158] Shoval I, Ludwig A, Kalcheim C. Antagonistic roles of full-length n-cadherin and its soluble bmp cleavage product in neural crest delamination. Development 2007; 134:491–501.

[159] Reiss K, Maretzky T, Ludwig A, et al. Adam10 cleavage of n-cadherin and regulation of cell-cell adhesion and beta-catenin nuclear signalling. EMBO J 2005;24:742–52.

[160] Perl AK, Wilgenbus P, Dahl U, Semb H, Christofori G. A causal role for e-cadherin in the transition from adenoma to carcinoma. Nature 1998;392:190–3.

[161] Cano A, Pérez-Moreno MA, Rodrigo I, et al. The transcription factor snail controls epithelial-mesenchymal transitions by repressing e-cadherin expression. Nature Cell Biology 2000;2:76–83.

[162] Yook JI, Li XY, Ota I, Fearon ER, Weiss SJ. Wnt-dependent regulation of the e-cadherin repressor snail. J Biol Chem 2005;280:11740–8.

[163] Aybar MJ, Nieto MA, Mayor R. Snail precedes slug in the genetic cascade required for the specification and migration of the xenopus neural crest. Development 2003; 130:483–94.

[164] Barrallo-Gimeno A, Nieto MA. The snail genes as inducers of cell movement and survival: implications in development and cancer. Development 2005;132:3151–61.

[165] Dissanayake SK, Wade M, Johnson CE, et al. The wnt5a/protein kinase c pathway mediates motility in melanoma cells via the inhibition of metastasis suppressors and initiation of an epithelial to mesenchymal transition. J Biol Chem 2007;282:17259–71.

[166] Cheung M, Chaboissier MC, Mynett A, Hirst E, Schedl A, Briscoe J. The transcriptional control of trunk neural crest induction, survival, and delamination. Dev Cell 2005;8:179–92.

[167] Wang H, Leav I, Ibaragi S, et al. Sox9 is expressed in human fetal prostate epithelium and enhances prostate cancer invasion. Cancer Res 2008;68:1625–30.

[168] Nakahara H, Otani T, Sasaki T, Miura Y, Takai Y, Kogo M. Involvement of cdc42 and rac small g proteins in invadopodia formation of rpmi7951 cells. Genes Cells 2003; 8:1019–27.

[169] Chen Y, Zeng J, Cen L, et al. Multiple roles of the p75 neurotrophin receptor in the nervous system. J Int Med Res 2009;37:281–8.

[170] Schor NF. The p75 neurotrophin receptor in human development and disease. Prog Neurobiol 2005;77:201–14.

[171] Yamashita T, Tucker KL, Barde YA. Neurotrophin binding to the p75 receptor modulates rho activity and axonal outgrowth. Neuron 1999;24:585–93.

[172] Roux PP, Barker PA. Neurotrophin signaling through the p75 neurotrophin receptor. Prog Neurobiol 2002;67:203–33.

[173] Underwood CK, Coulson EJ. The p75 neurotrophin receptor. Int J Biochem Cell Biol 2008;40:1664–8.

[174] Kanning KC, Hudson M, Amieux PS, Wiley JC, Bothwell M, Schecterson LC. Proteolytic processing of the p75 neurotrophin receptor and two homologs generates c-terminal fragments with signaling capability. J Neurosci 2003;23:5425–36.

[175] Parkhurst CN, Zampieri N, Chao MV. Nuclear localization of the p75 neurotrophin receptor intracellular domain. J Biol Chem 2010;285:5361–8.

[176] Bronfman FC. Metalloproteases and gamma-secretase: new membrane partners regulating p75 neurotrophin receptor signaling? J Neurochem 2007;103 Suppl 1:91–100.

[177] Marchetti D, Aucoin R, Blust J, Murry B, Greiter-Wilke A. p75 neurotrophin receptor functions as a survival receptor in brain-metastatic melanoma cells. J Cell Biochem 2004;91:206–15.

[178] Chan MM, Tahan SR. Low-affinity nerve growth factor receptor (p75 ngfr) as a marker of perineural invasion in malignant melanomas. J Cutan Pathol 2010;37:336–43.

[179] Bechetoille N, Haftek M, Staquet MJ, Cochran AJ, Schmitt D, Berthier-Vergnes O. Penetration of human metastatic melanoma cells through an authentic dermal-epidermal junction is associated with dissolution of native collagen types iv and vii. Melanoma Res 2000;10:427–34.

[180] Berking C, Takemoto R, Satyamoorthy K, Elenitsas R, Herlyn M. Basic fibroblast growth factor and ultraviolet b transform melanocytes in human skin. Am J Pathol 2001;158:943–53.

[181] Eves P, Layton C, Hedley S, et al. Characterization of an in vitro model of human melanoma invasion based on reconstructed human skin. Br J Dermatol 2000;142:210–22.

[182] Haass NK, Smalley KSM, Li L, Herlyn M. Adhesion, migration and communication in melanocytes and melanoma. Pigment Cell Res 2005;18:150–9.

[183] Hsu MY, Shih DT, Meier FE, et al. Adenoviral gene transfer of beta3 integrin subunit induces conversion from radial to vertical growth phase in primary human melanoma. Am J Pathol 1998;153:1435–42.

[184] Meier F, Nesbit M, Hsu MY, et al. Human melanoma progression in skin reconstructs : biological significance of bfgf. Am J Pathol 2000;156:193–200.

[185] Juhasz I, Albelda SM, Elder DE, et al. Growth and invasion of human melanomas in human skin grafted to immunodeficient mice. Am J Pathol 1993;143:528–37.

[186] Medalie DA, Eming SA, Tompkins RG, Yarmush ML, Krueger GG, Morgan JR. Evaluation of human skin reconstituted from composite grafts of cultured keratinocytes and human acellular dermis transplanted to athymic mice. J Invest Dermatol 1996; 107:121–7.

[187] Bhowmick NA, Neilson EG, Moses HL. Stromal fibroblasts in cancer initiation and progression. Nature 2004;432:332–7.

[188] Gaggioli C, Hooper S, Hidalgo-Carcedo C, et al. Fibroblast-led collective invasion of carcinoma cells with differing roles for rhogtpases in leading and following cells. Nat Cell Biol 2007;9:1392–400.

[189] Ridky TW, Chow JM, Wong DJ, Khavari PA. Invasive three-dimensional organotypic neoplasia from multiple normal human epithelia. Nature medicine 2010;.

[190] Biedermann T, Pontiggia L, Böttcher-Haberzeth S, et al. Human eccrine sweat gland cells can reconstitute a stratified epidermis. J Invest Dermatol 2010;130:1996–2009.

[191] Pontiggia L, Biedermann T, Meuli M, et al. Markers to evaluate the quality and self-renewing potential of engineered human skin substitutes in vitro and after transplantation. J Invest Dermatol 2009;129:480–90.

[192] Gershenwald JE, Soong SJ, Balch CM, on Cancer (AJCC) Melanoma Staging Committee AJC. 2010 tnm staging system for cutaneous melanoma...and beyond. Ann Surg Oncol 2010;17:1475–7.

[193] Lipkin G. Plasticity of the cancer cell: implications for epigenetic control of melanoma and other malignancies. J Invest Dermatol 2008;128:2152–5.

[194] Becker JC, Houben R, Schrama D, Voigt H, Ugurel S, Reisfeld RA. Mouse models for melanoma: a personal perspective. Exp Dermatol 2010;19:157–64.

[195] Bedogni B, Powell MB. Hypoxia, melanocytes and melanoma - survival and tumor development in the permissive microenvironment of the skin. Pigment Cell & Melanoma Research 2009;22:166–74.

[196] Pouysségur J, Dayan F, Mazure NM. Hypoxia signalling in cancer and approaches to enforce tumour regression. Nature 2006;441:437–43.

[197] Hsu MY, Meier FE, Nesbit M, et al. E-cadherin expression in melanoma cells restores keratinocyte-mediated growth control and down-regulates expression of invasion-related adhesion receptors. Am J Pathol 2000;156:1515–25.

[198] Costea DE, Loro LL, Dimba EAO, Vintermyr OK, Johannessen AC. Crucial effects of fibroblasts and keratinocyte growth factor on morphogenesis of reconstituted human oral epithelium. J Invest Dermatol 2003;121:1479–86.

[199] Schneider J, Biedermann T, Widmer D, et al. Matriderm versus integra: a comparative experimental study. Burns 2009;35:51–7.

[200] Hoek KS, Eichhoff OM, Schlegel NC, et al. In vivo switching of human melanoma cells between proliferative and invasive states. Cancer Res 2008;68:650–6.

[201] Follenzi A, Naldini L. Generation of hiv-1 derived lentiviral vectors. Meth Enzymol 2002;346:454–65.

[202] Wong CE, Paratore C, Dours-Zimmermann MT, et al. Neural crest-derived cells with stem cell features can be traced back to multiple lineages in the adult skin. J Cell Biol 2006;175:1005–15.

[203] Thurber AE, Douglas G, Sturm EC, et al. Inverse expression states of the brn2 and mitf transcription factors in melanoma spheres and tumour xenografts regulate the notch pathway. Oncogene 2011;30:3036–48.

[204] Nguyen DX, Massagué J. Genetic determinants of cancer metastasis. Nat Rev Genet 2007;8:341–52.

[205] Kim R, Emi M, Tanabe K, Arihiro K. Tumor-driven evolution of immunosuppressive networks during malignant progression. Cancer Res 2006;66:5527–36.

[206] McAllister SS, Weinberg RA. Tumor-host interactions: a far-reaching relationship. J Clin Oncol 2010;28:4022–8.

[207] Schatton T, Schütte U, Frank NY, et al. Modulation of t-cell activation by malignant melanoma initiating cells. Cancer Res 2010;70:697–708.

Curriculum Vitae

PERSONAL DATA

Name	Gregor Kiowski
Nationaltiy	Swiss, German
Address	Ackerstrasse 12 8005 Zürich
Phone	+41 (0) 79'416'89'28
E-Mail	g.kiowski@hispeed.ch

EDUCATION

PhD Cell Biology
University of Zurich, Switzerland Nov. 2007 - Dez. 2011
Title - The Role of Melanoma Stem Cells in Metastasis

- Course in Clinical Cancer Research
- Course in Molecular and Cell Biology of Cancer
- Course in Business Know-How

Master of Science ETH
Swiss Federal Institute of Technology, Zurich, Switzerland Oct. 2001 - Oct. 2007
Thesis - Characterization of a Tumor Stem Cell in Human Neuroblastoma

- Major in Biochemistry and Molecular Biology
- Minors in Cell Biology and Pharmacology

PROFESSIONAL EXPERIENCE

Swiss Investment Company Oct. 2005 - Feb. 2006
Division of Funds accounting

- Basic tasks in fund management and accounting.
- Daily publication of funds operating figures.
- Assistant to the division head.

Swiss Private Bank Leu Jun. 2004 - Feb. 2005
Division of private banking tax and inheritances

- Compiled historical tax reports for the german tax amnesty.
- Internal monitoring
- Processing of account statements and inquiries.

TALKS

- USGEB (Union of the Swiss Societies of Experimental Biology) Meeting
- Seminar for the department of Dermatology, University Hospital Zurich
- Cancer Network Zurich Retreat
- Workshop "Experimental Neuro-oncology"
- Cancer Biology PhD Program Student Retreat

PUBLICATIONS

Engineering melanoma progression in a humanized environment *in-vivo* (Kiowski G, Biedermann T, Widmer DS, et al., J Invest Dermatol 2011)

LANGUAGES

- German native
- Proficient in English (Cambridge ESOL Certificate of Proficiency)
- Basic knowledge in French and Italian

INTERESTS

Soccer, Snowboarding, Mountain biking, Diving, Hiking, Photography, Cooking, Wine